

**CLASS VI PERMIT APPLICATION NARRATIVE**

**40 CFR 146.82(a)**

**GULF COAST SEQUESTRATION  
PROJECT GOOSE LAKE**

## **Table of Contents**

1.0	Facility Information .....	5
2.0	PROJECT BACKGROUND .....	6
2.1	Project goals .....	6
2.2	Ownership.....	6
2.3	Proposed injection mass/volume and CO <sub>2</sub> source .....	6
2.4	Applicable permits.....	7
2.4.1	Hazardous Waste Management program under RCRA. (40 CFR 239 -282) .....	7
2.4.2	UIC Program. (LAC 43:XVII.3603.E.1) .....	7
2.4.3	NPDES. (40 CFR.d.122, LAC 33: Chapter IX).....	7
2.4.4	PSD Program. (40 CFR 144.31(e)(6)(iv), LAC 33:III:509.A-P, LAC43:XVII.3607.B.9.d).....	7
3.0	GEOLOGY .....	8
3.1	Regional Geology .....	8
3.1.1	Regional Stratigraphy .....	10
3.1.2	Regional Structural Geology.....	15
3.1.3	Regional Cross Sections .....	17
3.1.4	Regional Groundwater Flow in the Injection Zone .....	19
3.2	Local Geology of the Project Goose Lake Site .....	21
3.2.1	Local Stratigraphy.....	21
3.2.2	Description of the Confining Zone and Injection Zone .....	22
3.2.3	Local Structure.....	26
3.2.4	Fault Transmissivity.....	28
3.2.5	Faulting within the Area of Review.....	37
3.2.6	Geomechanics of the Area of Review .....	40
3.3	Seismicity .....	43
3.3.1	Seismicity - Louisiana.....	44
3.3.2	Seismicity - Texas.....	44
3.3.3	Seismic Risk Analysis.....	45
3.3.4	Induced Seismicity .....	49
3.4	Hydrogeology .....	55
3.4.1	Regional Hydrogeology .....	55
3.4.2	Determination of the Lowermost Base of the USDW .....	58
3.4.3	Local Hydrogeology for the Project Goose Lake Site .....	62

3.4.4	Water Wells and Data Sets .....	65
3.4.5	Local Water Usage.....	65
3.5	Geochemistry.....	67
3.6	History of Economic Development .....	69
3.6.1	Regional Pressure Sources and Sinks .....	69
3.7	Geologic Summary .....	71
4.0	SITE CHARACTERISATION .....	72
4.1	Available Data Set and Basis for Evaluation.....	72
4.1.1	Seismic Data .....	72
4.1.2	Well Data .....	79
4.1.3	Interpretation and Evaluation Methodology .....	84
5.0	SITE SUITABILITY .....	90
5.1	Existing well penetrations in the Injection Zone .....	90
5.2	Model assumptions and conclusion.....	90
5.3	Check list of requirements.....	92
5.4	CO <sub>2</sub> trapping in the Injection Zone.....	92
5.5	Injection Zone Storage Capacity .....	92
5.6	Primary Confining Zone Integrity .....	92
5.7	Secondary Confinement .....	92
5.8	CO <sub>2</sub> interaction with subsurface and well materials.....	93
6.0	DESCRIPTION OF AoR AND CORRECTIVE ACTION PLAN .....	94
6.1	Description of the files submitted for the AoR and the Corrective Action plan .....	94
7.0	DESCRIPTION OF FINANCIAL RESPONSIBILITY .....	95
7.1	Description of the files submitted for the financial responsibility .....	95
8.0	DESCRIPTION OF WELL CONSTRUCTION PLAN .....	96
8.1	Well Construction Overview .....	96
8.2	Stimulation Program.....	96
8.3	Well Construction Procedures .....	96
8.3.1	Prevention of fluid movement into or between USDW's .....	96
8.3.2	Testing and monitoring devices within the borehole and annulus.....	96
8.3.3	Drilling contingency plans and USDW Protection .....	97
8.3.4	Effect of average down-hole temperature.....	98
8.3.5	Structural strength of the proposed casing.....	98
8.3.6	Details of proposed cement job.....	99

8.3.7	Mechanical integrity of the cement and casing.....	99
8.3.8	Description of the well construction plan .....	99
8.3.9	Description of the Tubing and Packers .....	103
8.3.10	Grade V5 liquid test.....	104
8.3.11	Grade V4 liquid test + axial loads .....	104
8.3.12	Grade V3 liquid test + axial loads + temperature cycling .....	104
8.3.13	Grade V1 gas test + axial loads + temperature cycling .....	105
9.0	DESCRIPTION OF PRE-OPERATIONAL LOGGING AND TESTING PLAN.....	106
9.1	Description of the documents that are submitted to the GSDT .....	106
10.0	DESCRIPTION OF WELL OPERATION PLAN .....	107
10.1	Operational Procedures.....	107
10.1.1	Injector Well No.1 .....	107
10.1.2	Injector Well No.2 .....	108
10.2	Description of the proposed Carbon Dioxide Stream.....	108
11.0	DESCRIPTION OF TESTING AND MONITORING PLAN .....	109
11.1	Description of the documents that are submitted to the GSDT .....	109
12.0	DESCRIPTION OF INJECTION AND WELL PLUGGING PLAN .....	110
12.1	Description of the documents that are submitted to the GSDT .....	110
13.0	DESCRIPTION OF POST-INJECTION SITE CARE AND SITE CLOSURE PLAN ..	111
13.1	Description of the documents that are submitted to the GSDT .....	111
14.0	DESCRIPTION OF EMERGENCY AND REMEDIAL RESPONSE PLAN.....	112
14.1	Description of the documents that are submitted to the GSDT .....	112
15.0	INJECTION DEPTH WAIVER AND ACQUIFER EXEPMTION EXPANSION.....	113
16.0	DESCRIPTION OF ANY ADDITIONAL INFORMATION REQUESTED.....	114
16.1	Description of the documents that has been requested by the UIC Program Director	
16.2	114 Optional Additional Project Information [40 CFR 144.4] .....	114
16.2.1	Wild and Scenic Rivers Act, 16 U.S.C. 1273 et seq .....	114
16.2.2	National Historic Preservation Act of 1966, 16 U.S.C. 470 et seq.....	114
16.2.3	Endangered Species Act, 16 U.S.C. 1531 et seq .....	114
16.2.4	Coastal Zone Management Act, 16 U.S.C. 1451 et seq.....	114
16.2.5	Subsurface cleanup sites .....	115
17.0	REFERENCES – See A.4.1 References .....	118

## **1.0 Facility Information**

**Facility name:** Project Goose Lake  
Well Numbers 1 and 2

**Facility contact:** Benjamin Heard, Principal  
2417 Shell Beach Drive, Lake Charles, LA 70601  
(713) 320-2497; [bheard@gcscarbon.com](mailto:bheard@gcscarbon.com)

**Well location:** Calcasieu Parish, Louisiana – Datum WGS 1984  
 

## **2.0 PROJECT BACKGROUND**

### **2.1 Project goals**

Once completed, this follow-on project to Project Minerva is designed to permanently store more than 40 million tons of carbon in a saline aquifer. Project Goose Lake has the capacity to sequester 1,330,000 tons of CO<sub>2</sub> annually and will have the same carbon offset impact as more than 300 utility-scale solar facilities or some quarter of a million-household rooftop solar panels.

Project Goose Lake envisions sourcing CO<sub>2</sub> volumes from industrial producers of CO<sub>2</sub> in the Eastern Texas and Southwestern Louisiana industrial corridors. The goal is to enable the United States manufacturing and industrial base in the Texas and Louisiana Gulf Coast to continue to provide jobs and economic opportunity while minimizing the amount of CO<sub>2</sub> emitted into the earth's atmosphere. GCS maintains that both economic and environmental stewardship can advance in unison with an asset such as Project Goose Lake and intends to see this vision become a reality.

### **2.2 Ownership**

GCS is a wholly owned subsidiary of the Stream family, a multi-generational single-family office, based in Lake Charles, Louisiana. In addition to other investments, the Stream family are long-term landowners in Southwestern Louisiana, owning and operating land assets for well over a century in and near Lake Charles. The Stream family have protected and restored tens of thousands of acres of wetlands and sustainably managed thousands of acres of timber assets. The addition of Project Goose Lake to the GCS sequestration "hub" is a natural fit for the existing operations.

### **2.3 Proposed injection mass/volume and CO<sub>2</sub> source**

Project Goose Lake is designed for two individual injection wells drilled from one well pad site located in southwestern Calcasieu Parish. Two injection wells were selected to maximize access to the available pore volume of the late Oligocene Upper Frio Formation situated on Stream owned acreage. The project is designed to operate for thirty years at a planned capacity per annum of 1.33 million metric tons of CO<sub>2</sub> split between both injection wells.

CO<sub>2</sub> is anticipated to be sourced from industrial facilities in Southwestern Louisiana and Southeastern Texas, primarily from the Lake Charles and Beaumont industrial corridors. According to Environmental Protection Agency ("EPA") Facility Level Information on Greenhouse Gases Tool ("FLIGHT") the total CO<sub>2</sub> emissions from the four counties/parishes adjacent to Project Goose Lake emitted nearly 57 million metric tons of CO<sub>2</sub> in 2018 (EPA FLIGHT database at <https://ghgdata.epa.gov/ghgp/>). The two counties in Texas are Jefferson and Orange and the two parishes in Louisiana are Cameron and Calcasieu. Project Goose Lake does not have a dedicated source of CO<sub>2</sub> under contract, however, is in advanced stage discussion on offtake arrangements with several counterparties with assets in the four county/parish area discussed above.

## **2.4 Applicable permits**

### ***2.4.1 Hazardous Waste Management program under RCRA. (40 CFR 239 -282)***

The Resource Conservation and Recovery Act (RCRA) is the law that outlines the proper management of hazardous and non-hazardous solid waste. Currently, the disposal of certain wastes from the exploration and production of oil, natural gas, and geothermal energy are excluded from hazardous waste regulations under Subtitle C of RCRA. The disposal of wastes from the drilling of Class V stratigraphic test wells and Class VI carbon sequestration wells are not excluded wastes; therefore, analytical testing of the material may be required to ensure that any environmental contaminations present are below regulatory levels. If no specific beneficial onsite use can be established, the cuttings may be transported offsite to a landfill. Local and state requirements and restrictions may place restrictions on offsite use and will be investigated during site planning.

### ***2.4.2 UIC Program. (LAC 43:XVII.3603.E.1)***

Class VI wells cannot be authorized by rule to inject carbon dioxide. GCS is applying for a Class VI permit to develop Project Goose Lake.

### ***2.4.3 NPDES. (40 CFR.d.122, LAC 33: Chapter IX)***

The NPDES program requires permits for the discharge of “pollutants”, meaning dredged spoil, solid waste, incinerator residue, filter backwash, sewage, garbage, sewage sludge, munitions, chemical wastes, biological materials, radioactive materials, heat, wrecked or discarded equipment, rock, sand, cellar dirt and industrial, municipal, and agricultural waste discharged into water, from any “point source”, meaning any discernible, confined, and discrete conveyance, including but not limited to, any pipe, ditch, channel, tunnel, conduit, well, discrete fissure, container, rolling stock, concentrated animal feeding operation, landfill leachate collection system, vessel or other floating craft from which pollutants are or may be discharged. This term does not include return flows from irrigated agriculture or agricultural storm water runoff, into “waters of the United States”. Any construction activity, including grading, clearing, excavation, or other earth moving process may require an NPDES storm water permit for construction under the NPDES Storm Water Program. A NPDES permit is not required for the development of Project Goose Lake.

### ***2.4.4 PSD Program. (40 CFR 144.31(e)(6)(iv), LAC 33:III:509.A-P, LAC43:XVII.3607.B.9.d)***

The requirements of this program apply to the construction of any new major stationary source, a source that emits more than 10 tons or more per year of a single hazardous air pollutant (HAP) or 25 or more tons per year of all HAPs, or any project at an existing major stationary source in an area designated as attainment or unclassifiable under Sections 107(d)(1)(A)(ii) or (iii) of the Clean Air Act. No new major stationary source or major modification shall begin actual construction without a permit that states that the major stationary source or major modification will meet those requirements. Carbon dioxide (CO<sub>2</sub>) has been identified as a greenhouse gas and is therefore a regulated NSR pollutant under the PSD major source permitting program. A NPDES permit is not required for the development of Project Goose Lake.

## **3.0 GEOLOGY**

### **3.1 Regional Geology**

The Gulf of Mexico is a relatively small ocean basin covering an area of more than 579,000 square miles (1.5 million square kilometers) (Ocean Exploration and Research Website, 2018). It began to form via rifting during the Triassic/Jurassic period (Figure 3.1-1). Sediment input has been particularly voluminous since the start of the Paleogene and is responsible for extensive deformation of underlying salt and the resulting abundance of prolific hydrocarbon systems along the Gulf Coast of Louisiana and Texas (Foote et al., 1984). For this project, the proposed site is comprised of more than 8,000 ft of regionally extensive clastic strata. A regional geologic stratigraphic column is provided in Figure 3.1-2 and Figure 3.1-3.

The earliest record of sedimentation in the Gulf of Mexico Basin occurred during the Late Triassic to Early Jurassic period, between 160 and 140 million years ago. Repeated cycles of seawater flooding and evaporation resulted in the formation of extensive salt accumulations that locally reached thicknesses of 10,000 ft to 15,000 ft thick. Subsequent, buoyancy-driven flow created the diapirs, pillows and massifs which characterize the Gulf Coast structure today (Foote et al., 1984). At this time, the early phases of continental rifting resulted in the deposition of non-marine red bed and deltaic sediments (shale, siltstone, sandstone, and conglomerate) of the Eagle Mills Formation in a series of restricted, graben fault-block basins (Figure 3.1-4). This thick sequence of anhydrite and salt beds (Werner Anhydrite and Louann Salt) are regionally extensive across coastal Louisiana and Texas.

The deposition of the Louann Salt beds was localized within major basins that were defined by the major structural elements in the Gulf Coast Basin. The clastic Norphlet Formation (sandstones and conglomerates) overlies the Louann Salt and is more than 1,000 ft thick in Mississippi but thins westward to a sandstone and siltstone in Texas. Norphlet conglomerates were deposited in coalescing alluvial fans near Appalachian sources and grade downdip into dune and interdune sandstone deposited on a broad desert plain (Mancini et al., 1985). Although the Norphlet Formation is unfossiliferous, based on dating of the overlying and underlying sequences, the Norphlet Formation is probably late Middle Jurassic or Callovian in age (Todd and Mitchum, 1977) (Figure 3.1-2).

The depositional environment rapidly changed from continental and evaporitic to shallow marine, with localized areas of deep marine (Foote et al., 1984). Broad carbonate banks composed of limestones, dolomites, and interbedded anhydrites developed along the edges of the basin, with fine carbonate muds deposited in deeper water areas (Foote et al., 1984). Reef construction and sedimentation kept pace with regional subsidence, which allowed thick carbonate sequences to accumulate (Foote et al., 1984). These shallow-water carbonates and clastic rocks make up the Smackover, Buckner, Haynesville formations and the Cotton Valley Group, and were deposited over the Norphlet Formation from the Upper Jurassic into the Lower Cretaceous. Jurassic, non-skeletal, carbonate sands and muds accumulated on a ramp-type shelf with reefal buildups developed on subtle topographic highs (Baria et al., 1982).

A high terrigenous clastic influx in eastern Louisiana and Mississippi occurred during deposition of the Haynesville and diminished westward where the Haynesville Formation grades into the Gilmer Limestone in East Texas. The top of the Jurassic occurs within the Cotton Valley Group,

with the Knowles Limestone dated as Lower Cretaceous (Berrassian) (Todd and Mitchum, 1977). The middle Cretaceous was a period of prolonged stability, permitting the development of extensive, shelf-edge reef complexes (Baria et al., 1982).

During the Upper Cretaceous, a large tectonic uplift formed the Rocky Mountains, while the Gulf of Mexico basin subsided. Large volumes of clastic sediments from the uplift were deposited as wedges into the basin. This effectively shut off the production of carbonates, except in the Florida and Yucatan regions. Since the Cretaceous, the rate of terrigenous sediment influx has been greater than the rate of basin subsidence, resulting in significant progradation of the continental shelf margin (Figure 3.1-5).

Sediment supplies during Cenozoic time overwhelmed the general rate of subsidence, causing the margins to prograde up to 240 miles from the edges of Cretaceous carbonate banks to the current position of the continental slopes off Texas and Louisiana (Foote et al., 1984). The geometry of Cenozoic deposition in the Gulf Coast Basin was primarily controlled by the interaction of the following factors:

- Changes in the location and rates of sediment input, significantly shifting the areas of maximum sedimentation
- Changes in the relative position of sea level, developing a series of large-scale depositional cycles throughout Cenozoic time
- Diapiric intrusion of salt and shale in response to sediment loading
- Flexures and growth faults due to sediment loading and gravitational instability

Early Tertiary sediments are thickest in the Rio Grande Embayment of southern Texas, reflecting the role of the ancestral Rio Grande and Nueces Rivers as sediment sources to the Gulf of Mexico basin (Figure 3.1-6). By Oligocene time, deposition had increased to the northeast, suggesting that the ancestral Colorado, Brazos, Sabine, and Mississippi Rivers were increasing in importance. Miocene time is marked by an abrupt decrease in the amount of sediment entering the Rio Grande Embayment, with a coincident increase in the rate of sediment supply in southeast Texas, Louisiana, and Mississippi. Throughout the Pliocene and Pleistocene Epochs, the maximum depocenters of sedimentation were controlled by the Mississippi River and are located offshore of Louisiana and Texas.

Tertiary sediments accumulated to great thickness where the continental platform began to build toward the Gulf of Mexico, beyond the underlying Mesozoic shelf margin and onto transitional oceanic crust. Rapid loading of sand on water-saturated prodelta and continental slope muds resulted in contemporaneous growth faulting (Loucks et al., 1986). The effect of this syndepositional faulting was a significant expansion of the sedimentary section on the downthrown side of the faults. Sediment loading also led to salt diapirism, with its associated faulting and formation of large salt withdrawal basins (Galloway et al., 1982a).

Sediments of the Tertiary progradational wedges were deposited in continental, marginal marine, nearshore marine, shelf, and basinal environments and present a complex depositional system along the Texas Gulf Coast.

Overlying the Tertiary progradational wedges along the Texas Gulf Coast are the Pleistocene and Holocene sediments of the Quaternary Period. The voluminous infilling of the Gulf basin during Tertiary time was followed by sediment influx of similar proportions due to the profound effects

of continental Pleistocene glaciation (Foote et al., 1984). Pleistocene sedimentation occurred during a period of complex glacial activity and corresponding sea level changes. As the glaciers made their final retreat, Holocene sediments were deposited under the influence of a fluctuating, but overall rising, sea level. Quaternary sedimentation along the Louisianan Gulf Coast occurred in fluvial, marginal marine and marine environments.

### ***3.1.1 Regional Stratigraphy***

The intervals of interest at Project Goose Lake are the Oligocene and Miocene. During these epochs, four sediment-dispersal axes dominated the Gulf margin (Figure 3.1-6). The Houston and central Mississippi deltas provided a source of coarse-grained sediment for SW Louisiana and SE Texas (Swanson and Karlsen, 2009). Oligocene- and Miocene-age sediments were deposited as major progradational wedges along the margin of the Gulf Coast Tertiary basin (Houston Embayment and South Louisiana Salt Basin sub-basins) (Swanson et al., 2013). The Gulf Coastal Plain was characterized by rapid subsidence in areas of high sediment loading through multiple cyclic depositional episodes. These cycles represented various transgressive and regressive stages and were caused by variations in sediment supply and subsidence.

Major progradational wedges are typically characterized by an up-dip section of interbedded continental and marginal marine sediments underlain by a thick marine section composed of under compacted slope and basin claystone. The instability caused by the direct and rapid loading of water saturated, unconsolidated sediments resulted in the development of large scale, syndepositional, down-to-the-basin faults and intraformational deformation (Galloway et al., 1982a).

Oligocene and Miocene deposits are subdivided according to depositional cycles and paleontological zones (Foote et al., 1984 and Swanson et al., 2013) (Figure 3.1.1-1).

1. Vicksburg Group: Lower Oligocene-aged. Represents a transgressive phase (mainly shale and some sandstone lenses)
2. Frio Formation: Middle Oligocene-aged. Represents a dominantly regressive phase. (Mixture of marginal marine and deltaic sandstones and shales, with localized deep marine shales and turbidite sandstones) Downdip equivalent of the continental Catahoula Formation (Swanson et al., 2013)
3. Anahuac Formation: Upper Oligocene-aged. Represents transgression (marine shales and thin sandstones)
4. Fleming Formation: Miocene-aged. Represents a very high number of alternating regressive and transgressive phases (progradational sandstones and retrogradational shales)

#### ***3.1.1.1 Vicksburg Formation***

The Vicksburg Formation lies within the Tertiary depositional wedge of the Gulf Coastal Plain and is regionally extensive across the Texas and Louisiana Gulf Coast. Alluvial sands were funneled through broad valleys and grade seaward into deltaic sands and shales, and then into prodelta silts and clays. These sediments were deposited during periods of marine transgression, separated by thicker sections deposited during a period of regression in the early Oligocene. The shoreline advanced and retreated in response to both changes in the rates of subsidence and sediment supply. Rapid down dip thickening occurs along the syndepositional Vicksburg Flexure

fault zone, where there may be as much as a ten-fold increase in formation thickness. The Vicksburg Flexure marks the shelf margin during early Oligocene time.

In southeast Texas and western Louisiana, the early Oligocene-aged Vicksburg Formation comprises mainly shales with some interbedded sands. In the Houston Embayment and western South Louisiana Salt Basin (Figure 3.1-6), Vicksburg sediments were deposited in a series of stacked deltas through Vicksburg time (Coleman and Galloway, 1990). Productive fields in the Houston Embayment are generally separated into three distinct trends, which are notated after their associated characteristic fossil. The shallowest and furthest up-dip trend, up-dip of the Vicksburg Flexure, is identified as the *Textularia warreni* producing trend (Gregory, 1966). Sands in this trend were deposited in proximal deltaic environments in inner neritic depths. The second trend, the *Clavulina byramensis* producing trend, lies in fault blocks down-thrown to the first and second Vicksburg growth faults. These sands were deposited in an upper Vicksburg delta complex. The lower Vicksburg is primarily a prodelta front environment in this area. The third trend, the *Loxostoma B* delicate trend, lies seaward of the second trend, and occurs in deeper waters. Sands in this area were deposited in delta front or prodelta environments, preferentially located in paleotopographic lows (Coleman and Galloway, 1990).

### **3.1.1.2 Frio Formation**

The Oligocene Frio Formation is a thick sequence of mainly regressive sediments that were deposited rapidly in alluvial, lagoonal, marginal marine and deep marine environments, forming a major progradational wedge along the Gulf. Frio thickness and depth increases southwards, with localized variations occurring around salt diapirs and major faults. These trends are demonstrated in the Late Oligocene Upper Frio Formation (Injection Zone) in Figure 3.1.1.2-1 and Figure 3.1.1.2-2. Non-marine sands were deposited in constantly shifting deltas and are interbedded with marine shales that were deposited during periods of local transgression. In areas between major delta systems (e.g. Mississippi Embayment, Figure 3.1-6) shoreface and shallow marine environments deposited broad sandstone units interbedded with marine silts/shales during transgressive periods. Deposition of the progradational Frio wedge was initiated by a major global fall in sea level, with subsequent Frio sediments being deposited under the influence of a slowly rising sea (Galloway et al., 1982b).

On a regional scale, the Frio Formation and Catahoula Formation (up-dip equivalent) can be divided into a number of distinct depositional systems that are related spatially and in time. Three major progradational delta complexes, designated the Central Mississippi, Houston and Norias delta systems, identified by Galloway et al., (1982b), were centered in the South Louisiana Salt Basin, Houston Embayment and Rio Grande Embayment, respectively (Figure 3.1-6). Three fluvial systems, the ancestral Mississippi, Chita/Corrigan, the Gueydan, supplied sediment to the delta complexes.

The Houston delta system of Texas and southwestern Louisiana is centered in southern Harris County, Texas. The system is composed of several minor, laterally coalescent, and frequently shifting delta lobes (Galloway et al., 1982b). The Chita/Corrigan fluvial systems supplied sediment. Up-dip deltas exhibited wave-dominated, arcuate geometries, while lobate delta geometries characterized episodes of maximum progradation or an area where high subsidence rates were associated with salt withdrawal basins (Galloway et al., 1982b). Due to constant

switching of delta lobes, the rate of coastal progradation was slow for the Houston delta system (Galloway et al., 1982b).

A major global sea level rise occurred during the late Cretaceous, creating the Mississippi Embayment and allowing the farthest inland transgression of a shallow epicontinental sea (Vail et al., 1977). This embayment is part of the Mississippi Alluvial plain and supplied sediment to the southwestern portion of Louisiana. By Oligocene time, deposition had increased from the northeast, suggesting that the ancestral Colorado, Brazos, Sabine, and Mississippi Rivers were increasing in importance. Miocene time is marked by an abrupt decrease in the amount of sediment entering the Rio Grande Embayment, with a coincident increase in the rate of sediment supply in southeast Texas, Louisiana, and Mississippi. This continued through the Pliocene and Pleistocene epochs, with the major depocenters of sedimentation controlled by the Mississippi River and these are located offshore of Louisiana and Texas.

The Norias delta system of South Texas constitutes the main Frio Formation depocenter in the South Texas Coastal Plain. Typical sand content ranges from 25% to 40% for a total Frio Formation section that can be more than 12,000 ft thick. The lateral boundaries of the Norias delta system remained fairly fixed through time, centering on Kennedy County, Texas. Deposition of the system prograded the continental margin more than 60 miles basin ward, primarily during deposition of the lower and middle Frio Formation sections. This major off lapping episode was terminated by the shale-rich Anahuac Formation transgression, but the rate of sediment supply to the Norias system was sufficient to severely limit up-dip incursion of transgressive marine shelf facies. The Upper Frio Heterostegina-Marginulina delta complexes continued to prograde locally across the Frio platform in the face of regional onlap (Galloway, 1982b). Individual deltas of the Norias system exhibit wave-modified, lobate geometries to wave-dominated, cuspatate geometries (Galloway et al., 1982b).

Separating the delta complexes was a broad, strike-parallel barrier island/strandplain system along the south-central Texas coast called Greta/Carancahua. It comprises a linear sandstone belt, separating marine from brackish-water (back-barrier lagoon) shales. Shoreline conditions remained fairly constant during Frio Formation deposition. This, coupled with aggregational processes, developed a thick, narrow, homogenous sand section (Galloway et al., 1982b). Strike-parallel growth faults accentuated the coast-parallel geometry of the Greta/Carancahua barrier island/strandplain system. A similar but smaller barrier strandplain system (Buna) was developed by longshore currents off the eastern flank of the Houston delta system in east Texas/southwest Louisiana (Galloway et al., 1982b).

Within Louisiana the Upper Frio Formation transitions into fine-grained, mix-load dominated fluvial sediments up-dip, north of Beauregard Parish, ultimately pinching out in central Louisiana, ~80 miles north of the Project Goose Lake area. To the south (offshore Gulf of Mexico) the downdip limit of the Upper Frio Formation is defined by large-scale fault-related juxtaposition against thick, fine-grained formations in the overlying Neogene (Swanson et al., 2013). Local structural highs are the result of salt diapirism, and associated faulting, in combination with the regional structural fabric of major faults dipping dominantly southwards, parallel with the Gulf coastline.

### ***3.1.1.3 Hackberry Trend***

A transgressive, deep-water shale and sandstone unit referred to as the “Hackberry Trend” occurs in the middle to lower part of the Frio Formation and is localized to southwest Louisiana and eastern Texas (Figure 3.1-6 and Figure 3.1.1.3-1). Shales and sandstones of the Hackberry Trend pinch out to the north along the “Hartburg” flexure and formed a southward-thickening wedge (Swanson et al., 2013). The “Hartburg” flexure represents a zone of Oligocene-aged growth faulting which likely generated an area of deep marine environment.

In up-dip areas (north of Project Goose Lake area), submarine canyons up to 800 ft deep were incised through pre-Hackberry sediments (Figure 3.1.1.3-2) (Swanson et al., 2013). Here, the Hackberry Trend is characterized by thick shales punctuated by sand-rich channel-fill facies deposited in submarine canyons. Further downdip (across the Project Goose Lake area, and south), basin floor turbidite fan systems and isolated slope channel-fill sandstones typically appear encased in thick shale sequences (Swanson et al., 2013).

### ***3.1.1.4 Anahuac Formation***

As sea level continued to rise during the late Oligocene, the underlying Upper Frio Formation progradational platform flooded. Wave reworking of sediment along the encroaching shoreline produced thick, time transgressive blanket sands at the top of the Frio Formation and base of the Anahuac Formation section. The transgressive marine shale-rich Anahuac Formation deposited conformably on top of the blanket sands throughout the Texas and Louisiana coastal region. The Anahuac Formation was deposited in an inner-shelf, shallow marine, proximal deltaic, distal deltaic, and slope environments (Swanson et al., 2013). It is typically composed of calcareous, marine shales with localized, lenticular, micritic limestone units. See [REDACTED]

[REDACTED] for structure and isopach maps. In western and central parts of Louisiana (Project Goose Lake area) the interval mostly comprises shales with lesser sandstones. Limestones and calcareous clastics dominate in eastern Louisiana and the eastern Gulf of Mexico, where clastic influx was minimal (Swanson et al., 2013).

The Anahuac Formation dips towards the Gulf of Mexico and thickens regionally from its inshore margin to nearly 2,000 ft offshore (Galloway et al., 1982b) [REDACTED] In southwestern Louisiana, the Anahuac Formation reaches a thickness of more than 1,300 ft [REDACTED] An erosional unconformity marks the top of the Anahuac Formation, and the start of a regressive period in the basal Miocene interval. Local variations in gross thickness are likely the result of this unconformity combined with variable fault movement along regional faults, and around salt diapirs.

### ***3.1.1.5 Fleming Formation***

The Miocene strata of the Gulf Coastal Plain contain more transgressive-regressive cycles than any other epoch. Rainwater (1968) has interpreted the middle Miocene as a major delta-forming interval comparable to the present-day Mississippi Delta system. The middle Miocene is representative of much of the entire Miocene interval, with only the site of deposition changing in response to various transgressions and regressions. The result is a complex of interbedded shallow neritic clays; restricted marine clays, silts, sands; and deltaic deposits of sands, silts, and clays. If a composite were made of the thickest Miocene intervals around the Gulf Basin, more than 40,000

ft of accumulated sediment would be obtained, of which about 20,000 ft were deposited in southern Louisiana (Rainwater, 1968).

The Oakville Formation and the Lagarto Formation form the major units of the thick Miocene Fleming Formation that were deposited throughout the Gulf Coast region. The Miocene sediments of the Fleming Formation of Louisiana are equivalent to the Oakville and Lagarto Formations of Texas and the Catahoula, Hattiesburg, and Pascagoula Formations of Mississippi (Figure 3.1.1.5-1).

Deposition of the Fleming Formation occurred in relatively shallow water across a broad, submerged, shelf platform constructed during Frio and Anahuac deposition. Three major depositional regimes characterize the Fleming Formation. Figure 3.1.1.5-2 shows the distribution of the lower Miocene depositional systems across the Texas Coastal Plain.

A major fluvial system (Santa Cruz fluvial system) extended across South Texas and supplied sediment to the North Padre delta system (Figure 3.1.1.5-2). The Hebbronville and George West fluvial axes are interpreted as two principal depositional loci of a single major river that shifted southward through Miocene time (Galloway et al., 1982a). The high sand content and internal structures of the fluvial system indicate low-sinuosity, braided, bed-load channel deposition (Galloway et al., 1982a). The Santa Cruz fluvial system grades basinward into delta-plain deposits of the North Padre delta system. The delta system is generally coincident in geographic distribution with the underlying Oligocene Norias delta system of the Frio Formation. The North Padre delta system is characterized by sand-rich, strike-parallel, delta-margin, facies tracts typical of coastal-barrier and beach-ridge facies, characteristic of highly destructive, wave-dominated deltas (Galloway, 1985).

Along the Texas-Louisiana border, the Newton fluvial system supplied sediment to the Calcasieu delta system of southeast Texas and southwest Louisiana (Figure 3.1.1.5-2). Sands of the Newton fluvial system are fine to medium-grained, with thick, vertically, and laterally amalgamated sand lithosome geometries typical of meander belt fluvial systems (Galloway, 1985). Depositional patterns within the Oakville Formation (lower Fleming) of southeast Texas show facies assemblages typical of a delta-fringing strandplain system (Galloway, 1985). The Calcasieu delta system is best developed in southeast Texas in the Lagarto Formation of the upper Fleming. The delta system consists of stacked delta-front, coastal-barrier, and interbedded delta/shoreline sandstones that compose the main body of the delta system, with interbedded prodelta mudstones and progradational sandy sequences deposited along the distal margin of the delta (Galloway, 1985).

Along the south-central Texas Coast, flanking the two Miocene delta systems, is a broad, strike-parallel barrier island/strandplain system. The Matagorda barrier/strandplain system is cored by a prominent strike-parallel belt of sandstone, bounded both up-dip and downdip by mud rich bays and lagoons, and marine shales, respectively (Galloway, 1985). The shore-zone complex has been interpreted by Galloway (1985) and Galloway et al., (1986) to consist of a mix of microtidal barrier-island and sand-rich strandplain deposits. Where streams of the Moulton/Point Blank stream plain infilled the back-barrier bays and lagoons, fluvial channel deposits merge directly with shore-zone sands (Galloway, 1985).

### ***3.1.1.6 Pliocene-aged Formations***

Conformably overlying the Fleming Formation is the Pliocene-aged Goliad Formation. The sedimentary sequence of the Goliad Formation is similar in character to underlying Upper Miocene units, having been deposited in a fluvial, deltaic, and marginal marine setting. The section thickens gradually to the south and is approximately 700 to 750 ft thick at the Project Goose Lake site where it is composed of interbedded fluvial and deltaic sandstones plus local minor conglomerates. Sandstones of the Goliad Formation are the lowermost units containing fresh to slightly saline water, and form the upper Evangeline aquifer in Harris County, Texas (Wesselman and Aronow, 1971). However, at the Project Goose Lake site, the Goliad is significantly deeper than the base of the defined lowermost USDW.

### ***3.1.1.7 Pleistocene-aged Formations***

Lying conformably above the Goliad are the Pleistocene-aged sediments of the Willis Formation that were deposited under the influence of the complex glacial and interglacial climatic sea level changes of the Pleistocene. The Willis Formation was deposited in both fluvial and deltaic environments and thickens in a southeastward dip direction as well as southwest along strike toward the southwest. Pleistocene sediments thicken along the Texas/Louisiana border and in a dip direction where there was significant deposition along growth faults during Pleistocene sea level lowstands (Wesselman and Aronow, 1971). Willis Formation sediments grade conformably into the overlying Holocene depositional units. Pleistocene and Holocene units contain fresh water and comprise the Chicot aquifer.

### ***3.1.1.8 Holocene-aged Formation***

With the retreat of the Pleistocene glaciers, sea level began a final irregular rise to its present-day level. As sea level rose, the lower reaches of coastal plain river valleys slowly filled with brackish-to-marine water and subsequently began filling with fluvial sediments. In southeastern Louisiana and eastern Texas, Holocene sediments were deposited in river valley meander belts and are primarily composed of point bar sandstones with interbedded, fine-grained over bank deposits.

The slow rise of the Holocene sea level marked the beginning of the recent geologic processes that have created the present Louisiana/Texas coastal zone. During recent times, sediment compaction, slow basin subsidence, and minor glacial fluctuations have resulted in insignificant relative sea level changes. The coastal zone in southwest Louisiana/southeast Texas has evolved to its present condition through the continuing processes of erosion, deposition, compaction, and subsidence periods. Recent alluvial deposition in the area is restricted to the geomorphic flood plain of the present-day San Jacinto River system and to the entrenched valleys of the ancestral San Jacinto River system, which had down-cut into the underlying Pleistocene deposits during sea level lowstands (Wesselman and Aronow, 1971).

## ***3.1.2 Regional Structural Geology***

The Gulf of Mexico continental margins and deep ocean basin regions are relatively stable areas (Foote et al., 1984). The area is characterized by structural dip towards the Gulf, with frequent Miocene/Oligocene interval normal and growth faults aligned parallel to the contemporaneous shelf edge, stair-stepping down towards the Gulf (Figures 3.1.2-1 and 3.1.2-2). Tectonism driven

in large part by sediment loading and gravity has played a key role in contemporaneous and post-depositional deformation of Tertiary strata (Foote et al., 1984). Deeper fault zones are present at basement level, mirroring the trend of the shallower Oligocene-level faults, but do not appear to be directly linked.

Salt mobilization led to extensive diapirism across the Louisiana and Texas Gulf Coast. This remobilized salt, originating from the deep Louann Salt Formation, may be present in a number of geometrical forms, including diapirs and pillows. In the region of the Project Goose Lake site, salt features typically occur as diapirs, or “salt domes.” Such diapirs buoyantly moved upwards through many thousands of feet of younger strata concurrently with sedimentation during the Oligocene and Miocene. An example can be seen at the Vinton Dome, northwest of the Project Goose Lake site (Figures 3.1.1.2-2 and 3.1.2-3). Regional salt features may be deep-rooted and extend vertically for several thousands of feet or may have been totally severed from its deeper source.

Associated faulting is caused either in response to local salt mobilization or evacuation, or on a larger scale where significant volumes of strata have been transported on listric fault surfaces which likely detach along deeper shales and/or salt intervals. Faulting induced by salt evacuation commonly causes an expanded sedimentary section on the downthrown side of the fault (growth fault), usually either down-to-the-coast or down-to-the-basin. Faulting associated with salt movement in the Project Goose Lake site area includes local radial faulting emanating from Vinton Dome.

A second cause of faulting most common to the Texas/Louisiana Gulf Coast is the cause-and-effect relationship between rapid progradation of sediments and slope failure in the vicinity of the shelf edge or outer platform margin. Sediment accumulated in a series of wedges that thicken and dip gulfward. As a result of rapid progradation and sediment loading, large growth-fault systems formed near the downdip edge of each sediment wedge within the area of maximum deposition. Faulting typically aligned parallel with the contemporary shelf edges in the Gulf Coast region. The greatest displacement of faults and thickest accumulations of Oligocene and Miocene sediments occurred in an area known as the Frio Expanded Zone (Figures 3.1.2-1 and 3.1.2-2).

[REDACTED] demonstrate regional structural trends of the Upper Frio and Anahuac formations. Depth increases significantly from north to south and is likely linked to frequent normal and growth faults striking perpendicular to dip, detaching along deep shale or salt intervals. Such faults are only resolvable with 3D seismic data and appear as noise in lower resolution structural maps generated from regional well data. Localized structural highs are commonly associated with salt diapirism. Within the broad structural regime, synclines may result from the interplay of major regional faults with salt domes and the associated counter-regional faulting.

[REDACTED] demonstrate the significant increase in Oligocene strata thickness observed as the “Frio Stable Shelf Fault Zone” (north Orange County and Central Calcasieu) trends southeastwards into the “Frio Expanded Fault Zone” (Figures 3.1.2-1 and 3.1.2-2) (Swanson et al., 2013). While no major growth faulting is observed in the Project Goose Lake 3D seismic dataset, it is believed that regionally, Oligocene sediments greatly expanded and filled vast amounts of accommodation space created by movement along growth faults within the “Frio Expanded Fault Zone” (Swanson et al., 2013).

The shallower Oligocene-Holocene section thickens basinward, periodically interrupted by low-relief, broad salt domes and anticlines. Some minor fault displacement occurs as well, particularly where the system overlies deep-seated Eocene or Oligocene growth-fault trends (Galloway et al., 1982a). Structural modification is greatest where the Cenozoic sedimentary section is warped upwards along the margins of salt diapers.

### **3.1.3 Regional Cross Sections**

[REDACTED] shows the locations of two regional cross sections, in structural format, hung on TVDSS (true vertical depth sub-sea) [REDACTED]. The cross sections run approximately parallel to strike (E-W) and parallel to dip (N-S) and comprise a selection of the most data-rich wells that form the basis of the geological evaluation. All available well logs are shown for each well. Where a scan of the original field log (raster log) is available, it is displayed. When unavailable, digital logs (LAS logs) are displayed. Formation tops and all logs have been made available in [REDACTED]. Predicted formation depths are displayed as dashed lines when log coverage is insufficient.

The following geological intervals are defined where wells have sufficient well log coverage:

1. USDW Interval (underground source of drinking water)
  - a. Base lowermost USDW mapped using a 2-ohm cutoff on resistivity logs (deep resistivity preferred). See Section 3.4.2 Determination of the Lowermost Base of the USDW for detailed explanation.
2. Miocene Interval (secondary Confining Zone)
  - a. Mapped as an interval of high frequency alternations between low and high SP, GR and resistivity log values. Interpreted as alternating sand-silt-shale beds linked to a long period of frequent shoreline transgressions and regressions during the Miocene epoch.
3. Anahuac Formation (Confining Zone)
  - a. Mapped as an interval of sustained/relatively uniform high values in spontaneous potential (SP), gamma ray (GR) and resistivity logs. Indicative of a dominantly shale-rich interval with only minor sandy sections, primarily at the base of the formation (regional continuity of sandy sections unclear from log data).
  - b. Top formation marked by a sharp drop in log values and an increase in log variability (serrated log character); indicative of a regional unconformity related to a drop in sea level and a transition to a period of frequent transgression and regressions.
4. Upper Frio Formation (Injection Zone)
  - a. Mapped as an interval with frequent fluctuations between high and low SP, GR and resistivity logs.
  - b. Intervals of low resistivity, gamma ray and spontaneous potential are interpreted to be sand-rich units. Interval thickness is very variable and may be up to 100 ft thick or less than 5 ft.

- c. Intervals of higher resistivity, gamma ray and spontaneous potential are interpreted to be shale-rich units.
- d. Transition between sand-rich and shale-rich intervals may be sharp, creating blocky log character, gradual, with fining or coarsening upwards trends, or a combination of all.
- e. Top formation marked variably by a sharp or gradational increase in SP, GR and resistivity and a transition to more uniform log character.

5. Middle Frio Formation (Hackberry Trend at Project Goose Lake)

- a. Mapped as an interval of uniform log character punctuated by sporadic, relatively infrequent deviations in log values.
- b. Top formation is typically defined by an increase in SP log values and an increase and a reduction in the variability of SP and resistivity.
- c. Overall log character varies depending on proximity to the paleo-shoreline and intersection of deep marine channel/turbidite sandstones and basin floor fan complexes.
- d. Across the Project Goose Lake area and up-dip (proximal), the Middle Frio interval typically appears uniform in log character, with infrequent deviations, interpreted as shale-dominated strata punctuated by isolated submarine channel/turbidite sandstones. Correlation of sand-rich intervals is generally not possible with the density of data available.
- e. Distal areas, downdip of Project Goose Lake, may exhibit very variable, serrated log curves, or similar character to that described above. Variability may be linked to sampling of sandy basin floor turbidite fan complexes.

### 3.1.3.1 East-West Cross Section

[REDACTED] provides a regional strike-line view through the Project Goose Lake area, from the west to east:

1. The Injection and Confining zones are demonstrably regionally continuous from west to east of the Project Goose Lake area
2. Relatively uniform log character in each defined interval along strike. Depositional environment interpreted to vary most strongly north-south

### 3.1.3.2 North-South Cross Section

[REDACTED] provides a regional dipline view through the Project Goose Lake area, from the north (proximal/continental platform) to the south (distal/Gulf of Mexico Basin):

- The Injection and Confining zones are demonstrably regionally continuous from north to south of the Project Goose Lake area.
- [REDACTED]



### ***3.1.4 Regional Groundwater Flow in the Injection Zone***

The Project Goose Lake site is located within the Gulf Coast basin in southwestern Calcasieu Parish and northwestern Cameron Parish. It is located on the floodplain of the Sabine River (west of the site) and at the seaward margin of the Gulf Coastal plain physiographic province. Sedimentary strata of the Gulf Coast basin consist of poorly lithified units which strike nearly parallel to the coast and thicken to the south. Hydrostratigraphic units of importance range in age from Miocene to recent and include in ascending order:

- Fleming Formation
- Goliad
- Willis
- Lissie (subdivided into the Montgomery and Bentley formations)
- Beaumont
- Holocene/Recent sediments

Within this stratigraphic section are the two main aquifers of the area, the Chicot and the Evangeline.

The Lower Miocene-aged Fleming Formation is the deepest unit in the ground water section and consists of pro-delta mudstones and deltaic sandstones. The clay-rich section of the Fleming Formation is known as the Burkeville aquiclude, which is the confining layer that separates the Evangeline aquifer from the Jasper aquifer.

The Pliocene-aged Goliad Formation conformably overlies marine sediments of the Fleming Formation, and together, they form the Evangeline aquifer. Sediments of the Goliad Formation are predominately fluvial-deltaic sands, marginal marine sands and occasional conglomerates, with a total thickness in this area of approximately 700 ft.

Lying conformably above the Goliad are Pleistocene sediments of the Willis, Lissie, and Beaumont units which are associated with the Chicot aquifer. These deposits reflect the complex glacial and interglacial climatic and sea level changes of the period. The Willis Formation contains both fluvial and deltaic sediments, whereas the overlying Lissie Formation is primarily fluvial. The younger Beaumont Formation is geologically similar to the Lissie Formation and is less than 100 ft thick in the area. Combined thickness of the Pleistocene formations in the vicinity of the Project Goose Lake site is approximately 1,100 ft, which coincides with the base of the USDW (the deepest occurrence of ground water having less than 10,000 mg/l total dissolved solids).

At the top of the stratigraphic section are Holocene deposits that mark glacial retreat and a corresponding rise in sea level. In the local area, Holocene sediments consist of meander belt point bar sandstones and interbedded finer-grained overbank deposits, coastal marsh, mud flat, and beach deposits. At the Project Goose Lake site, Holocene alluvial sediments are composed of basal coarse-grained sand and gravel, which grade upward into finer-grained sandstones, siltstones, and clays with a total thickness of approximately 50 ft. The combined Pleistocene-Holocene section comprises the Chicot aquifer. A detailed discussion on regional and local hydrogeology is contained in Section 3.4.

The Injection Zone at the Project Goose Lake site lies within the deeper saline sands of the Upper Frio Formation, below the Miocene-aged Jasper aquifer. The saline waters in the Injection Zone flow down-dip, towards the Gulf of Mexico.

#### ***3.1.4.1 Frio Formation Fluid Background Velocity***

Many of the studies for flow rates in deep saline aquifers come from the search for nuclear waste isolation sites. These studies show sluggish circulation to nearly static conditions in the deep subsurface (Bethke et al., 1988). Flow rates in the deep saline aquifers (Clark, 1988), were found generally to be in the order of inches per year. A south-southeastern (down-dip) direction of regional flow established for the Upper Frio Formation is consistent with the theory of deep basin flows and the physical mechanisms (topographic relief near outcrops and deep basin compaction) identified as contributing to natural formation drift (Bethke et al., 1988; Clark, 1988; Kreitler, 1986).



### **3.2 Local Geology of the Project Goose Lake Site**

A structural and stratigraphic picture of the geology beneath proposed Project Goose Lake site has been developed from a series of structure and stratigraphic maps and cross sections prepared from the available well control in the area (including offset Class I Plant Wells and oil and gas exploration/production wells). The analysis of regional and local geology near the proposed project site demonstrates that the subsurface is geologically ideal for injection. The massive sandstones of the Oligocene-aged Upper Frio Formation provide effective injection reservoirs in terms of their lateral extent, mineralogical composition, and petrophysical characteristics.

Initial studies show that the Injection Zone (Upper Frio Formation) has the permeability, porosity, thickness, and lateral continuity to accept and contain waste. Shales of the overlying Anahuac Formation possess the necessary Confining Zone criteria to be effective barriers to upward movement of CO<sub>2</sub>. Effective secondary sealing is provided by a shale-rich Miocene interval (Figure 3.2-1).

Figure 3.2-5 provides a schematic cross section view of the total system. Significant separation exists between the top of the Anahuac Formation (Confining Zone) and the base of the lowermost USDW, as illustrated by isopach maps.

The following sections provide a detailed assessment of the local geology as it pertains to the Project Goose Lake site.

#### ***3.2.1 Local Stratigraphy***

Analysis of the regional and local geology near Project Goose Lake demonstrates that the subsurface system is geologically ideal for injection. The stratigraphy of interest is as follows (See Figure 3.2.1-1):

- Injection Zone: Upper Frio Formation (Late Oligocene)
- Confining Zone: Anahuac Formation (End Oligocene)
- Secondary Confining Zone: Miocene interval
- Base of the Lowermost USDW: Quaternary interval (glacial sediments and regional potable water aquifers)

Correlations of the major stratigraphic intervals for the proposed Project Goose Lake site have been developed using all available well logs for 1,000+ wells within a 20-mile radius of the Area of Review (AoR), referred to as the “study area”. Two cross sections are provided as part of this report to illustrate the detailed stratigraphy within the AoR. Locations of these cross sections can be found on [REDACTED]. Lateral extent of the maximum AoR, final stable plume, major faults mapped on 3D seismic data and proposed injection well sites are included in the following figures for context:



Logs utilized in the cross-section interpretations are contained in APPDX B - AoR Data.

### ***3.2.2 Description of the Confining Zone and Injection Zone***

In this Class VI application request, the Confining Zones, Injection Zone, and injection intervals have been designated. Each is described in the following sub-sections.

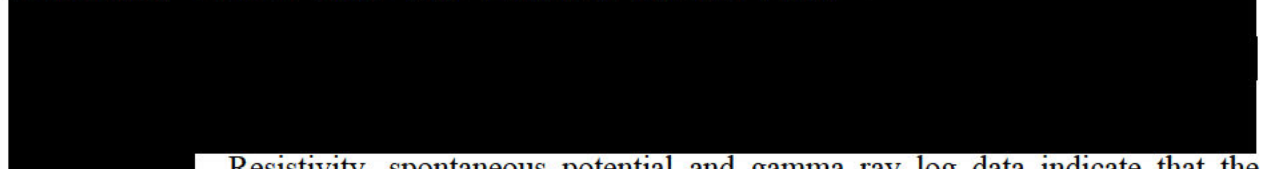
The massive sandstones of the Oligocene-aged Upper Frio Formation provide effective injection reservoirs in terms of their lateral extent, mineralogical composition, and petrophysical characteristics. Detailed studies show that the Injection Zone has the permeability, porosity, thickness, and lateral continuity to accept and contain waste. Shales of the overlying Anahuac Formation possess the necessary confining zone criteria to be effective barriers to upward movement of CO<sub>2</sub>. Additionally, more than 7,000 ft of overlying, shale-rich Miocene section provides a secondary Confining Zone unit. The following sections detail the regulatory zones at the Project Goose Lake site.

#### ***3.2.2.1 Confining Zone***

A Confining Zone is defined as a zone that separates the injected wastes within the Injection Zone from the overlying groundwater zones. In accordance with the Environmental Protection Agency (EPA) 40 CFR §148.21(b) standard, the Confining Zone is a laterally extensive and sufficiently low in permeability and porosity layer, which restricts the vertical flow of injectate. Within the Project Goose Lake study area, there are two identified confining zones; a primary and a secondary. These two Confining Zones meet the EPA Standards and restrict the vertical flow of injectate within the designated Injection Zone.

##### ***3.2.2.1.1 Confining Zone – Anahuac Formation***

The Confining Zone is defined as corresponding to the shale-rich Anahuac Formation, which conformably overlies Upper Frio Formation Injection Zone.



Resistivity, spontaneous potential and gamma ray log data indicate that the Anahuac Formation has high shale content both regionally and within the AoR. Additionally, the Anahuac Formation acts as a very effective, thick regional seal to many prolific hydrocarbon fields and so can be assumed to be rich in sealing lithologies.



An important conclusion in this study is that the sluggish circulation within the deep saline aquifers “demonstrates that geological confinement is effective on both a local and regional scale.”

Porosities for the Anahuac Formation (Confining Zone) for the Project Goose Lake site were determined using correlations developed for Gulf Coast shales as presented in Porter and Newsom, 1987 (see Table 3.2.2.1.1-3).

The “effective” shale porosity, which discounts the bound water within the clay structure as well as water contained in dead-end pores, represents an appropriate choice of a porosity value for such a calculation. At the depths of interest, an effective clay/shale layer porosity is based upon Table 3.2.2.1.1-3 (Porter and Newsom, 1987).

Rock compressibility's were estimated by combining data from taken from (Zheng et al., 2019), (Zimmerman, 1990), and (Yale, 1993).

### *3.2.2.1.2 Secondary Confining Zone – Miocene Overburden*

Interbedded sand units within the secondary Confining Zone provide an additional level of safety as buffer aquifers that could capture and retain any fluids that might migrate vertically through an undetected potential breach in the Injection Zone (Upper Frio Formation) and the Confining Zone (Anahuac Formation). [REDACTED] demonstrate the continuity of the Miocene interval across the AoR.

### *3.2.2.1.3 Lower Confining Zone*

### *3.2.2.2 Injection Zone – Upper Frio Formation*



Log data within the Injection Zone indicate individual or stacked sand-rich beds alternating with shale-rich intervals and/or siltstones [REDACTED]

1. Sand-rich intervals

- a. Interpreted as a negative deflection in spontaneous potential, resistivity, and gamma ray log values
- b. Multiple feet to >100 ft thick
- c. May appear as individual beds or amalgamated/stacked
- d. Variably sharp or gradational upper- and lower-unit boundaries give log curves a blocky or serrated character
- e. May be correlated laterally at the scale of the AoR and are therefore interpreted to be laterally extensive shoreface sandstones

2. Fine grained/shale-rich intervals

- a. Interpreted as a positive deflection in spontaneous potential, resistivity, and gamma ray log values
- b. Multiple feet to hundreds of feet thick

This interpretation conforms with published analysis of Oligocene Gulf Coast depositional environments. The upper Oligocene Frio Formation is described as a thick sequence of mainly regressive sand-rich sediments interbedded with silts/shales, deposited rapidly in alluvial, lagoonal, marginal marine and deep marine environments, forming a major progradational wedge along the Gulf (Swanson et al., 2013).

Sand-rich beds can be correlated across the AoR, are considered to be pay intervals and are likely to have very good lateral communication and variable vertical communication through intra-Frio shales/siltstones.

Core data is available from [REDACTED]

[REDACTED]

Site-specific data will be collected in pre-operational data testing prior to commencement of injection to verify this data.

[REDACTED]

### ***3.2.2.3 Lateral Extent of the Confining and Injection Zones***

The Injection Zone (Upper Frio Formation) and the Confining Zone (Anahuac Formation) are both regionally extensive along Gulf Coast Texas and Louisiana. Figure 3.2.2.3-1 illustrates the combined gross thickness and mappable large-scale extent (Swanson et al., 2013). Figures 3.1.1.2-1, 3.1.1.4-1, 3.1.3-2, and 3.1.3-3 demonstrate the regional continuity of both zones across the Project Goose Lake area of interest. Within the 30 yr. AoR the base lowermost USDW, top Confining Zone and top/base Injection Zone are clear, consistent picks in the available well log data. Both zones are represented by and mapped on well-defined seismic reflectors in 3D seismic data [REDACTED] The Injection and Confining Zones are demonstrably laterally extensive, exhibiting no evidence of pinchout of sand-rich intervals within main AoR.

[REDACTED]

[REDACTED]

[REDACTED]

[REDACTED]

[REDACTED]

[REDACTED]

[REDACTED]

### ***3.2.3 Local Structure***

Project Goose Lake takes advantage of a broad monocline of [REDACTED]

[REDACTED]

Project Goose Lake benefits from the following trapping mechanisms (described in full detail in Section 3.2.7 Trapping mechanisms):

- Buoyancy trapping against the Anahuac Formation
- Relative permeability hysteresis
- Dissolution of gaseous phase CO<sub>2</sub> into the formation's aqueous phase
- Localized buoyancy trapping within 4-way closures, where they may exist

All major faults intersecting the Injection and Confining Zones, within the AoR, have been fully mapped using 3D seismic data [REDACTED]. Detailed fault analysis has been completed to determine key fault characteristics and assess vertical and lateral transmissibility with respect to CO<sub>2</sub> and pressure. Full details are provided below, in Section 3.2.3 Fault Transmissivity.

The following section details the local faulting and structures at the proposed Project Goose Lake site.

### ***3.2.3.1 Description of Faulting***

The predominant direction of faulting in the area is parallel to the edge of the Gulf of Mexico basin. It is a result of the deposition of large quantities of sand and mud along the margins of the Gulf of Mexico. As a result of rapid sediment loading, large growth-fault systems formed near the downdip edge of each sediment wedge within the area of maximum deposition. Previous research suggests that deeper, thick Jurassic salt was mobilized by the weight of the overburden into a series of ridges and troughs (Swanson, et al., 2013). This growth faulting and rapid subsidence of Cenozoic shelf margins in the NW Gulf of Mexico is also related to large-scale, deep-seated gravity sliding of the continental slope (Swanson, et al., 2013). [REDACTED]

High quality 3D seismic data is available across the entire injection area, which facilitates detailed structural interpretation and seismic horizon mapping throughout the AoR and beyond [REDACTED]

[REDACTED] As part of the evaluation workflow, all faults within the AoR have been mapped where 3D seismic is available. [REDACTED] provide a map view of all faults at Frio and Anahuac Formation depths. Faults located away from salt domes tend to have strikes between 70 and 90 degrees, however, radial faults around salt domes have a wide variation in strikes due to the complex structural regime associated with diapiric salt structures.

Faults within the AoR are not sufficiently transmissive to allow migration of fluid vertically from the Injection Zone. Because the very thick section of ductile shale and sands beneath the Project Goose Lake at the depths of interest, the juxtaposition of shale beds or sand-to-shale beds across a fault will form a vertical barrier (seal) to fluid flow due of their very low vertical permeability. A further vertical permeability barrier between the Injection and Confining Zone and the USDW is achieved by thousands of feet of fault seal along the fault plane itself. Significant shale gouge and

shale smear along the fault plane has been calculated as part of the BEG fault study and provides ample seal to the potential vertical migration pathway. This is further supported by the existence of a working petroleum system in the region that relies heavily on fault seals over millions to years to prevent the upward migration of hydrocarbons.

[REDACTED]

### 3.2.3.2 [REDACTED]

[REDACTED]

### 3.2.3.3 [REDACTED]

[REDACTED]

The dome resulted from the upward movement of deep, mid Jurassic salt through many thousands of feet of younger strata.

[REDACTED]

There is evidence of sediment dispersal patterns being diverted around salt-related seafloor topography during deposition. Additionally, post-depositional movement resulted in erosional surfaces, steepening of bedding dip near the salt column and the creation of many complex fault blocks. The cumulative result is that the Injection Zone thins and/or pinches out along the dome flanks and is completely absent over the crest.

[REDACTED]

[REDACTED]

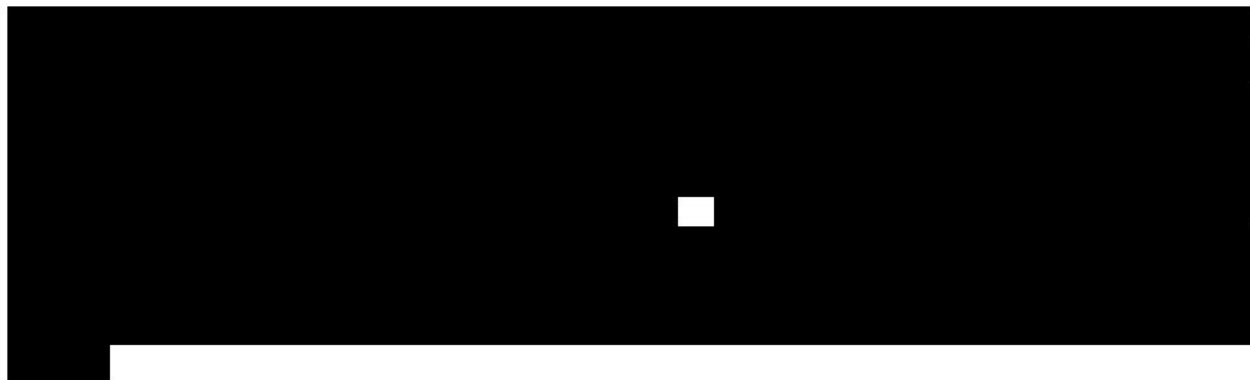
### 3.2.4 *Fault Transmissivity*

Faults within the area are not sufficiently transmissive to allow migration of material from the Injection Zone. The transmissivity of fluids across a fault must be considered with respect to both lateral (horizontal) and vertical components, requiring an assessment of the likelihood of a sealing

surface (top seal and/or lateral seal) being present. Faults, in and of themselves, do not seal (Downey, 1984). However, faults can place porous intervals against seals and form non-transmissive barriers (traps). Additionally, materials entrained within the fault zone can also provide a seal (*i.e.*, clay smear). In a sand-shale geologic sequence, faulting will result in the juxtaposition of like and/or unlike lithology across the fault plane in three manners:

1. Sand-to-sand
2. Sand-to-shale
3. Shale-to-shale

Fault planes are normally considered to be inconsequential to migrating fluids, and generally are of significance as sealing surfaces only because they may juxtapose rocks of differing capillary properties and fluid pressures (Downey, 1984; Smith, 1966). Each fault case, based on the juxtaposition of lithologies across the fault, must be considered during an assessment for both lateral and vertical transmissivity.



#### ***3.2.4.1 Vertical Fault Transmissivity***

This property of viscoelastic deformation behavior will cause any fractures and/or faults to close very rapidly in response to the in-situ compressive stresses, like squeezing into the fault plane from both sides. This well-known ductile (or plastic) behavior of the geologically young Gulf Coast shales is amply demonstrated by the presence of shale diapir structures and the natural closure of uncased boreholes with time (Johnston and Greene, 1979; Gray et al., 1980; Davis, 1986; Clark et al., 1987; Warner and Syed, 1986; and Warner, 1988). Jones and Haimson (1986) have found that due to the very plastic nature of Gulf Coast shales, faults will seal across shale-to-shale contacts, allowing no vertical fluid movement along the fault plane.

The Miocene strata in this area is saline, therefore, the Miocene can be considered to perform as an additional barrier to vertical fluid migration as well as allowing for pressure dissipation and as a monitoring zone to assure that no fluids are migrating though the Anahuac Formation.

In 1991, the DuPont Sabine River Works Plant (now known as the INV – Orange Site located approximately 17 miles west of the study area) conducted a borehole closure test at the Orange Dome field. This closure test demonstrated the plastic nature of the Gulf Coast shales and the rapidity of shale movement to seal off open areas in the subsurface. The test conclusively

demonstrated that the young Miocene shales of the Gulf Coast will flow and seal off an open area in the subsurface in a very short time period (test duration was approximately one week) (Clark et al., 1991).

The vertical sealing nature of shale-to-shale juxtaposed lithologies can be seen in the numerous Gulf Coast oil and gas fields that have fault traps where both the top and the lateral seals are provided by shale beds.

Smith (1980) presents a mechanism whereby shale may be emplaced along the fault plane to provide an effective seal against vertical fluid movement (Figure 3.2.4.1-1). Shale can be deformed more readily prior to failure than sandstone in a sand-shale sequence. Continued deformation will eventually fault the shales, however, a zone of deformed shale may become-greatly attenuated and trapped along the plane of the fault, resulting in a vertical seal.

Therefore, the only mechanism available for vertical movement up along a fault is through "stair-stepping", whereby the fluid potentially moves laterally across juxtaposed sand-to-sand beds. However, at Project Goose Lake site, the preponderance of shale within the confining intervals

Criteria can be developed to determine which faults in the vicinity of the site are potentially vertically transmissive or are sealed based on the juxtaposition of lithologies across the fault:

- 1) Juxtaposed shales present in the geologic section have a ductile nature and are likely to have squeezed in from both sides of the fault plane, sealing the fault to fluid movement. The juxtaposition of shale across from a sand bed would also seal the fault to fluid movement. This characteristic of Gulf Coast shales to seal open spaces in the subsurface is a well-known and documented phenomenon.
- 2) Where the geologic section is predominately sand, upward fluid movement may take place and would be expected to dissipate through "stair-stepping" into the overlying, juxtaposed sand units, similar to the oil migration in the Niger Delta (Weber and Daukoru, 1975). Were the CO<sub>2</sub> to migrate up through the injection interval and cross the fault, the CO<sub>2</sub> would still be in the Injection Zone on the other side of the fault.

The overlying geologic section of predominately shales (present in the section between the lower Miocene-aged Fleming Formation and the Upper Frio Injection Interval), which provide extensive shale to shale contacts along the fault plane, will prevent CO<sub>2</sub> migration out of the Injection Zone.

### ***3.2.4.2 Lateral Fault Transmissivity***

Lateral fault seal can arise from juxtaposition of porous and permeable reservoir rock against nonporous or no permeable rock, or by the development of fault rock having a high entry pressure. While faults may not act as seals themselves (Downey, 1984), they can place porous intervals against seals that form non transmissive barriers (traps). Fault planes are normally inconsequential to migrating fluids, and generally are of significance only in the circumstance of shallow, near-surface faulting in an overall tensional regional stress environment. In such cases, field

observations and theory (see Secor, 1965, for example) show that the fault plane may act as an open transmissive fracture. However, the process of faulting may result in a "disturbed" fault zone between the offset lithologies. Therefore, a two-tiered analysis approach may be required. First-order fault seal analysis involves identifying reservoir juxtaposition areas over the fault surface using mapping techniques. Second-order fault seal analysis ascertains whether the reservoir-to-reservoir contact is likely to support a pressure difference. Several mechanisms have been recognized whereby fault planes can act as seals (Knipe, 1992):

- a) Juxtaposition, in which reservoir rock are juxtaposed against a low-permeability unit with a high entry pressure
- b) Clay smear or entrainment of clay/shale into the fault plane, thereby giving the fault "disturbed zone" a high entry pressure
- c) Cataclasis, which is the crushing of sand grains to produce a fault gouge of finer grained material, giving the fault "disturbed zone" a high capillary pressure
- d) Diagenesis, where preferential cementation along a previously permeable fault plane may partially or completely remove porosity, creating a hydraulic seal

Juxtaposition seals can be recognized by mapping the contact of the various units across a fault. To identify or predict sealing via clay smear, cataclasis, or diagenesis requires an ability to relate these mechanisms to measurable properties or processes in the subsurface. The initial host rock is an important control on the fault disturbed zone material and properties, and thus, on seals. The host-rock properties that exert the most influence are the clay or phyllosilicate content, porosity, and permeability (Knipe, 1997).

Each of the sealing mechanisms is described in the following subsections. Note that none of the attributes described is, in itself, a measure of the sealing capacity of the fault surface. Instead, these attributes are an estimate of the sealing nature or relative likelihood of a seal being developed along a fault surface. To be useful they must be calibrated from known seal and non-seal situations.

#### **3.2.4.2.1 Connectivity of Juxtaposed Lithologies**

The initial consideration in the evaluation of lateral transmissivity across a fault is the determination of juxtaposition of porous lithologies across a fault and the connectivity of the juxtaposed porous lithologies. In a sand-shale geologic sequence, such as those beneath the Project Goose Lake site, faulting will result in the juxtaposition of like and/or unlike lithologies across the fault plane in three manners: a) sand-to-sand, b) sand-to-shale, and c) shale-to-shale. Each fault case must be assessed separately for the lateral transmissivity of the juxtaposition of lithologies across the fault. In the case of a sand and shale sequence, the connectivity considers that fraction of net sand that is in geometric contact with sand across the fault. The lower the connectivity, the more likely the fault will tend to act as a seal and, therefore, the greater the effect of the fault on impeding fluid flow, resulting in increased pressure buildup. The determination of the percentage of connectivity requires an accurate depiction of the stratigraphy on both sides of the fault for its entire length. For complex situations, a fault-plane section (a display of the geometry of the stratigraphy brought into contact by fault displacement, i.e., two sides of a fault juxtaposed) can be prepared to show relationships (Allan, 1989). The plane of the Allan Section is not vertical, but dips along the plane of the fault. Alternatively, a "juxtaposition diagram" (Knipe, 1997) can

be constructed from the stratigraphy on either side of the fault to evaluate lithological cross-contacts. High sand-to-sand connectivity at the fault plane will have minimal impact on the lateral transmissivity of the reservoir.

Fault planes are normally inconsequential to migrating fluids, and generally are of significance as sealing surfaces only because they may juxtapose rocks of differing capillary properties and fluid pressures (Smith, 1966, and Downey, 1984). Much of the knowledge base for characterizing fault seal/non-seal emanates from studies in oil fields, which deal with unlike fluid phases (oil-water) juxtaposed across a fault. In these examples, where porous intervals are juxtaposed, significant additional pressure (displacement pressure) may be needed to overcome capillary properties and force hydrocarbon molecules into connate water-filled pore spaces through and across a fault that would otherwise be transmissive to like-phase fluids (Smith, 1966). The forces that need to be overcome include the hydrocarbon-water interfacial tension and wettability of the reservoir rock, prior to initiation of hydrocarbon fluid flow. The discounting of the existence of the pressure differential effect due to differing capillary properties has probably influenced field study conclusions where there are insufficient data to recognize this phenomenon as the cause for sealing.

### **3.2.4.2.2 Clay Smear**

In cases where thick, under-compacted clay shales are interspersed between porous intervals, clay smears can develop and be emplaced along a fault plane (Smith, 1980). Under-compacted clays can be deformed much more readily prior to failure than sandstone can in a sand-clay sequence. Continued deformation will eventually fault the clay/shales; however, a zone of deformed clay/shale may become greatly attenuated and trapped along the plane of the fault, resulting in a vertical and horizontal seal. Such fault-plane clay smears are common small-scale features and have been reported in East Texas outcrops (Smith, 1980), coal mines in Germany (Weber, 1978), and have been inferred from log interpretation of fault zones (Weber, 1978, Berg and Haveman, 1995). Conclusions from faulting case histories indicate that the fault-zone clay/shale thickness and petrophysical properties of the clay/shale, in the displaced section at the time of faulting, are the primary factors that govern whether or not a clay/shale will "smear" and form boundary fault-zone material for sealing. Lehner and Pilaar (1991) observed from fault outcrops that clay smear, as an effective sealing mechanism, is likely to occur only in soft sediments and at sufficiently slow fault slip velocities. Smith (1980) found that growth faults, which form relatively near the surface contemporaneously with deposition (*i.e.*, syndepositional faults), have a greater potential to be sealing due to clay smear than post-depositional faults, forming when sediments are more indurated. Harding and Tuminas (1989) and Jev et al., (1993) also concluded that syndepositional faulting usually favors clay smear sealing because the muds are generally uncompactated at the time of displacement and are more likely to smear along the fault plane. However, even in cases of initial fault seal, fault plane seal breakdown may occur along weak areas, as the result of increased pressure differentials (resulting from production or injection) from one side of the fault to the other (Bouvier et al., 1989).

The following factors have been found to control the likelihood of clay/shale smearing:

1. Thicker source beds can produce thicker clay smears
2. Shear-type smears decrease in thickness with increasing distance from the source layer
3. Abrasion-type smears decrease in thickness with increasing fault throw

#### 4. Multiple source beds can give a combined continuous smear (Yielding et al., 1997)

Several algorithms have been proposed for providing a quantitative approach to clay smear prediction. Bouvier et al., (1989) presents a study of the Nun River field in the Niger Delta, describing the “Clay Smear Potential” as a means of estimating the likelihood of clay smearing in areas of sand-to-sand juxtaposition. The clay smear potential is a measure of the amount of clay that has been smeared from individual shale source beds at a certain point along a fault plane:

$$CSP = \sum \frac{(Shale - bed - thickness)^2}{(Distance - from - source - bed)}$$

The Clay Smear Potential models the behavior of shear-type smears for distance tapering and additive effect of compound clay beds. Yielding et al., (1997) modified the specific formula for the Clay Smear Potential equation to a more general form, called “Smear Factor”:

$$SF = \sum \frac{(Shale - bed - thickness)^n}{(Distance - from - source - bed)^m}$$

The exponents “m” and “n” can be determined via experimental or observational studies. Note that as “n” increases above a value of one, thicker source beds are proportionally weighted higher than are thin beds (i.e., a bed twice as thick is weighted by more than twice as much).

Lindsey et al., (1993) proposed a “Shale Smear Factor” based on observations of abrasion smears in a lithified sequence:

$$SSF = \frac{Fault - throw}{Shale - layer - thickness}$$

Note that the Shale Smear Factor remains constant between the offset terminations because it does not depend on smear distance. However, lateral changes in fault throw would have a corresponding change on the calculated Shale Smear Factor. Lindsey et al., (1993) concluded that shale smears with a Shale Smear Factor of up to seven are likely to be continuous.

Yielding (1997) recognized that the clay smear potential and shale smear factor may be difficult to apply in thick heterogeneous sequences due to the complications inherent in mapping every shale bed and then considering its contributive effect at the fault surface. They suggested an approach that considers the bulk properties of the sequence at the scale of the reservoir mapping utilized, termed the “Shale Gouge Ratio”:

$$SGR = \frac{\sum [(Zone - thickness) \times (Zone - clay - fraction)]}{Fault - throw} \times 100\%$$

The Shale Gouge Ratio represents the proportion of shale or clay that might be entrained in the fault zone by a variety of mechanisms. Wall rocks with a high shale content tend to produce greater proportions of shale or clay in the fault zone. Investigation of fields in three different basins (Niger Delta; Northern North Sea; and Offshore Trinidad) show seal threshold on the order of 10 to 20 percent Shale Gouge Ratio (Yielding et al., 1997).

#### **3.2.4.2.3 Cataclasis**

Cataclasis involves the fracture, crushing, and rotation of mineral grains along a fault plane. It is a mechanism of brittle deformation. When deformation is severe, cataclasis may result in a "gouge" zone along the fault that is comprised of a fine-grained matrix of crushed grains, which can form a seal even when sandstones are juxtaposed (Engelder, 1974; Pittman, 1981). A seal forms because the petrophysical and textural characteristics of the disturbed zone material differ from the juxtaposed lithologies on either side of the fault.

Cataclasis can increase or decrease the porosity of the material in the disturbed zone of the fault relative to the material in the juxtaposed lithologies. In severe cataclasis, the deformed zone material may consist of crushed grains that have a lower porosity, smaller mean grain size, and poorer sorting than the juxtaposed lithologies.

These characteristics may result in reduced permeabilities in the disturbed zone due to the smaller pore throat size of the gouge material, thereby increasing the potential for seal, especially between immiscible fluids, where the capillary pressures would be significantly higher in the disturbed zone material (Berg, 1975). Knipe (1992) found that cataclastic fault gouge can have pore throat radii less than 0.001 millimeters. Antonellini and Aydin (1994) and Pitmann (1981) found that deformation bands within the fault gouge can have a porosity one order of magnitude and a permeability three orders of magnitude less than the undeformed surrounding host rock. Gouge due to cataclasis generally only forms under conditions of significant friction along a fault plane, under high effective confining pressures (Smith, 1966).

Therefore, permeability reduction and/or seal by grain crushing and/or fracturing effects at the Project Goose Lake site are expected to be minor since the faulting occurred at a shallow depth when the sands of interest were essentially unconsolidated.

#### **3.2.4.2.4 Cementation/Secondary Mineralization**

Cementation of fractures along the fault plane and/or of the disturbed zone material by secondary mineral deposits from circulating subsurface formation fluids may produce a zone that forms a vertical barrier to lateral fluid flow. A high degree of cementation may completely infill the voids within the pore throats of the disturbed zone, reducing the transmissivity of the material to virtually zero.

#### **3.2.4.2.5 Field Studies Identifying Lateral Fault Seal**

Field studies of Gulf Coast salt dome reservoirs (20 cases from Good Hope Field, Louisiana and others) show that where parts of the same sandstone body are juxtaposed across a fault (30 - 300 ft of throw), the faults are laterally transmissive (Smith, 1980). Even in those cases where "fault gouge" material was present in a disturbed zone along the fault, the faults were laterally transmissive when the same sandstone body (including the thin shale beds in the sandstone body) was juxtaposed across the fault (Handin, 1963). Weber and Daukoru (1975) determined from field evidence that in a young, growth-faulted basin similar to the Texas Gulf Coast, laterally non-transmissive faults are only likely when a given sand body on the high side (upthrown) of the fault is passed by a sedimentary sequence on the downthrown side that contains more than 25 percent shale beds (excluding the thin shale beds in the sandstone body).

Gulf Coast salt dome studies to determine the widths of fault zones, indicate that faulting is associated with relatively thin fault zones, and, in some places, these faults may be represented by a discrete surface (Smith, 1980). Evidence of this can be found in cores from Raccoon Bend Field, Austin County, Texas (Teas and Miller, 1933). The Antrim faults in exposed Eocene sediments of northwestern Houston County, Texas, were found to occur as discrete fault surfaces or thin zones less than one foot thick (Smith, 1980). Similarly, outcrops in the Frechen mines (near Cologne, West Germany) indicate the shear zone widths vary with the lithological compositions of the fault walls over the throw interval. Here, where sand is juxtaposed against sand, the fault shear zones are usually only a few centimeters wide (Weber, 1978). In the Nigerian oil fields, which are similar geologically to the Gulf Coast, the examination of 1:20 scale dipmeter logs shows that the widths of shear zones of normal faults generally range from less than a foot to ~2 ft.

Bouvier et al. (1989) developed a "Clay Smear Potential" (CSP), which represents the relative amount of clay that has been smeared from individual shale source beds at a certain point along a fault. To determine the local clay-smear sealing vs. non-sealing cutoff values, individual CSP values were calibrated against known trapped hydrocarbons in sand-to-sand contacts along a fault plane(s). Jev et al. (1993), in their analysis of several fault planes in a Nigerian oil field, were able to develop a useful guideline for predicting sealing potentials along a fault plane by incorporating into the CSP the sonic log data (to differentiate hard shales from soft shales), gamma-ray log data to detect the lithology, and fault throw. Knott (1993) analyzed 297 sealing and non-sealing faults in the North Sea and determined that the most useful parameters in fault sealing prediction are fault displacement, net-to-gross sand ratio, and the amount of sand in communication: sand connectivity having a quantifiable effect on the probability of sealing. Knott (1993) developed a Fault Seal Probability (FSP) method, plotting the maximum fault throw of faults against their total reservoir thickness (including the interbeds of shale within a sandstone body). The results show that when reservoir sands of the same sand body are in juxtaposition, the faults tend to be non-sealing.

Oil and gas field production histories can be used to document instances of laterally sealed faults. Example cases are given below:

#### Eugene Island Block 330 Field Example

Alexander and Handschy (1998) analyzed the sand-to-sand juxtaposition across the major bounding field faults forming the Eugene Island Block 330 Field. Fault plane analysis, as well as pressure and geochemical data, indicate that Field Fault F is sealing to lateral fluid flow in the majority of cases where sands of differing ages are juxtaposed (coeval juxtaposed sands tend to be

laterally transmissive). Six cases of sand-to-sand juxtaposition of sands with differing pore fluids are documented in Table 3.2.4.2.5-1, indicating that Fault F is a lateral seal that prevents fluid flow across the fault. In the case of the downthrown KE-2 Sand and the upthrown LF Sand, a  $261 \pm 114$  psi pressure differential exists across the fault, demonstrating that Fault F is a seal to pressure as well (Alexander and Handschy, 1998).

#### Javelina-East McCook Field Example

Berg and Haveman (1995) present evidence of laterally sealed faults set up by fault shear zones in the Javelina-East McCook Field of South Texas. A normal fault with a shear zone is interpreted in the Shell Davis 3 well, immediately overlying the productive “Y” Sand, forming a “high-side” seal. A shallower fault in the same well sets up a “low side” seal against the fault shear zone in the “R” sandstone.

#### **3.2.4.2.6 Field Examples of Laterally Transmissive Faults**

Oil and gas field production histories can be used to document instances of laterally transmissive faults. Example cases are given below:

#### Akaso Field Example

Jev et al., (1993) present evidence that laterally transmissive fault conditions exist between Akaso Field and the adjacent Cawthorne Channel Field in Nigeria. During development of Akaso Field (1990), formation pressure testing results from the initial field wells indicated that the unproduced Akaso G sands had undergone significant pressure depletion (140-311 psi) as compared to the shallower field sands, which were hydrostatically pressured. Additionally, the Akaso G sands (0.404 psi/ft in 1990) and the Cawthorne Channel E sands (0.406 psi/ft in 1988, originally hydrostatic) showed a remarkably similar pressure gradient with respect to time. Geologically, the Akaso G sands are juxtaposed against the E sands of the Cawthorne Channel Field, which have been producing since 1970 (see Figure 3.2.4.2.6-1). Cawthorne Channel Field E sands have produced over 2.5 billion gallons of oil since being brought online (Jev et al., 1993). The similar pressures in the two juxtaposed sands and the pressure depletion (subhydrostatic) in the Akaso G sand relative to the shallower sands, conclusively demonstrate communication across the fault that separates the two fields.

#### Gulf Coast Gas Field Example

Conoco provided a Gulf Coast example of a field that is known to have pressure communication across faults based on the production history of the wells. The field was produced for more than 25 years. Figure 3.2.4.2.6-2 shows the structure at the top of the productive sand, a cross section through the field at the level of the productive sand, and several pressure decline curve comparisons for wells in adjacent fault blocks. Pressure decline curves (bottomhole pressure with time) were constructed for individual wells in each of the fault blocks. Pressure decline curve comparisons were made for the two sets of adjacent fault blocks (Blocks D & I and Blocks C & E) that are known to be in pressure communication (Figure 3.2.4.2.6-2). The pressure decline curves in the adjacent blocks overlay, clearly demonstrating that the blocks are in pressure communication.

### 3.2.4.2.7 Lateral Fault Transmissivity Considerations

Criteria can be developed from these case studies to potentially determine which faults in the vicinity of the Project Goose Lake Site are laterally transmissive or are laterally sealed:

- 1) Where the sand-shale ratio of the faulted geologic section indicates a substantial amount of impermeable shale (25% or greater in shale beds) is present, the shale can be expected to be smeared along the fault plane during the growth of the fault. This clay smear would impede fluid movement laterally to juxtaposed sand, resulting in a laterally non-transmissive fault.
- 2) A fault is laterally sealing where the entire injection interval sand is juxtaposed with a low permeability layer such as clay or shale.
- 3) A fault is laterally non-sealing where parts of the same sandstone body (excluding shale beds within a sandstone body) are juxtaposed (Smith, 1966; Smith 1980).

### 3.2.5 *Faulting within the Area of Review*

The injection wells themselves have been specifically located away from faulting, to be able to effectively model and predict CO<sub>2</sub> migration in the reservoir modelling process.



### 3.2.5.1 Fault Mapping and Modeling

The faults visible on 3D seismic data have been mapped and modeled in fine detail. The seismic horizons and faults were used to construct a structural framework within the geologic model. This model was populated with several properties, including shale content, which, combined with fault thickness (calculated from using a fault displacement – fault thickness ratio) used to determine fault permeability (Jolley et al., 2007).

It is possible to calculate the variation of clay values (and related fault permeability distribution) across fault planes in the simulation model from its faulted corner-point structure. This method uses the dynamic model's geocellular geometry and property grids to calculate unique SGR and fault permeability values for each faulted cell face in the model. To do this, the method first compares fault throws that are explicit within the geocellular model construction (from the model corner-point x/y/z and non-neighbor cell connection tables) with the properties of the stratigraphic layering (Vshale, porosity and permeability). This calculates unique SGR values for each explicitly faulted cell face in the model. These values are then used as a proxy for clay percent in order to assign fault permeability values derived from measured data) using an empirically derived formula from the Brent Province, North Sea (Jolley et al., 2007):

$$k_f = a * SGR^{-b}$$

Where:

$k_f$  = fault transmissibility (mD)

$a$  = position coefficient of the power-law relations between  $k_f$  and clay % for the data (for which SGR calculated from the simulation corner-point model is a proxy)

$b$  = curvature coefficient of the power-law relations between  $k_f$  and clay % for the data (for which SGR calculated from the simulation corner-point model is a proxy)

The coefficients  $a$  and  $b$  have been found to vary as a function of the burial depth-range of the data (Jolley et al., 2007). For the purpose of this study these parameters have been checked to match the expected depth range of the study area.

Fault permeability values are combined with fault rock thickness and adjoining cell length and permeability, to calculate unique fault transmissibility multiplier ( $T$ ) values for each contact between cells divided by a fault in the model using the formula, as per Manzocchi et al., 1999:

$$T = \left[ 1 + t_f \frac{(2/k_f - 1/k_i - 1/k_j)}{(L_i/k_i + L_j/k_j)} \right]^{-1}$$

Where:

$t_f$  = fault thickness in the fault cell between two adjoining model formation cells

$k_f$  = fault transmissibility in the fault cell between two adjoining model formation cells

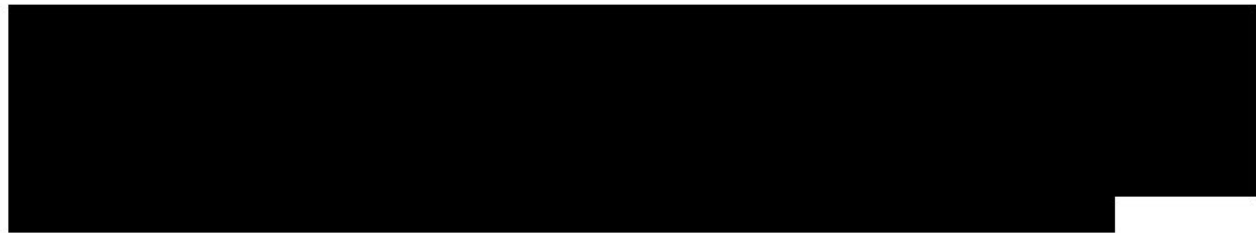
$L_i$  = length of cell I on one side of the fault

$k_i$  = permeability of cell I on one side of the fault

$L_j$  = length of cell J on opposite side of the fault to cell I

$k_j$  = permeability of cell J on opposite side of the fault to cell I

### ***3.2.5.2 Fault Stability***



### ***3.2.5.3 Fault Sealing Capacity/Transmissibility***



### ***3.2.5.4 Uncertainties in Fault Study***



## ***3.2.6 Geomechanics of the Area of Review***



Additional geomechanical and petrophysical characterization of the Injection and Confining Zones will be undertaken as part of pre-operational testing.



A series of 15 horizontal black bars of varying lengths, decreasing from left to right. The bars are set against a white background and are evenly spaced vertically. The lengths of the bars decrease in a regular, linear fashion from the first bar on the left to the last bar on the right.

### **3.3 Seismicity**

An earthquake is a motion or trembling that occurs when there is a sudden breaking or shifting of rock material beneath the earth's surface. This breaking or shifting produces elastic waves which travel at the speed of sound in rock. These waves may be felt or produce damage far away from the epicenter - the point on the earth's surface above where the breaking or shifting occurred.

The Texas-Louisiana Gulf Coast is historically an area of low seismicity with naturally occurring earthquakes being rare and of exceptionally low magnitude. Project Goose Lake is in one of the areas recognized as having low to the lowest level of seismic risk in the continental United States (USGS, 2014) (Figure 3.3-1). Rare instances of fluid injection-induced and fluid withdrawal-induced earthquakes from oil field operations have been documented along the Gulf Coast. However, fluid injection-induced earthquakes are associated with much higher injection pressures and volumes than those anticipated to be encountered in Project Goose Lake injection operation, while fluid withdrawal-induced earthquakes are most associated with large-scale oil and gas production of magnitudes greater than any past or present production near the site.

The frequency of small and large earthquakes is related in a predictable way, called the “Gutenberg-Richter relation” that states that for every 1,000 magnitude four earthquakes there will be approximately 100 magnitude five events, 10 magnitude six events, and one magnitude seven event. Thus, the occurrence of two earthquakes with magnitude near 6 in the twentieth century suggests that a magnitude seven may occur every few hundred years or so.

Faulting in the Gulf Coast Basin is predominantly two types: listric normal growth faulting (Figure 3.3-2) and radial faulting associated with shale or salt piercement structures (Figure 3.3-3). Growth faults form contemporaneously with sedimentation so that their throw increases with depth and strata on the downthrown side are thicker than the correlative strata on the upthrown side of the fault (Figure 3.3-2). The faults form in clastic sequences that build out into unconfined depositional sites that have prograded to the edge of the continental margin, resulting in contemporaneous failure of the prograding sediments (Jackson and Galloway, 1984). Although growth faults may be common throughout the Gulf Coast Basin as a whole, none are present within, or immediately surrounding the Project Goose Lake AoR. Listric faults are locally present but are restricted to the deeper Jurassic and Upper Cretaceous sedimentary intervals well below the Injection Zone.

In any particular region, the level of earthquake hazard depends on many different factors. These include the size, location, and frequency of earthquakes that may occur, as well as the population density, topography and nature of manmade improvements. For any particular earthquake, the expected intensity also depends on the type of construction and the thickness of surficial and near-surface soil. For any region, the most important factor affecting seismic risk is the historical record of earthquake activity. Regions that have had large earthquakes in the past will likely experience them again. Although hazard estimates include information about mapped faults, in practice, the information is not always influential since many faults are not seismically active and many unmapped faults exist.

### ***3.3.1 Seismicity - Louisiana***

The Louisiana-Texas Gulf Coast is historically an area of low seismicity, with naturally occurring earthquakes being rare and of low magnitude (Figures 3.3.1-1, 3.3.1-2, and 3.3.1-3). The natural seismicity of the area is attributed to one or more of the following:

- Faulting along zones of flexure caused by sediment loading
- Earthquakes induced by fluid injection and/or fluid withdrawal from oil field operations
- Events related to salt or shale diapirism

Seismic event data through April 2022, for a 186-mile radius around Project Goose Lake, is shown in Figures 3.3.1-1 and 3.3.1-2 and tabulated in Table A.1 Seismic Events, APPDX C - Reg Seis. Earthquake events are grouped by geological regime, with those in the “Gulf Coast” area being analogous to the Project Goose Lake area. Those events in the “Sabine Uplift” area are less relevant to the area of interest. These data were secured from the USGS Earthquake Catalog.

The data show that southwestern Louisiana is low risk from a historical perspective, with only one recorded seismic event near Project Goose Lake. On October 16, 1983, a magnitude 3.8 earthquake occurred west of Lake Charles in southwestern Louisiana (13 miles north of Project Goose Lake). The earthquake was felt over an area of 1,004 square miles and had a maximum Modified Mercalli intensity of V. The focal mechanism of the earthquake was determined based on P-wave first motions from 22 local and regional monitoring stations along a predominantly east-west trending, southeast-dipping normal fault with a small strike-slip component. The depth of this event (3.1 miles) provides significant evidence that normal faulting within the crystalline basement may control shallower growth faults along the Gulf Coast.

The largest recorded earthquake within the Gulf Coast geological regime occurred on October 19, 1930, with the epicenter near Donaldsonville, LA (~146 miles east of Project Goose Lake). This earthquake measured 4.2 on the Richter scale and was felt over an area of approximately 15,000 square miles (Shake Out website).

### ***3.3.2 Seismicity - Texas***

In Texas, the regions at greatest risk for seismicity are in West Texas, where earthquakes of magnitude of about six occurred in 1931 and 1995, and in the Panhandle area, where at least six earthquakes with magnitude above 4 have occurred since 1900. Earthquakes of similar magnitude may occur again in these areas. Geologically, some features of the Panhandle are similar to the Missouri-Tennessee area, however, large continental quakes are extraordinarily rare (occurring less often than once per 500 years in any particular place). Within the twentieth century there have

been more than 100 earthquakes large enough to be felt in Texas; their epicenters occur in 40 of Texas's 257 counties. Four of these earthquakes have had magnitudes between five and six, making them large enough to be felt over a wide area and produce significant damage near their epicenters.

In four regions within Texas there have been historical earthquakes that indicate potential earthquake hazard. Two of the regions, near El Paso and in the Panhandle, have had earthquakes with magnitudes of about 5.5-6.0 occurring every 50-100 years, with even larger earthquakes possible. In northeastern Texas, the greatest hazard is from very large earthquakes (magnitude 7 or above), which might occur outside of Texas, particularly in Oklahoma or Missouri-Tennessee. In south-central Texas and along the Gulf Coast the hazard is generally low, however, small earthquakes can occur there, including some that are triggered by oil or gas production. Elsewhere in Texas, earthquakes are exceedingly rare. However, the hazard level is not zero anywhere in Texas; small earthquakes remain possible.

Within a 186-mile radius around Project Goose Lake, 21 Texas earthquakes have occurred since 1900. All lie outside of the Gulf Coast geological province and were in or along the fringes of the Sabine Uplift area (Figures 3.3.1-1 and 3.3.1-2 and Table A.1 Seismic Events, APPDX C - Reg Seis). The majority of these earthquakes occurred post-2012 and are likely linked to oil and gas drilling activity within the Haynesville Shale area of the Sabine Uplift. The geological regime in this area is significantly different to that at Project Goose Lake, and thus it is not seen as a good analogue for predicting future earthquakes.

In the Project Goose Lake study area, the likelihood of an earthquake caused by natural forces or fluid injection is considered remote. Injection of carbon dioxide at Project Goose Lake is expected to be at comparatively low pressures and take place into deep, high porosity-high permeability formations that are extensive over a broad area that is not subject to natural earthquakes. Therefore, the probability of an earthquake of sufficient intensity to damage the injection system, injection well, or the confining layer is very low.

### **3.3.3 Seismic Risk Analysis**

A preliminary seismic risk evaluation has been conducted for the project area. The GCS sequestration area is located in Calcasieu Parish, on the extreme western edge of southwestern Louisiana, near the border with Texas. These portions of Louisiana and Texas lie within the geologic tectonic province known as the Gulf Coast Basin. It is within this deep basin that basement rock structures are covered by a thick sequence of unconsolidated to loosely compacted sedimentary rocks. Overall seismic risk is rated very low based on:

1. Low frequency of natural earthquake events in and near the sequestration area
2. Low intensity of natural earthquakes felt in the sequestration area, with maximum ground motion on the surface being less than or equal to an intensity range of MMI=V
3. Low population density in Calcasieu and Cameron Parishes limit exposures and impacts, with only about 13,500 total population across the sequestration area in southwestern Calcasieu Parish (District 12)
4. Lack of injection-induced seismicity in Class I wells operating in similar Tertiary sediments along the Texas to Mississippi Gulf Coast

5. Incremental injection pressures are less than those required to induce slip along pre-existing faults

Typical geologic structures characteristic of this province are gently southerly dipping and thickening sedimentary strata. These strata are disrupted by three types of faults: radial faults originating from salt or shale piercement domes; syndepositional growth and regional systems (listric normal faults, and post-depositional faults). The major fault systems can trend for considerable distances, roughly paralleling the coastline. The regional fault systems in south Louisiana are syndepositional growth faults, originally formed during periods of accelerated basin subsidence and sedimentary deposition. In general, mechanisms invoked to explain the formation of growth faults have included overloading in areas of rapid sedimentation, differential compaction of deposited sediments, abnormally high fluid pressures, and gravity sliding. An extensional stress province is associated with growth faulting from northeastern Mexico to Louisiana maximum horizontal stress ( $SH_{max}$ ) is subparallel to the coastline, following the strikes of the growth faults (Snee and Zoback, 2016).

The seismic activity in this part of the coastal plain is among the lowest in the United States (Figure 3.3-1) and has been assigned the lowest coefficients (Leeds and Associates, 1989). This is also shown on Seismic Risk Maps prepared by FEMA (<https://www.fema.gov/emergency-managers/risk-management/earthquake/hazard-maps>) that indicate that the sequestration project is located in an area with “very small probability of experiencing damaging earth-quake effects.” Underground tectonic forces that are continually applied to brittle rocks tend to deform or bend the rocks slightly. In this scenario, stress in brittle rocks builds up during the “inter-seismic” period until they rupture seismically and deforms instantaneously when the stress from the forces built-up over time exceeds the strength of the rocks. These instantaneous movements produce seismic waves that travel through the earth and along the surface of the earth and are responsible for the trembling and shaking known as an earthquake. It should be noted that none of the earthquakes that has occurred in Louisiana has been attributed to any specific fault, however, this may be due to the paucity of seismograph stations located in the state (Stevenson and McCulloh, 2001).

Note that near Houston, there are many examples of faults that are known to be active, but which do not have any associated earthquakes because the shallow Tertiary sediments are not brittle. In these cases, the strain is continuously released as the sediments creep along the fault plane. For example, land in some communities southeast of Houston such as Clear Lake and Dickenson areas is subsiding because large volumes of groundwater have been pumped out from the ground for many years. The subsidence appears to be associated with slip/creep along active, near-surface faults. In these cases, such slip is a slow or continuous creep and does not cause an earthquake.

To cause an earthquake the faults need to "lock" then “unlock” suddenly to radiate seismic waves. However, none of the earthquakes that has occurred in Louisiana have been attributed to any specific fault. This is in large part because of the paucity of seismograph stations located in the state. Earthquakes have also been located in Southeast Texas. The 1887 Wellborn, 1910 Hempstead and 1914 Anderson shocks may have been related to salt dome growth or minor adjustments from sediment loading in the Gulf Coast basin. The 1891 Rusk and the 1981 Center and Jacksonville earthquakes in Northeast Texas were all located on or near a 50-mile segment of the Mount Enterprise fault system.

Fluid withdrawal is usually associated with aseismic subsidence and faulting such as occurs in the Houston area. However, small earthquakes are sometimes reported. In 1925, small shocks were

associated with subsidence produced from oil production at the Goose Creek old field southeast of Houston. Larger earthquakes in East Texas also may have resulted from fluid withdrawal as tentative relations between withdrawal and seismicity have been proposed for the 1932 Mexia-Wortham and the 1957 Gladewater earthquakes and evidence exists for the earthquakes in some oil and gas fields in South Texas.

The size of an earthquake can be expressed by either intensity or magnitude. Magnitude is based on an instrumental recording that is related to energy released by an earthquake, while intensity describes the felt effects of an earthquake:

**Intensity** - effect of the ground motion on man, structures, and on natural features. The measure currently in use (since 1931) is known as the Modified Mercalli Intensity Scale (MMI). Before 1931, the quite similar Rossi-Forel Intensity Scale was used. Intensity observations are employed to construct isoseismal maps wherein the areas of equal shaking are contoured.

**Magnitude** - instrumental measure of an earthquake. It is the response of a specified instrument (seismograph) with narrowly defined dynamic response. With the magnitude scale, earthquakes can be measured at a distance. Seismic stations should all achieve similar determinations from the same event since adjustments are made for distance and instrumental constants. The magnitude scale was devised by Dr. Charles F. Richter. There are now several versions of the magnitude scale, depending on the type of seismic wave observed, epicentral distance, and several other factors.

Instrumental seismology is equally as important as the historic record, for instrumentation permits measurement and location of seismic events much smaller than those which may be felt. Thus, a catalog of seismic events may contain events that are instrumentally recorded but not felt by man. Also, since seismic ground motion attenuates with distance and the entire country is not adequately covered by seismographs, many small events are felt but not recorded or escape all detection.

### **3.3.3.1 Model Earthquake – Sequestration Project Area**

A model earthquake is used to evaluate the potential effects, if any, of natural earthquakes on structures associated with the sequestration project. In general, a source mechanism is required when designing a “model” earthquake. In these cases, it is usual to have a “known” active fault system with a measured strain or stress field. In more active regions of the earth, faults with strain (movement across the fault without a rupture) develop at a rate of up to five centimeters per year, or more (Leeds and Associates, 1989). As a meter or more of strain develops, stress accumulates and eventually the system releases this stored strain energy in the form of elastic waves (i.e., an earthquake).

Although the Texas/Louisiana Gulf Coast contains several geological features capable of storing and releasing stored energy, all are weak or ineffective in terms of generating even modest ground motion (Leeds and Associates, 1989).

Salt structures develop by buoyant flow of lower density salt through weaker zones of the thick Tertiary sediments. The salt is generally so plastic that it tends to flow rather than develop large fractures. The surrounding sediments are badly faulted by the intrusion of salt and are almost as physically incompetent as the salt, also having low densities, poor cementation, and low shear strength with resulting low shear moduli (Leeds and Associates, 1989). It is doubtful that the salt

dome as a seismogenic source could develop earthquakes with magnitudes greater than 3.0 and intensity MMI>IV (Leeds and Associates, 1989). These events could be felt locally but are unlikely to propagate damaging ground motions. The events might be perceptible, but the level of shaking could not be considered damaging.

Growth faults have also developed along the Texas/Louisiana Gulf Coast which may be responsible for seismic activity. Considering the Gulf Coast as a whole, a level of Mb=4.2 is considered an upper level for this kind of source in this area (Leeds and Associates, 1989). The several low magnitude events within about 50 miles of the coastline are probably attributable to this mechanism.

The possibility that growth faults may be triggered by faults in the basement is suggested by Stevenson and Agnew (1985) in their discussion of the Lake Charles Earthquake. Details of the event were developed from recordings of Department of Energy supported microseismic networks deployed for monitoring geothermal experiments (withdrawal and injection) in southern Louisiana. The interpreted depths of 14+ km for these events are deeper than have previously been reported and well beneath anticipated injection depths for the sequestration project. Additionally, none of the events were attributable to the geothermal extraction/reinjection operations (Stevenson (pers comm.), in Leeds and Associates, 1989).

### **Design Earthquake for the Risk Analysis**

In the evaluation of the potential effect of seismicity on a Class I Injection Well Facility located near the western margins of the sequestration project, Leeds and Associates (1989) used a modeled seismic event with a body-wave magnitude, Mb of  $4.2 \pm 0.2$  as a conservative working model for the design earthquake and presumed that the source area for the event would be along one of the nearby coast parallel growth faults.

The maximum ground motion on the surface generated by the design earthquake would be within the intensity range of MMI=V. This intensity equates to a horizontal surface acceleration of 0.05g (Leeds and Associates, 1989). This is the same value used as an “Operating Basis Earthquake” (OBE) for Gulf Coast nuclear power plant electric generating stations. The Nuclear Regulatory Commission's estimate of the risk each year of an earthquake intense enough to cause core damage to the reactor at River Bend (north of Baton Rouge) was 1 in 40,000, according to an NRC study published in August 2010 (Hiland, 2010). The empirical correlation between intensity and acceleration has a wide spread of data, with recordings varying from horizontal accelerations of 0.025 to 0.15g for an Intensity MMI=V event.

The operational basis earthquake (OBE) is defined by US Federal Regulations 10 CFR 100, Appendix A, as follows:

“The Operating Basis Earthquake is that earthquake which, considering the regional and local geology and seismology and specific characteristics of local subsurface material, could reasonably be expected to affect the plant site during the operating life of the plant; it is that earthquake which produces the vibratory ground motion for which those features of the nuclear power plant necessary for continued operation without undue risk to the health and safety of the public are designed to remain functional.”

The design earthquake in this study is based on the empirical data of normal shallow focus (<12 miles) earthquakes on soft sites (Leeds and Associates, 1989). It is also assumed that in the Gulf coastal seismic environment, the release of energy from less competent materials than usual, would result in longer surface rise times; therefore, the ground motion would be biased to longer periods with lower frequencies and result in low accelerations, large displacements, and long durations.

Studies over the years of the effect of depth on seismic ground motion have all noted the attenuation that is realized with depth. Observations in deep mines and boreholes have confirmed this phenomenon. The data strongly indicate dampening of amplitude with depth and are an average of one-half, or less, of the ground motion. The motion may be as low as one-fifth and for small motions, where the materials remain completely elastic, the diminution of amplitude may be as small as much one-tenth (Leeds and Associates, 1989).

The effect of ground motion on saturated granular soils is the buildup in pore water pressure. If the water table is located near the surface (within about 15 to 20 ft), if the sands are reasonably well sorted and clean (free of clay), and if accelerations exceed about 0.25g, a type of soil failure known as liquefaction can occur (Leeds and Associates, 1989). Liquefaction causes a loss of shear strength of the soil and may result in ejection of sand and water to the surface (sand boils), and collapse of the foundations of structures supported by soils. In extreme cases, multistory buildings have rolled over (Niigata, Japan Earthquake in 1964) and buried tanks have “floated” to the surface (Leeds and Associates, 1989). Following liquefaction, there is settlement and ensuing densification of the soil. The sequestration project area does not meet the conditions expected to trigger liquefaction since the acceleration levels (0.05g) are only about one-fifth that required (Leeds and Associates, 1989).

As depth increases there is attenuation and reduction of motion. While pore pressures could increase, the soils framework is not used as support the lithostatic sediment column. Additionally, within the short duration of shaking, there is insufficient time or place for the fluid to go to. Thus, it remains incompressible. (Leeds and Associates (1989) conclude that possible interactions between sedimentary horizons due to casing penetration and cement are minimal since there is only minor differential movements as the seismic wave passes through the matrix. They conclude that there might be only several centimeters of displacement over the wavelength of the seismic waves and that the normal elasticity of well casing and tubing is sufficient to accommodate the strain (Leeds and Associates, 1989). It is only in extreme cases, such as in Kern County, California, where surface accelerations can reach 0.5g and there are many miles of surface rupture, that existing wells may be affected. The 1952 event, approximately 2% of the wells in the area had some surface damage due to settlement of surficial soils (Leeds and Associates, 1989). This event caused some subsurface damage including collapsed tubing near the surface due to the sharp rise in casing pressure accompanied the shock. However, all wells returned to normal status within 2 or 3 weeks of the event (Leeds and Associates, 1989).

### ***3.3.4 Induced Seismicity***

Seismicity related to fluid injection normally results from activity involving high pressures and large volumes, such as those associated with high-pressure water flood projects for enhanced oil recovery. This seismicity is caused by increased pore pressure, which reduces frictional resistance and allows the rock to fail. Fluid withdrawal has caused land subsidence and earthquakes due to de-watering and differential compaction of the sediments. Earthquakes of magnitude 3.4 to 4.3 on

the Richter scale appear to have been caused by fluid withdrawal near some oil fields in east Texas (Davis et al., 1989), such as Sour Lake, Mexia, and Wortham Fields.

Since 2010, the occurrence of earthquakes with a magnitude greater than 3.0 have increased from 20 events per a year (1967-2000) to over 100 events per a year (2010-2013) in the central and eastern US region (Ellsworth, 2013). The increased rate of occurrence in previously inactive seismic areas has been correlated with the increased use of injection wells located near faults. Fluid injection induced earthquakes are most likely caused by the increased pore pressure from injection operations which have reduced effective stress of faults leading to failure. This mechanism has been used to explain the best-known cases of injection-induced seismicity which was first studied in the Rocky Mountain Arsenal near Denver. New case studies have increased with the use of wastewater injection wells associated with hydraulic fracking. In many sites, smaller seismic occurrences have shown to be precursors to larger events. More data has become available since the Rocky Mountain study in the 1960's, leading to a better understanding of factors and processes associated with induced seismicity.

One of the most notable regional cases of induced seismicity associated with injection wells occurred in Youngstown, Ohio. In 2011, 12 low-magnitude seismic events occurred along a previously unknown fault line (Ohio DNR, 2012). These events occurred less than a mile from Class II injection well Northstar I. Previously, the area was seismically inactive, with earthquakes beginning a few months after the injection of wastewater. The injectable pressure at Northstar I was increased twice over 6 months (Ohio DNR, 2012) and may have reduced the effective stress on a fault. After the well was shut down by the Ohio Department of Natural Resources, the seismic activity declined. As a result of this case, seismic monitoring prior to injection and after injection has become common in Class II sites.

A case study in the Dallas-Fort Worth area tied small seismic events to a Class II injection well. 11 hypocenters have been observed at a focal depth of 2.7 miles and 0.3 miles from a deep saltwater disposal (SWD) well (Frohlich et al., 2010). Injection at this well began 8 weeks prior to the first recorded seismic event. A northeast trending fault is located approximately at the same location of the DFW focus (Frohlich et al., 2010). As a result of fluid injection into the disposal well, the stress upon the fault had been reduced and thus reactivated the fault (Frohlich et al., 2010). All of the seismic events associated with the DFW focus are small magnitude events (less than 3.3) and occurred very shortly after initial injection.

In Oklahoma, one of the largest earthquakes in the state's history may have been a result of wastewater injection at a Class II disposal site. In 2011, Prague, Oklahoma was the location of a 5.7 magnitude earthquake that was followed by thousands of smaller aftershocks. Waste-water had been pumped continuously into an old oil well for 17 years. As the pore spaces filled, the wellhead pressure was increased to continually inject the wastewater. This reduced the effective stress upon the Wilzetta fault located 2,133 ft from the well (Keranen et al., 2013). The fluid was injected into the same sedimentary strata at which 83% of the aftershocks originated (Keranen et al., 2013). In this case, the seismic event occurred years after the initial injection phase. Since the area was considered low risk seismically, there is no data on smaller earthquakes that may have preceded the event in 2011.

In north-central Arkansas, multiple earthquakes have been triggered because of a Class II injection well. Since the operation of the disposal well in 2009, the site has experienced an increase from two events in 2008 to 157 events in 2011 (Horton, 2012). It was also tied to the discovery of a

new vertical fault. 98% of earthquakes within this area occurred within 3.7 miles of one of three waste disposal sites (Horton, 2012). The depth of the earthquake foci occurred between 4.2 and 4.7 miles. Injection of fluid occurred at a depth of 1.6 miles. At this disposal site, and E-W trending (Enders Fault) cut into the aquifer in which the fluid was injected and then acted as a conduit to the new fault at the depth of 4.2 to 4.7 miles (Horton, 2012). The disposal wells were shut down in 2011 by the Arkansas Oil and Gas Commission. The rate and size of the earthquakes steadily decreased following the shutdown of the wells (Horton, 2012).

In Texas there are at least two known examples of previously seismically inactive areas becoming seismically active after major injection programs began. One site is located in the Central Basin Platform, near Kermit, and the other is in the Midland Basin near Snyder. In both cases, large scale, high pressure, oil field related, water flooding projects were under way, and earthquakes with a magnitude of over 4.0 on the Richter scale were recorded. Historically, induced earthquakes in Texas have not exceeded 4.6 magnitudes (Frohlich et al., 2010). Factors for an induced earthquake are limited to the distance a well is located from a fault, the stress state of the fault, and a sufficient quantity of fluids from the injection well at a high enough pressure and enough time to cause movement along the fault (Ohio DNR, 2012). A hydraulic conduit from the Injection Zone to a fault may also induce earthquakes (Ellsworth, 2013). The largest injection-induced events are associated with faulting that is deeper than the injection interval, suggesting that the increased pressure into the basement increases the potential for inducing earthquakes (Ellsworth, 2013). In all cases, faults have been reactivated at or in close proximity to Class II injection sites. In some cases, previously unknown faults have been discovered. No induced earthquakes have been known or are postulated to have been caused by Class I injection operations (Davis et al., 1989).

#### ***3.3.4.1 Induced Seismicity Analysis at Site***

A working model for the project is available from Class I injection well sites located along the Texas-Louisiana-Mississippi Gulf Coast, roughly extending from Corpus Christi in South Texas to Pascagoula, Mississippi. These sites include both hazardous and nonhazardous fluid effluent disposal wells that typically operate in the +/-300 to 500 gallons per minute injection range, with maximum injection approaching 1,000 gallons per minute. Many of these sites have been operating since the 1970's and a few as far back as the 1950's. The geological environments of these operations are largely identical to those anticipated in the Project Goose Lake study area. Typical geologic structures characteristic of these areas includes gently coastward dipping and thickening sedimentary strata of Tertiary to Cretaceous age that are disrupted by radial faults originating from salt or shale piercement domes, syndepositional growth and regional fault systems, and post-depositional faults. There is no known evidence of injection-induced seismicity or suspected injection-induced seismicity at or near any of these facilities, many of which are near high-population areas. Assessment of the potential for induced seismicity at these locations follow the methodology outlined below, using the very conservative "zero-cohesion Mohr-Coulomb failure criterion" recommended by the U.S. Geological Survey (Wesson and Nicholson, 1987). These analyses indicate very low potential for induced seismicity due to pressures resulting from the injection activity (examples such as long-term Class I injection operations at sites like INV-Victoria, INV-Orange, Lyondell Channel View, Rubicon etc., among others) regulated by the EPA.

Known examples of injection-induced seismicity due to injection include areas in the Fort Worth-Dallas area of Texas, Youngstown, Ohio, Central Oklahoma, and north-central Arkansas. These areas with known cases of induced seismicity are hydro-mechanically very dissimilar to those found in the Goose Lake sequestration area and are often in areas of critically stressed faults. Additionally, the sequestration project will be injecting into sandstones of the Upper Frio Formation, which is located many thousands of feet above the crystalline basement complex. Injection into strata near or at the basement, with activation of pre-existing faults, has been identified as contributing to induced seismicity in those parts of the country where deep injection occurs. Despite the long history of Class I and Class II disposal along the Texas-Louisiana Gulf Coast, there are no regional-scale or operational trends associated with induced seismicity in or near the sequestration project or in similar hydro-mechanical areas such as those documented in Skoumal et al. (2018) and Weingarten et al. (2015).

GCS employs conservative assumptions to the causative mechanisms of induced seismicity and the geomechanical conditions within the Project Goose Lake study area to conservatively constrain parameters. The potential for induced seismicity at Project Goose Lake can be evaluated using the very conservative "zero-cohesion Mohr-Coulomb failure criterion," recommended by the U.S. Geological Survey (Wesson and Nicholson, 1987). This method is based on the following equation:

$$P_{crit} = \frac{S_v(3\alpha - 1)}{2} \quad (1)$$

where:

$P_{crit}$  = the critical Injection Zone fluid pressure required to initiate slippage along faults and fractures

$S_v$  = the total overburden stress (which represents the maximum principal stress in the Gulf Coast region)

$\alpha$  = the ratio of the minimum principal stress (horizontal in the Gulf Coast region) to the maximum principal stress (overburden stress)

Inherent in Equation (1) are a number of conservative assumptions, guaranteed to produce a worst-case lower bound to the critical fluid pressure for inducing seismicity. These are:

- 1) It neglects the cohesive strength of the sediments
- 2) It assumes that a fault or fracture is oriented at the worst possible angle
- 3) It assumes a worst-case value of 0.6 for the coefficient of friction of the rock. See Figure 3.3.4.1-1 (Wesson and Nicholson, 1987)

For present purposes, Equation (1) can be expressed in a more convenient form by introducing the so-called matrix stress ratio ( $K_i$ ) (Matthews and Kelly, 1967; Eaton, 1969), which is defined as the

ratio of the minimum to the maximum "effective" principal stresses. Effective principal stress is equal to actual principal stress minus fluid pore pressure ( $p_o$ ). Thus:

$$K_i = \frac{\alpha S_v - p_o}{S_v - p_o} \quad (2)$$

Substituting Equation (2) into Equation (1) yields:

$$\Delta P_{crit} = \left( \frac{3K_i - 1}{2} \right) (S_v - p_o) \quad (3)$$

where  $\Delta P_{crit}$  is the critical Injection Zone pressure build-up required to induce seismicity, with:

$$P_{crit} = p_o + \Delta P_{crit} \quad (4)$$

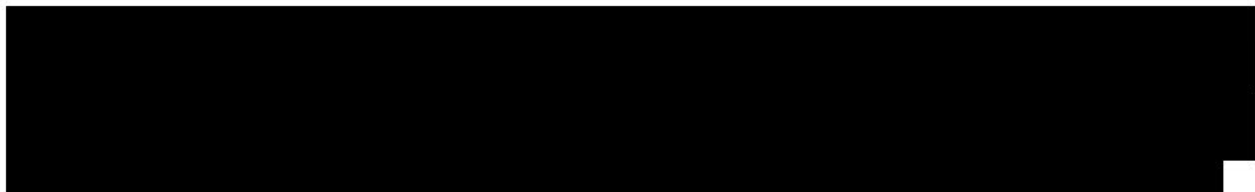
Equation (3) will be used to evaluate induced seismicity at Project Goose Lake.

Reservoir modeling indicates that, at the injection depths, the initial pore pressure ( $p_o$ ) is  $0.456 \pm 0.015$  pounds per square inch (psi) per foot of depth (Hovorka et al., 2018), (Nicholson, 2012) and (Seni et al., 1997) at a datum depth of -8,000 ft TVDSS.  $S_v$  is  $1.0 \pm 0.1$  psi per foot of depth (Nicholson, 2012), (Meckel et al., 2017) and (Ramos et al., 1994). (Nicholson, 2012) assumed a value of 85% of  $S_v$  for the minimum horizontal stress. values consistent with work published by (Engelder et al., 1997). (Meckel et al., 2017, p34) assumed a value of 0.85 psi/ft (85% of 1 psi/ft for the vertical stress gradient).

Matthews and Kelly (1967) provide a plot of the matrix stress ratio ( $K_i$ ) for tectonically relaxed reservoir sediments along the Louisiana and Texas Gulf Coast. Therefore, the  $P_{crit}$  for the Upper Frio Formation Injection Zone at Project Goose Lake can be determined. See Table 3.3.4.1-1.



### 3.3.4.2 Estimated Fracture Gradient of the Frio Formation



Plan revision number: v3  
Plan revision date: 06/16/2023

A black and white image showing a series of horizontal bars. The bars are black with white outlines, arranged in a staggered pattern. The top bar is the shortest, followed by a longer bar, then a medium bar, then a very long bar, then a medium bar, and finally a long bar at the bottom. The bars are set against a white background.

### **3.4 Hydrogeology**

The primary regulatory focus of the USEPA injection well program is protection of human health and the environment, including protection of potential underground sources of drinking water (“USDW”). The USDW is defined by the EPA as an aquifer which supplies any public water system and contains fewer than 10,000 mg/l total dissolved solids (TDS). The following sections detail the regional and local hydrogeology and hydrostratigraphy.

#### ***3.4.1 Regional Hydrogeology***

The regional aquifer system is called the Gulf Coast Aquifer System and stretches from Texas, across Louisiana, Mississippi, and Alabama, and includes the western most portion of Florida. Miocene and younger formations contain usable quality water (<3,000 milligrams per liter (mg/L) TDS) and potentially usable quality water (<10,000 mg/L TDS), which is defined as base of lowermost USDW within this system. These aquifer systems regionally crop out in bands parallel to the coast and consists of units that dip and thicken towards the southeast. Baker (1979) describes four major hydrogeologic units that comprise the Gulf Coast Aquifer System in the Texas and Louisiana region. In ascending order, the four units are:

- Jasper aquifer
- Burkeville confining system
- Evangeline aquifer
- Chicot aquifer

The Burkeville confining system hydrologically separates the Evangeline aquifer from the underlying Jasper aquifer. However, the Chicot and Evangeline aquifers are thought to be hydrologically connected. A hydrogeologic stratigraphic column for southwestern Louisiana is contained in Figure 3.4.1-1. The following sections provide details on the regional expanse and parameters pertaining the hydrostratigraphy for the defined systems from deepest to shallowest intervals. A regional stratigraphic section (A-A') parallel to dip from Baker (1979) depicting the aquifers in the regional area of Southeast, Texas is contained in Figure 3.4.1-2.

#### ***3.4.1.1 Hydrostratigraphy***

##### ***3.4.1.1.1 Jasper Aquifer***

The Jasper Aquifer is a hydrostratigraphic unit contained within the Miocene sands in the southwestern portion of Louisiana and Texas. The base of the aquifer coincides with the stratigraphic lower boundary of the Miocene-aged Fleming Formation. In parts of Texas, this also includes the Oakville sands. However, in the project site this geologic interval is not present. The Jasper aquifer is separated from the deeper saline formation waters of the Upper Frio Formation by the shale-rich Anahuac Formation and is a confined system overlain by the Burkeville confining unit (Figure 3.4.1-2). The system is laterally extensive throughout the southern portion of Louisiana and along the Gulf Coast of Texas. Regionally, the Jasper aquifer system dips southwards and becomes deeper and increases in salinity towards the Gulf of Mexico.

In Louisiana, the Jasper Aquifer System is only used as a freshwater source in Vernon, Beauregard, Rapides and Allen Parishes, located north of Project Goose Lake. In the Project Goose Lake area,

the Jasper aquifer contains saline waters, ranges in thickness from 50 ft to 2,400 ft thick regionally and is comprised of medium- to fine-grained sands. It is geologically isolated from other aquifers by laterally extensive overlying and underlying clay strata with recharge to the system north of the project site (up-dip). In the local area, the saline-bearing Jasper aquifer strata is truncated against the West Hackberry salt dome.

#### ***3.4.1.1.2 Burkeville Confining System***

The Burkeville Confining System separates the Jasper and Evangeline aquifers and retards the interchange of water between the two aquifers. The Burkeville Confining System is comprised of compacted clays and fine-grained silts, with occasional lenses of sands. This system is shown to be an effective confining unit due to the differing hydrostatic pressures within the Jasper (underlying) and Evangeline (overlying) aquifers. A typical thickness of the Burkeville is 300 ft (Baker, 1979). However, the unit thickness can vary from 100 to 1,000 ft within the Gulf Coast area. The regional cross section presented in Figure 3.4.1-2 depicts the confining system dipping down towards the Gulf.

The system is comprised of fine-grained silts and clays and is evident across the well logs for the area. The Burkeville contains some sand lenses that may act as perched aquifers up-dip providing freshwater in localized areas.

#### ***3.4.1.1.3 Evangeline Aquifer***

Within southwestern Louisiana, the Evangeline aquifer is situated within sands associated with the Pliocene-aged Goliad Formation. These sands underlie the Chicot Aquifer System and are comprised of sands that range from loosely consolidated sands and gravels, with interbeds of silts and clays. The sands are moderately well sorted and overlay the confining Burkeville Confining unit, retarding flow from between the aquifer systems. The upper portion of the Evangeline is separated from the Chicot by thin clay beds, but in some areas, these confining strata are missing. This puts the deeper Evangeline sands in contact with basal sands of the Chicot.

Recharge to the Evangeline aquifer occurs via rainfall inland from the Gulf of Mexico, and minimally, by leakage downwards from other shallow aquifers. The hydraulic conductivity of the Evangeline aquifer varies between 20 to 100 ft/day (DEQ of Louisiana, 2009). The freshwater interval thickness ranges from 50 to 1,900 ft in the Evangeline.

#### ***3.4.1.1.4 Chicot Aquifer***

The Chicot Aquifer System is the main regional aquifer system that provides usable groundwater for southwestern Louisiana. The Chicot Aquifer System is largely comprised of one, major undifferentiated sand, that splits down-dip. These Pleistocene-aged sands are predominately comprised of unconsolidated to loosely consolidated gravels and coarse graded sands. They dip and thicken towards the Gulf Coast and thin to the west (towards Texas) and slightly thicken towards the east (towards Mississippi). The aquifer system thickens and deepens to the south at a rate of about 30 ft/mile (Nyman et al., 1990). The upper sand section contains freshwater underlain by saltwater in Cameron Parish (Nyman, 1984), except along the southeastern coast where no freshwater is present (Smoot, 1988). A freshwater to saline interface is driven northwards from the coast by water production for public supply, rice irrigation, and aquaculture. The southern limit of freshwater in the upper aquifer occurs near the coastline (Nyman et al., 1990).

Recharge to the system in Louisiana occurs where the Chicot outcrops in southern Rapides and Vernon Parishes, and in northern Allen, Beauregard, and Evangeline Parishes. There is also minimal recharge to the system via vertical leakage from the shallow overlying alluvial deposits.

### **3.4.1.2 Regional Groundwater Usage**

Groundwater withdrawals from aquifers within Louisiana in 2015 are presented in Figure 3.4.1.2-1 (from USGS and Louisiana Department of Transportation (DOTD)). The primary focus of this assessment is on the Jasper, Evangeline, and Chicot aquifers in the southwestern portion of the state.

The Jasper aquifer is not a major source for regional freshwater use along the Gulf Coast, except in Beauregard, Rapides and Vernon Parishes (Figure 3.4.1.2-2). As the aquifer dips downwards towards the south (towards the coast), the groundwater increases in chlorides and is less commercially ideal to produce in comparison to the overlying Chicot and Evangeline aquifers. In Louisiana, the Jasper aquifer is primarily used as source only near its recharge areas. Its primary uses are for public water supply and industry with approximately 47.95 million gallons per day (Mgal/d).

Groundwater withdrawal from the Evangeline aquifer in Louisiana is almost half of that then from the Jasper aquifer. The Evangeline is used most heavily in Evangeline Parish, as well as Allen, Avoyelles, and Beauregard Parishes for public supply and industry (Figure 3.4.1.2-3). Approximately 28.56 Mgal/d were withdrawn from the aquifer in 2015.

The Chicot aquifer yields the highest amount of groundwater for the State of Louisiana. It is the primary source of water for Acadia, Calcasieu, Cameron, and Jefferson Davis Parishes (Figure 3.4.1.2-4). As the aquifer nears the coast, the lower units become saline and only the upper portions of the aquifer are used as a source of groundwater. Approximately 849.90 Mgal/d are produced from the entire aquifer. The largest beneficiary of withdrawal is rice irrigation and aquaculture (crawfish harvesting), which are seasonal. As a result, during the off-peak irrigation season, the aquifer recharges, with the water level rebounding back to normal levels. The Chicot is also the largest supplier of public supply at 95.60 Mgal/day for the region and supports large cities such as Lake Charles.

Overall, regional groundwater withdrawals within the Chicot aquifer have declined since 1985. Since the water levels are stabilized, withdrawal from the aquifers is not expected to have an effect on either the safety of the injection site (non-endangerment of USDWs) or injection operations. The Upper Frio Formation Injection Zone at Project Goose Lake is separated by over 7,000 ft of shale-rich geologic section from the shallow USDWs (<10,000 mg/L TDS) [REDACTED] Multiple additional saline “buffer aquifers” also exist between the top of the Confining Zone and base of the lowermost USDW, mitigating the vertical transmission of fluids upwards.

Regional aquifer data on the characteristic for the systems is contained in Table 3.4.1.2-1 (from Wesselman and Arrow, 1971) for the aquifers in the Beaumont and Orange, Texas. These data are regional and applicable across the Sabine River into southwestern Louisiana.

### ***3.4.1.3 Regional Groundwater Flow***

Groundwater moves through aquifer systems from areas of high hydraulic head to areas of lower hydraulic head. Regional uses from industry and the public water systems have some impacts on diverting the direction of flow.

The Chicot regional flow is in the direction of development. Major development of groundwater occurs around the Lake Charles area. In Cameron Parish, due to aquifer development, the direction of groundwater flow is primarily north and northeast (Lovelace et al., 2004).

A map of the potentiometric surface for the Chicot aquifer (Figure 3.4.1.3-1) shows the direction of groundwater flow. Lovelace et al. (2004) indicated that the flow direction is towards major pumping areas such as Lake Charles in Calcasieu Parish and the northern part of Acadia Parish and south Evangeline Parish, where there is heavy pumping for industrial and irrigation uses. Control points and wells in the analysis are located on Figure 3.4.1.3-1. The direction of flow of groundwater is downgradient at 90 degrees to the potentiometric contours. An additional issue from pumping and heavy groundwater usage is the upwards coning of saltwater that can occur as response to freshwater withdrawal. The result is higher salinity waters being pulled upwards as pumping increases in aquifers that are hydraulically connected. Along the coast in the southwestern and southern portion of Louisiana, saltwater is being slowly pulled inland (northwards) due to over pumping of groundwater aquifers for industry and agriculture, especially during the peak rice irrigation and aquaculture harvesting seasons. Two regional cross sections (Figure 3.4.1.3-2) extending across Calcasieu Parish show that the southern portion of the parish is impacted by saltwater encroachment in the Chicot aquifer (and by default the Evangeline) from the Gulf of Mexico. Increasing chloride concentrations between 1968 and 1984 indicated that a northwards or upward movement of the freshwater-saltwater interface in areas east and south of Lake Charles.

### ***3.4.2 Determination of the Lowermost Base of the USDW***

The most accurate method for determining formation fluid properties is through the analysis of formation fluid samples. In the absence of formation fluid sample analyses, data from open-hole geophysical well logs can be used to calculate formation fluid salinity by determining the resistivity of the formation fluid ( $R_w$ ) and converting that resistivity value to salinity value. The two primary methods to derive formation fluid resistivity from geophysical logs are the “Spontaneous Potential Method” and the “Resistivity Method.” The “Spontaneous Potential Method” derives the formation fluid resistivity from the resistivity of the mud filtrate, and the magnitude of the deflection of the spontaneous potential response (SP) of the formation (the electrical potential produced by the interaction of the formation water, the drilling fluid, and the shale content of the formations). The “Resistivity Method” determines formation fluid resistivity from the resistivity of the formation ( $R_t$ ) and the formation resistivity factor (F), which is related to formation porosity and a cementation factor (Schlumberger, 1987).

#### ***3.4.2.1 Spontaneous Potential Method***

The spontaneous potential curve on an open-hole geophysical well log records the electrical potential (voltage) produced by the interaction of the connate formation water, conductive drilling fluid, and certain ion selective rocks (shales). Opposite shale beds, the spontaneous potential curve usually defines a straight line (called the shale baseline), while opposite permeable formations, the

spontaneous potential curve shows excursions (deflections) away from the shale baseline. The deflection may be to the left (negative) or to the right (positive), depending primarily on the relative salinities of the formation water and the drilling mud filtrate. When formation salinities are greater than the drilling mud filtrate salinity, the deflection is to the left. For the reverse salinity contrast, the deflection is to the right. When salinities of the formation fluid and the drilling mud filtrate are similar, no spontaneous potential deflection opposite a permeable bed will occur.



### **3.4.2.2 Resistivity Method**

The Resistivity Method determines formation fluid resistivity from the resistivity of the formation ( $R_t$ ) and the formation resistivity factor (F), which is related to formation porosity and a cementation factor (Schlumberger, 1987). The resistivity of a formation ( $R_t$  in ohm-meters) is a function of: 1) resistivity of the formation water, 2) amount and type of fluid present, and 3) the pore structure geometry. The rock matrix generally has zero conductivity (infinitely high resistivity) with the exception of some clay minerals, and therefore is not generally a factor in the resistivity log response. Induction geophysical logging determines resistivity or  $R_t$  by inducing electrical current into the formation and measuring conductivity (reciprocal of resistivity). The induction logging device investigates deeply into a formation and is focused to minimize the influences of borehole effects, surrounding formations, and invaded zone (Schlumberger, 1987). Therefore, the induction log measures the true resistivity of the formation (Schlumberger, 1987). The conductivity measured on the induction log is the most accurate resistivity measurement for Resistivity under 2 ohm-meters.

Electrical conduction in sedimentary rocks almost always results from the transport of ions in the pore-filled formation water and is affected by the amount and type of fluid present and pore structure geometry (Schlumberger, 1988).

In general, high-porosity sediments with open, well-connected pores have lower resistivity, and low-porosity sediments with sinuous and constricted pore systems have higher resistivity. It has been established experimentally that the resistivity of a clean, water-bearing formation (*i.e.*, one containing no appreciable clay or hydrocarbons) is proportional to the resistivity of the saline formation water (Schlumberger, 1988). The constant of proportionality for this relationship is called the formation resistivity factor (F), where:

$$F = \frac{R_t}{R_w} \quad (3)$$

Where:

$R_t$  = Formation resistivity

$R_w$  = Formation water resistivity

For a given porosity, the formation resistivity factor (F) remains nearly constant for all values of  $R_w$  below 1.0 ohm-meter. For fresher, more resistive waters, the value of F may decrease as  $R_w$  increases (Schlumberger, 1987). It has been found that for a given formation water, the greater the porosity of a formation, the lower the resistivity of the formation ( $R_t$ ) and the lower the formation factor. Therefore, the formation factor is inversely related to the formation porosity. In 1942, G.E Archie proposed the following relationship (commonly known as Archie's Law) between the formation factor and porosity based on experimental data:

$$F = \frac{a}{\phi^m} \quad (4)$$

Where:

$\phi$  = porosity

$a$  = an empirical constant

$m$  = a cementation factor or exponent.

In sandstones, the cementation factor is assumed to be two, but can vary from 1.2 to 2.2 (Stolper, 1994). In the shallower sandstones, as sorting, cementation, and compaction decrease, the cementation factor can also decrease (Stolper, 1994).

Experience over the years has shown that the following form of Archie's Law generally holds for sands in the Gulf Coast and is known as the Humble Relationship (Schlumberger, 1987):

$$F = \frac{0.81}{\phi^2} \quad (5)$$

Combining the equations for the Humble relationship and the definition of the formation factor, the resistivity of the formation water ( $R_{we}$ ) is related to the formation resistivity ( $R_t$ ) by the following:

$$R_t = \frac{R_{we} \times 0.81}{\phi^2} \quad (6)$$

### 3.4.2.3 Methodology used in the Evaluation of the Project Goose Lake Site

To determine the formation water resistivity in a particular zone, the resistivity of the drilling mud filtrate (obtained from the log header) at the depth of the zone must first be determined. Resistivities of saline solutions vary as a function of NaCl concentration and temperature. The relationship between temperature, NaCl concentration, and resistivity are typically shown in the form of a nomograph for computational ease [REDACTED]. From [REDACTED] the resistivity of the drilling mud filtrate can be corrected to the temperature of the zone of interest. A shale baseline is next established on the spontaneous potential curve and the deflection away from the shale baseline measured. A chart containing the graphic solution of the spontaneous potential

equation [REDACTED] gives the solution for the ratio between the resistivity of the mud filtrate and the formation water ( $R_{mf}/R_{we}$ ) based on the measured spontaneous potential curve deflection. The resistivity of the formation water at formation temperature can be determined from the  $R_{mf}/R_{we}$  ratio and converted to the equivalent NaCl concentration from [REDACTED]. Once the base of the lowermost USDW is established, a formation resistivity ( $R_t$ ) cut off on the deep induction log can be established using Equation (6). This formation resistivity cut-off value is used to establish the base of the lowermost USDW at the Project Goose Lake Site.

[REDACTED]  
Deeper intervals with higher temperatures will have a higher resistivity cut off value for analysis. From this water resistivity value and an estimate of formation porosity, a formation resistivity ( $R_t$ ) cut-off can be calculated.

[REDACTED]  
From Equation (6), a formation resistivity ( $R_t$ ) cut-off can be calculated if the approximate formation porosity is known. Therefore, solving Equation (6) gives the following result:

$$R_t = \frac{R_w}{(1 - \phi) \ln \left( \frac{R_w}{R_t} \right)}$$

Therefore, it is conservatively calculated that the sands with a formation resistivity of greater than 2.0 ohm-m were considered to be USDWs. This site-specific calculation agrees with the Louisiana Department of Natural Resources (LDNR) guidance, which indicates that the USDW should fall between:

- Ground surface to 1,000 ft: 3.0 ohms or greater is considered USDW
- 1,000 ft to 2,000 ft: 2.5 ohms or greater is considered USDW
- 2,000 ft and deeper: 2.0 ohms or greater is considered USDW

To be conservative in the current analysis, the base of the lowermost USDW across the evaluated logs was placed at the base of the deepest sand with a deep resistivity greater than 2.0 ohms. Additionally, for continuous sand beds with higher resistivities at the top, the USDW was placed at the bottom of the next deepest sand. For the Project Goose Lake Site, the USDW is found to occur at a depth range of approximately [REDACTED]

[REDACTED]  
These logs depths were then calculated back to a mean-sea level depth reference using known Kelly Bushing (KB) and Ground Level (GL) elevations.

For this portion of Louisiana, out of the 357 logs, 35 logs did not extend shallow enough (NSE) to be analyzed and 25 logs were of poor quality (PQL) and unable to provide clear-cut information for determination of the depth of the lowermost USDW. The remaining 297 logs provided sufficient data to resolve the location of the lowermost USDW across the Project Goose Lake site and extended area of interest.

As the site is located near the Texas-Louisiana state line, data was also acquired from the Texas Railroad Commission for those logs in the Sabine and Orange, Texas areas. Seven logs were evaluated and provided data on the USDW across the Sabine River in Texas.

The “Base of the Lowermost USDW” [REDACTED] is based on the 2.0 ohm-m resistivity cut-off value for available wells with shallow open-hole well logs with the Area of Review and extended area of concern.

[REDACTED]

### ***3.4.3 Local Hydrogeology for the Project Goose Lake Site***

The Project Goose Lake site is located within Calcasieu Parish in southwestern Louisiana. Hydrostratigraphic units of importance range in age from Miocene to recent-aged strata and include in ascending order: (1) Lagarto, (2) Goliad, (3) Willis, (4) Lissie (which is subdivided into the Montgomery and Bentley formations), (5) Beaumont Formation, and (6) Holocene/recent sediments (Figure 3.4.1-1). Within this stratigraphic section are the two main aquifers of local interest, which are the Chicot aquifer (Pleistocene-aged) and the Evangeline aquifer (Pliocene-aged). The base of the lowermost USDW is located approximately at the base of the Chicot aquifer 700-Foot Sand or at the top portion of the Evangeline aquifer. It is not a considered a stratigraphic marker across the Project Goose Lake site.

Within the local project area, the Evangeline aquifer predominantly contains saline ground water (greater than 10,000 mg/l TDS). Upper and lower boundaries to the Evangeline include the Goliad Formation and the upper part of the Fleming Formation, respectively. The Evangeline and Chicot aquifers are usually separated by thin layers of confining clay that comprise the top of the Goliad Formation. However, when this clay is absent, the geologic boundary between the two aquifers is indistinguishable with the Goliad grading into the Willis Formation. In general, the Evangeline aquifer tends to have greater sand to clay ratio with individual sand beds up to several tens of feet thick. Because the Evangeline aquifer is mostly saline within the Project Goose Lake area, it is not considered a USDW and is not used for groundwater in Calcasieu Parish.

The shallower Chicot aquifer contains upper and lower members separated by clay beds. The upper member of the Chicot aquifer consists of a basal sand overlain by clay and is comprised of the Willis, Lissie, and Beaumont Formations (Figure 3.4.1-1).

#### ***3.4.3.1 Chicot Aquifer***

In Calcasieu Parish, the major aquifer system is the Chicot aquifer. This aquifer is sub-divided into three sub-units that are separated by confining layers. The principal sand units within the aquifer are the 200-foot Sand, 500-foot Sand, and 700-foot Sand. In the northeastern portion of

the Parish, these sands merge and the unit contains undifferentiated sands that are connected hydraulically. The Chicot outcrops and dips towards the southwest, away from exposed areas in the Beauregard, Allen, Rapides, and Evangeline Parishes. Freshwater in the lower subsections of the Chicot deteriorates in quality with depth. Low TDS concentration groundwater is predominately found in the 200-foot Sand and 500-foot Sand of the Chicot Aquifer, which is heavily used by public and industrial users. The 700-Foot Sand contains areas of saltwater encroachment from leakage from underlying salt domes and from the Gulf of Mexico as it approaches the coast.

#### **3.4.3.1.1 200-Foot Sand**

The 200-foot Sand generally grades from fine to medium sand at the top to a coarse sand or gravel at the base (Harder, 1960). This upper sand is used to primarily supply water for domestic and industrial uses. The chloride content from this sand is generally less than 100 ppm, except in the eastern part of the parish where it increases up to 300 ppm and the dissolved solids are as high as 700 ppm (Harder, 1960). This shallow aquifer sand contains the lowest TDS concentration waters in the aquifer. In general, dip of the 200-Foot Sand is southward (from its recharge outcrop in Beauregard Parish) at a rate of 4 to 10 ft per a mile (Harder, 1960). However, in the southwestern portion of the Parish, the dip can vary up to 50 ft per a mile based upon a thickness increase in the strata.

#### **3.4.3.1.2 500-Foot Sand**

The 500-foot Sand generally grades from fine sand at the top to coarse sand and gravel near the base (Harder, 1960). This unit varies in thickness from 25 ft in southeastern Calcasieu Parish to approximately 310 ft in north-central Calcasieu Parish. [REDACTED]

[REDACTED] The average dissolved solids content is 302 ppm and the chloride content is generally low in the northern and central parts of the Parish, where the average well supplies 30 ppm TDS water (Harder, 1960). The dissolved solids content may increase up to 600 ppm where the 500-foot Sand directly overlays salt dome structures (*i.e.* Vinton Dome). The higher salinity for sands overlaying the salt domes is generally localized to the immediate areas surrounding the structure and do not appear to impact the water quality down-dip of the domes (down structure).

#### **3.4.3.1.3 700-Foot Sand**

The 700-foot Sand is generally tan to grayish and grades from fine sand at the top to a coarse sand at the base (Harder, 1960). This unit is thick and laterally extensive throughout Calcasieu Parish. The chloride content is much higher than what is found in either the 200-Foot Sand or the 500-Foot Sand. Across the state line, water wells near Orange, Texas (approximately eight miles west) produce fresh to slightly saline water from the lower unit of the Chicot aquifer at depths of approximately 700 ft.

Recharge to the Chicot aquifer occurs principally in the outcrop areas in Beauregard, Allen, Rapides, and Evangeline Parishes (Harder, 1960). The system receives more water than it can transmit laterally down dip to deeper portions of the sand. As result, streams such as the Calcasieu River are hydrologically connected to the Chicot aquifer. Soils in the vicinity of the Project Goose Lake site are classified as Gulf Coast marsh and range from old organic soils to firm mineral clay rich soils. These surface soils have lower permeability and poor drainage, with little recharge from

the immediate local area. The surficial confining layer thickness ranges from 40 ft in small areas in northwestern and northeastern Calcasieu Parish to 280 ft in the south-central part of the parish (Sargent, 2004)

[REDACTED]

Three localized cross sections are constructed to show the lateral continuity of the Chicot aquifer units and their relation to the base of the lowermost USDW. As indicated previously, the conservative 2-ohm deep resistivity cutoff value is used to define the lowermost USDW.

The following cross sections are provided, showing detailed interpretation of the aquifers and the base of the lowermost USDW (See APPDX D – USDW Xsec):

1. [REDACTED] is a north-south oriented cross section that is approximately parallel to dip
  - a. [REDACTED].  
USDW follows the base of the 700-Foot sand and increases in depth southwards until it reaches the Hackberry Field (salt dome), where some shallowing is evident.
2. [REDACTED]
  - a. Base USDW fluctuates between tracking the base of the 700-Foot sand and some deeper aquifers. Varies between ~1,000 ft and 1,200 ft TVDSS depth.

The cross sections show the projected base of the USDW fluctuates between the upper portion of the Evangeline aquifer and the base of the 700-Foot sand at the base of the Chicot aquifer. These aquifers are hydraulically connected and the base of the USDW is not a stratigraphic defined zone.

#### ***3.4.3.2 Base of the Lowermost USDW***

[REDACTED]

[REDACTED]

[REDACTED]

In some instances, the conservative 2-ohm resistivity log cut off occurs within the middle of the sand package. This is an indication of a transition from freshwater to brackish/saltwater within the lower portion of the sand package. To maintain

consistency, the base of the USDW was placed at the base of this sand, not at the transition point within the sand package.



However, the Evangeline is not considered a “usable” aquifer with Calcasieu Parish and is not developed for use within the area. The top of salt is deeper at West Hackberry, and there is less influence via vertical leakage into the overlying aquifers due to a thicker cap-rock. However, as the strata dips towards the coast, saltwater encroachment into the deeper aquifers (Evangeline and Jasper) is evident in the southern portion of Calcasieu Parish due to pumping operations.



#### ***3.4.4 Water Wells and Data Sets***

Water well data was gathered from the online database of LADNR, specifically the online GIS website SONRIS (<https://www.sonris.com/>). The data was combined into a digital GIS format to merge the two data sets. All data are current through July 2022.

A water well search was performed through SONRIS (Louisiana). Primary water well locations present within the AoR of the Project Goose Lake site are shown on [REDACTED]. All water wells within the AoR are located within Louisiana. A total of 17 water wells occur in the Maximum AoR and are tabulated in Table A.2 H2O Wells AoR 5-Mile Buff, APPDX E – Water Wells AoR Flag. These wells extend from depths of 225 ft to 568 ft into the 200-Foot sand and the 500-Foot in the Chicot Aquifer. No wells are in the deeper aquifers of the Evangeline or Jasper. 10 of these water wells are plugged and abandoned wells, seven are currently active.

Additionally, to be conservative, a 5-mile buffer around the AoR was searched for additional water data. These tabulated data are available in Table A.2 H2O Wells AoR 5-Mile Buff, APPDX E – Water Wells.

In Louisiana, there are 1,220 water wells (884 active, 326 plugged and abandoned, 7 abandoned, 2 destroyed, and 1 inactive) contained within the 5-mile AoR buffer. These wells range in depth from 0 ft to 2148 ft, and water is withdrawn from all sands within the Chicot aquifer. Primary use is water supply to rigs, and industrial, commercial, and domestic purposes.

#### ***3.4.5 Local Water Usage***

In Calcasieu Parish, with a population of 192,768 people, the main source of groundwater drinking water comes from the Chicot aquifer. In 2015, 98.30 Mgal/d were withdrawn from the Chicot aquifer for usage of public supply, agriculture, power generation, and industrial applications. Public supply accounted for 27.67 Mgal/d (or 28%) of the groundwater withdrawal. The largest local public consumer is the Lake Charles Water District. Major industry that withdraws from the

aquifer in Calcasieu Parish are those associated with chemicals and petroleum refining facilities. In smaller amounts, other industries such as lumber, rubber and plastics, and primary metals account for minimal impacts to groundwater withdrawal. The largest agricultural use is for rice irrigation, at 18.73 Mgal/d. However, this is a seasonal withdrawal, peaking during late spring. Overall, groundwater withdrawal trends have decreased steadily since 1985. (Data provided from the Calcasieu Parish Fact Sheet, 2017).

The 500-Foot Sand is the most heavily developed aquifer that supplies the public water for the towns of Sulphur, Carlyss, Vinton, and Lake Charles in southwestern Louisiana. The nearest major city, Lake Charles, Louisiana (northeast), is located approximately 25-miles northeast from the Project Goose Lake area. The Lake Charles Water District is a publicly owned, community water system that serves over 77,000 people. This district draws its water from 17 wells completed into the Chicot aquifer's 500-Foot Sand and 700-Foot Sand. The Chicot also provides public water for the town of Orange, Texas (across the Sabine River).

The rice irrigation wells are completed in the 200-Foot, 500-Foot, and 700-Foot sands generally yield between 1,500 and 2,000 gallons per minute (gpm). Some wells within the 700-Foot interval have produced up to 5,000 gpm, but the water quality is considered hard and requires treatment for public use. Occasional freshwater is found in perched aquifers (confined sand lenses), but these produce relatively low yields of water. The rice irrigation and the aquaculture of the local area is seasonal. During off-peak times, the water recharges and levels in the aquifer rebound. Direction of flow is consistent with pumping associated with public supply, mostly towards the city of Lake Charles.

### **3.5 Geochimistry**

A data collection program will be designed and implemented to fully characterize mineralogy in the Injection and Confining Zones. Based on regional analogues (e.g. BEG pilot injection program) no compatibility issues are predicted.

Geochemical modelling was confined to the dissolution of CO<sub>2</sub> into the formation fluids.

[REDACTED]

[REDACTED]  
[REDACTED]  
[REDACTED]

[REDACTED]  
[REDACTED]  
[REDACTED]

[REDACTED]  
[REDACTED]  
[REDACTED]  
[REDACTED]  
[REDACTED]

[REDACTED]

[REDACTED]  
[REDACTED]  
[REDACTED]  
[REDACTED]

[REDACTED]

The image consists of a series of horizontal bars, primarily black, set against a white background. The bars are of varying lengths and positions, creating a layered effect. There are several white rectangular cutouts and a few small white squares. The bars vary in length and position, creating a layered effect.

### **3.6 History of Economic Development**

The Frio Formation, including the Anahuac Formation, is the largest producer of hydrocarbons from the Paleogene on the Gulf of Mexico shelf (Swanson and Karlsen, 2013). Hundreds of millions of barrels of hydrocarbons have been produced in the history of Gulf Coast development and Project Goose Lake sits within a highly productive and extensively developed Frio-Anahuac hydrocarbon play (Figure 3.6-1) As such, the project benefits from a substantial dataset including geophysical well logs, core samples, production data, regional studies, and seismic surveys.

History of exploration at Project Goose Lake site:

1. 1920's: Early wells targeted the crest and flanks of Vinton Dome, Black Bayou, and West Hackberry salt domes; Relatively few shallow, Miocene wells drilled.
2. 1930's – 1950's: Large increase in drilling (hundreds of wells); salt dome flanks targeted, with wildcat wells extending further afield; large, less structurally complex fault block traps targeted in Miocene reservoir.
3. 1960's-1980's: Increasing use of 2D seismic encouraged the expansion of drilling into deeper reservoirs (Miocene and Upper Frio Formation) and more structurally complex areas of the salt dome flanks (e.g. Southern flank of Vinton Dome); peak of Miocene drilling in the 70's before decreasing in the 80's.
4. 1990's: Early 90's saw a dramatic drop in drilling in the area before the advent of 3D seismic in the late 90's allowed imaging of deeper Hackberry sandstone reservoirs and a clearer understanding of structural traps. Exploration moved into a new phase of drilling of deeper, over pressured wells. This is important to Project Goose Lake as it provides a modern, analogous data set for the area of interest (Frio and Anahuac Formations).
5. Early 2000's saw a huge increase in Miocene/Oligocene drilling across the flanks of Vinton Dome and Black Bayou; deep wells targeting Hackberry sandstone channels were drilled away from salt dome structures, notably in the structural low targeted by Project Goose Lake. The deeper wells targeting the Hackberry were enabled by the extensive 3D seismic shoots which began in the late 90's and continued through the 2000's. Modern log suites were acquired in these wells and provide a critical data source for the Project Goose Lake analysis.
6. Mid 2000's – present: More recently drilling has continued at a much-reduced rate, mainly targeting previously overlooked accumulations in fault blocks around Vinton Dome, Black Bayou and Phoenix with vertical and directional wells; some older wells drilled across dome crests recompleted to target previously overlooked reserves.

Historic development has provided a wealth of information and knowledge about the regional Upper Frio Formation Injection Zone and Anahuac Formation Confining Zone. Nearby production has predominately been from the shallower Miocene or deeper Hackberry (mid-lower Frio Formation). Both targeted intervals are separated from the planned Injection Zone by substantial thicknesses of extensive sealing shales, and as such, there are no depletion issues.

#### ***3.6.1 Regional Pressure Sources and Sinks***



A series of 15 horizontal black bars of varying lengths, starting from a short bar on the left and increasing to a long bar on the right. Each bar is preceded by a small vertical black bar of decreasing height from left to right.

### **3.7 Geologic Summary**

The analysis of regional and local geology near the proposed Project Goose Lake Site demonstrates the study area is geologically ideal for CO<sub>2</sub> injection and storage. The massive fluvial-deltaic sandstones of the Oligocene-aged Upper Frio Formation provide effective injection reservoirs in terms of their lateral extent, mineralogical composition, and petrophysical characteristics. The geologic assessment has also identified that the reservoir permeability, porosity, thickness, and lateral continuity would allow them to accept and contain the amount of injected material envisaged and at the required rate. The overlying aquiclude layers in the Upper Frio Formation are sufficiently thick, impermeable, and laterally continuous to contain the injected fluids in the Injection Zone. Shales of the overlying Anahuac Formation and Miocene-age Fleming Formation possess the necessary Confining Zone criteria to be effective barriers to upward movement. The thick Anahuac and Fleming Formation shales extend laterally across the region and are well over 1,000 times less permeable than the underlying injection reservoirs. The existence of multiple sand/shale layers between the top of the Injection Zone and the base of the lowermost USDW insures additional protection from contamination of a USDW.

## **4.0 SITE CHARACTERISATION**

### **4.1 Available Data Set and Basis for Evaluation**

#### ***4.1.1 Seismic Data***

Project Goose Lake benefits from extensive high quality 3D seismic data across the AoR, extending eastward towards the Lake Calcasieu River and westward into Texas. GCS has access to over 422 square miles of proprietary and licensed 3D seismic [REDACTED]. The dataset was collected starting in the late 1990's and GCS used the entire seismic data base as set forth below.





#### ***4.1.1.5 Limitations and Assumptions of the 3D Seismic Dataset***

As with any other seismic reflection survey, the surveys utilized in this project have limitations related to their different vintages, acquisition parameters, processing/reprocessing sequences applied, and ultimately their ability to distinguish between two features from one another known as the seismic resolution.

The Rayleigh's Limit of Resolution states that two events should be separated by half a seismic cycle model. To solve for thickness  $\Delta h \geq \lambda/4$ , where  $h$  corresponds to the thickness and  $\lambda$  to the wavelength. The vertical resolution can be calculated from the length of the propagation wave and the layer thickness below  $\lambda/4$ . It is possible to detect layers down to  $1/32\lambda$ , and hence why in some cases in the presence of faults, the reflections are not completely disassociated, but seem more continuous but with unexplained changes in their dipping angles.

Vertical resolution varies, normally decreasing with depth as the earth works as a filter rapidly attenuating high frequencies. As high frequencies play a key role on defining the vertical resolution, the low frequencies play a role in the penetration, therefore the importance of seismic survey of having a broad frequency spectrum.

Following Rayleigh's limit of resolution, an average vertical resolution at reservoir level has been calculated for all the seismic surveys used:



#### ***4.1.1.6 Seismic interpretation workflow overview***

The interpretation workflow is summarized below:

**1. Reconnaissance viewing of data. This process consists of a rapid screening of the entire seismic dataset aimed at:**

- a. Making a visual QC of the different seismic surveys available in the project and making a decision on which ones to use and for what specific purpose.

- b. Familiarize the interpreter with the structural styles present in the area such as type of faulting in terms of strike, dip, trough and heaves, and others such as the different domes.

The type of faulting present in the area is extensive, with no inversion seen so far, meaning that no extensional fault has been reactivated in the opposite direction to its original movement.

Fault troughs vary significantly, going from being within the data's detectability, to faults with considerable trough (Figure 4.1.1.6-1).

- c. Familiarize the interpreter with the interval of interest in terms of horizon continuity.

2. Synthetic seismogram generation for seismic-to-well tie.



### 3. Horizon interpretation

The image consists of a series of horizontal bars of varying lengths and positions. The background is white. There are several large, solid black horizontal bands. In the center, there is a cluster of shorter, black horizontal bars of varying widths. The image has a grainy, high-contrast texture, resembling a scan of a physical object or a specific experimental visualization.

#### 4. Fault Interpretation (including fault polygon generation)

A large black rectangular redaction box covers the top portion of the page content, from approximately the top third to the middle of the page. It is positioned on the left side of the page, with a thin white vertical line to its right.



**5. Creation of time structural maps**



**6. Velocity model generation & time-to-depth conversion**



#### 4.1.2 Well Data

A substantial amount of time was dedicated to building a comprehensive database. Figure 4.1.2-1 illustrates the key inputs built into the primary subsurface database in Petra. [REDACTED]

as well as regional, publicly available tiff logs. ArcGIS was also extensively used for spatial analysis of wells vs data such as infrastructure, and terrain.

#### 4.1.2.1 Core and Rock Data Description

#### **4.1.2.1.1 Use of Current Core Dataset**

*Project Narrative for Project Goose Lake*  
Permit Number: INSERT PERMIT NUMBER  
**CONFIDENTIAL BUSINESS INFORMATION**





#### **4.1.2.5 Reservoir Engineering Data**

Site specific data will be collected as part of Pre-Operational Testing. In the meantime, a thorough literature review has been conducted of the available data pertinent to Project Goose Lake.

This data is separated into three sets. The first set is the generic data sourced from carbon capture and storage project studies in saline systems.

As an example, GCS cites the relative permeability and capillary pressure data. Data from generic studies is utilized such as (Zeidouni et al., 2009), (Ghanbari et al., 2006), (Juanes et al., 2006) and (Kumar et al., 2005).

Capillary pressure data from core samples which has been specifically analyzed for CCS purposes has been given by (Krevor et al., 2012). GCS uses the data to sense-check the characterization of CO<sub>2</sub> /brine capillary pressures for the Project Goose Lake work.

For studies specific to the Upper Frio Formation, there is capillary pressure data from (Jung et al., 2017), (Doughty, 2007) and (Hovorka et al., 2008). Lastly, there is data from the GEM simulation model from the Bureau of Economic Geology (Hosseini, 2019). Data for two rock types has been generated. Rock type 2 data appeared to be for a sandstone, whereas rock type 1 was for a tighter (potentially shale or mud stone) rock with a lower relative permeability to water and much larger capillary pressures. These had been history matched to measured data from the Upper Frio Formation CO<sub>2</sub> CCS pilot project (Hovorka et al., 2018) and therefore have added weight.

Other types of reservoir engineering data include; the formation pore pressure and temperature gradients and initial values at datum depth, salinity, rock compressibility, PVT properties of the *in-situ* formation fluids and CO<sub>2</sub> (density and viscosity as functions of pressure, temperature, salinity and dissolved CO<sub>2</sub> concentration), rock and fluid thermal properties (conductivities and heat capacities); the temperature, pressure and injection rates of the injected CO<sub>2</sub>, assumed well locations, perforated intervals and injection depths, composition of the injected fluids, aquifer properties (depth, length, thickness, permeability, porosity), geo-mechanical data (initial stress state, Biot coefficient, Young's modulus and Poisson's ratio versus depth, cohesion, coefficient of friction and the poro-elastic and thermo-elastic expansion coefficients), and the data to model CO<sub>2</sub> dissolution (equilibrium constant, fugacity coefficient and activity coefficient as functions of pressure, temperature and salinity).

All the assembled data was then incorporated into a software tool called "Reveal" to create what is referred to in all submitted permit documents as the "simulation model".

Details of the analysis of this data, with a complete bibliography, and its use in the Reveal simulation model, are described in other documents submitted to the EPA as part of the permitting process, such as the Post-Injection Site Care and Site Closure Plan 40 CFR 146.93(a) and Area of Review and Corrective Action Plan 40 CFR 146.84(b) documents.

Reveal is a reservoir simulation package produced by Petroleum Experts Limited of Edinburgh, UK. (Petroleum Experts, 2022). The version used for modelling during this project was IPM Version 12.5, build #109.

Reveal is a fully functional compositional, three-phase reservoir simulator, with black-oil functionality if required. GCS uses two phases: a gaseous phase for the injected supercritical CO<sub>2</sub> and an aqueous phase for the *in-situ* formation fluids.

Reveal models fluids using the Peng-Robinson equation of state (Peng and Robinson, 1976). Hysteresis in the saturation functions (from drainage to imbibition) may be modelled too. Reveal has full aqueous phase geochemistry modelling via an interface to PHREEQC. It uses PHREEQC ([www.usgs.gov/software/phreeqc-version-3](http://www.usgs.gov/software/phreeqc-version-3)) as its geochemical modelling engine. This is used to model CO<sub>2</sub> dissolution into the *in-situ* aqueous phase.

Reveal solves a complete energy balance equation. Reveal has geo-mechanical modelling capability, including fracture modelling for which it uses a finite element grid. It has advanced parallel solver options with a 5-point or 9-point template to formulate the finite difference equations for fluid flow. GCS used the 9-point option to minimize grid orientation effects.

Reveal is fully compatible with other modelling tools produced by Petroleum Experts, such as Prosper (a well modelling tool, (Petroleum Experts, 2022), PVTP (a fluids modelling package, Petroleum Experts, 2022) and GAP (for injection and production network modelling, Petroleum Experts, 2022). These are oil industry standard software packages with many years of development and used by oil and gas companies worldwide.

GCS uses Reveal because it takes the effect of pressure and temperature into account when calculating the density and viscosity of the CO<sub>2</sub>, and the effects of any contaminants such as methane on these properties of the gaseous phase. These are important factors in determining its distribution under buoyancy-drive and an imposed pressure gradient. It also models the dissolution of CO<sub>2</sub> into the aqueous phase as a function of pressure, temperature and salinity, an important trapping mechanism; and it calculates the effect of gas trapping during imbibition, accounting for hysteresis in the saturation functions. It allows the modeling of geo-mechanical effects to assess, for example, the risk of thermal fracturing as cool CO<sub>2</sub> is injected into a warmer formation.

#### **4.1.3 Interpretation and Evaluation Methodology**

Continual peer review and critical assessment of model inputs, outputs and assumptions by the GCS technical team and GCS senior advisors ensures reasonable results and ongoing model refinement.

The following steps provide an overview of the full-cycle GCS data, model and simulation workflow [REDACTED]

#### 4.1.3.1 Detailed description of Petrophysics

#### ***4.1.3.2 Petrophysics Next steps***

Pre-Operational Testing will include the acquisition of bespoke log suites, fluid samples and core across the Injection Zone, Confining Zone and overlying Miocene strata. The data acquisition will enable the calibration of petrophysical workflows for the Project Goose Lake site. Improvements to the petrophysical outputs will feed through to the geostatistical and reservoir simulation models and be supplied to the EPA prior to issuance of the Permit to Inject.

#### 4.1.3.3 Detailed description of Geostatistical Model Build

To accurately represent the subsurface over the wider context, GCS has developed a regional mapping workflow. The steps of the workflow are as follows:

Country	Percentage (%)
United States	13
Canada	14
United Kingdom	16
France	16
Germany	17
Italy	18
Spain	19
Portugal	19
Australia	20
New Zealand	21

The grid of the static geomodel model was populated with the results of the geostatistical modeling. To balance model size and achieve a sufficient level of detail, the properties of the cells in the geological model were vertically upscaled to a coarser grid over the central part of the simulation model [REDACTED] While outside of the central part of the simulation model the

areal size of the grid cells has been increased laterally, resulting in a less detailed picture of the subsurface [REDACTED]

#### ***4.1.3.4 Detailed description of Reservoir Simulation Model***

A comprehensive overview of the reservoir simulation model is set forth in a separate document:

[REDACTED]

[REDACTED]

[REDACTED]

[REDACTED]

[REDACTED]

[REDACTED]

[REDACTED]

[REDACTED]

The choice of injection site was predicated on a set of constraints. The constraints are:

1. Sufficient horizontal permeability to ensure injection pressures stayed well below fracturing pressure and the induced seismicity limit at the required injection rates
2. The injection depth should be below ~10,000 ft TVDSS to ensure a large vertical distance between the injection point and the confining Anahuac Formation, and to utilize the high pressure to ensure efficient use of the storage volume. It also reduces the incremental pressure required to store the required volume of CO<sub>2</sub> and this reduces the AoR.
3. Sufficient distance between neighboring injection wells to avoid interference and hence reduced injectivity; sufficient distance from faults (greater than 500 ft per fault) to reduce the risk of reactivating the fault

[REDACTED]

[REDACTED]

[REDACTED]

Plan revision number: v3  
Plan revision date: 06/16/2023



## 5.0 SITE SUITABILITY

## 5.1 Existing well penetrations in the Injection Zone

## 5.2 Model assumptions and conclusion

A high-contrast, black and white image featuring a series of horizontal bars. The bars are primarily black, with white segments at their top and bottom edges. The second bar from the top has a white rectangular gap in its center. The third bar from the top is the most prominent, with a large white rectangular area in its center and a smaller white square near its bottom right corner. The bottom-most bar is also black with white top and bottom edges. The overall pattern is a series of horizontal bands with varying white areas.

Country	Percentage of population aged 65 and older (2010)
United States	13.4%
Canada	13.3%
Australia	13.2%
United Kingdom	13.1%
France	13.0%
Germany	12.9%
Italy	12.8%
Spain	12.7%
Portugal	12.6%
Greece	12.5%
Ireland	12.4%
Belgium	12.3%
Netherlands	12.2%
Sweden	12.1%
Norway	12.0%

The trapping mechanisms are buoyant trapping against local and regional shales, capillary trapping, and dissolution.

No underground source of drinking water was endangered.

### **5.3 Check list of requirements**

Analysis of the regional and local geology near Project Goose Lake demonstrates that the subsurface system is geologically ideal for injection. The massive sandstones of the Oligocene-aged Upper Frio Formation provide effective injection reservoirs in terms of their lateral extent, mineralogical composition, and petrophysical characteristics. Initial studies show that the Injection Zone has the permeability, porosity, thickness, and lateral continuity to accept and contain waste. Shales of the overlying Anahuac Formation possess the necessary confining zone criteria to be effective barriers to upward movement. Additionally, the >7,000 ft overlying, shale-rich Miocene section providing secondary confining.

### **5.4 CO<sub>2</sub> trapping in the Injection Zone**

Carbon dioxide will be confined in the Injection Zone by means of local buoyant trapping in 4-way closures, capillary trapping and dissolution. Extensive modeling and a fault transmissibility study has shown that vertical leakage pathways are not an issue within the project area. Faults were determined to be laterally transmissible between the Injection pay intervals. Additionally, a full well integrity study was undertaken which concluded that there are no manmade leakage pathways within the AoR and no risk to the local USDW.

### **5.5 Injection Zone Storage Capacity**

The Upper Frio Formation Injection Zone is a laterally extensive, high net-to-gross interval with substantial storage capacity, as demonstrated by extensive historical O&G development regionally. Storage capacity has not been directly assessed but ongoing work has concluded that the total storage capacity of the Injection Zone is more than 180 MMT of CO<sub>2</sub>. This mass of CO<sub>2</sub> was securely stored within the storage formation and the maximum injection pressures were substantially less than the estimated fracturing pressure (Figure 3.2.5.2-1).

### **5.6 Primary Confining Zone Integrity**

There are no concerns regarding confining zone integrity on the basis of the work completed to date. The shale-rich Anahuac Formation is a regionally extensive sealing unit, averaging >800 ft gross thickness across Project Goose Lake. Anahuac Formation gross thickness and vertical permeability modeling indicates no breach of the seal by any planned injection activities. Fault analysis indicates no potential for movement of molecules from the Injection Zone vertically along fault planes within the Confining Zone (see Sections 0 Fault Transmissivity and 3.4 Hydrogeology).

### **5.7 Secondary Confinement**

Secondary confinement is not predicted to be necessary for USDW protection. However the Miocene strata that overlies the primary Anahuac seal (Figure 3.2-2), providing multiple additional thick, laterally continuous shale confining zones in a >7,000' thick interval [REDACTED]

## **5.8 CO<sub>2</sub> interaction with subsurface and well materials**

It has been assumed that there will be no geo-chemical interaction between the injected CO<sub>2</sub> and the subsurface formations, beyond the dissolution of some of the gaseous CO<sub>2</sub> into the formation fluids. Additional data collection and geochemical analysis will be undertaken to assess this.

## **6.0 DESCRIPTION OF AoR AND CORRECTIVE ACTION PLAN**

### **6.1 Description of the files submitted for the AoR and the Corrective Action plan**

The fully completed AoR and Corrective Action Plan Report has been submitted via the GSĐT in 'Confidential Business Information' form. All Tabs that require input data within the module have also been completed and submitted via the GSĐT.

The report covers in detail the computational modelling approach to the delineation of the Area of Review (AoR), the Corrective Action Plan relating to existing well penetrations within the AoR and the Reevaluation Schedule for AoR delineation once operations commence. A thorough review of the hydrogeology is also supplied, along with a comprehensive bibliography of references utilized during the AoR modelling execution and reporting phase.

The AoR and Corrective Action Plan Report satisfies rule requirements *40 CFR 146.82(a)(13), 146.84(b) and 146.84(c)*.

<b><i>AoR and Corrective Action GSĐT Submissions</i></b>
<b><i>GSĐT Module:</i></b> AoR and Corrective Action
<b><i>Tab(s):</i></b> All applicable tabs
<i>Please use the checkbox(es) to verify the following information was submitted to the GSĐT:</i>
<input checked="" type="checkbox"/> <i>Tabulation of all wells within AoR that penetrate confining zone [40 CFR 146.82(a)(4)]</i>
<input checked="" type="checkbox"/> <i>AoR and Corrective Action Plan [40 CFR 146.82(a)(13) and 146.84(b)]</i>
<input checked="" type="checkbox"/> <i>Computational modeling details [40 CFR 146.84(c)]</i>

## **7.0 DESCRIPTION OF FINANCIAL RESPONSIBILITY**

### **7.1 Description of the files submitted for the financial responsibility**

The fully completed Financial Responsibility Demonstration Report 40 CFR 146.85 has been submitted via the GSDT in 'Confidential Business Information' form. All Tabs that require input data within the module have also been completed and submitted via the GSDT.

The Financial Responsibility Demonstration submission will satisfy rule requirements *40 CFR 146.82(a)(14) and 146.85*.

#### ***Financial Responsibility GSDT Submissions***

***GSDT Module:*** Financial Responsibility Demonstration

***Tab(s):*** Cost Estimate tab and all applicable financial instrument tabs

*Please use the checkbox(es) to verify the following information was submitted to the GSDT:*

Demonstration of financial responsibility [*40 CFR 146.82(a)(14) and 146.85*]

## **8.0 DESCRIPTION OF WELL CONSTRUCTION PLAN**

### **8.1 Well Construction Overview**

Two injection wells are being proposed: Injector Well 1 and 2. Each Injector Well will have four permanent barriers between USDW and injection activities, two casings, and two cement sheaths. Two additional barriers will act to separate injection fluids from USDW, tubing metal wall and pressurized annular fluid. There will be a total of six man-made barriers and one natural barrier (Confining Zone/Anahuac Formation) to prevent fluids moving to USDW.

### **8.2 Stimulation Program**

No stimulation is planned, and this is not necessary to successfully access the pore volume of the Injection Zone.

### **8.3 Well Construction Procedures**

#### *8.3.1 Prevention of fluid movement into or between USDW's*

[REDACTED]

[REDACTED]

[REDACTED]

[REDACTED]

[REDACTED]

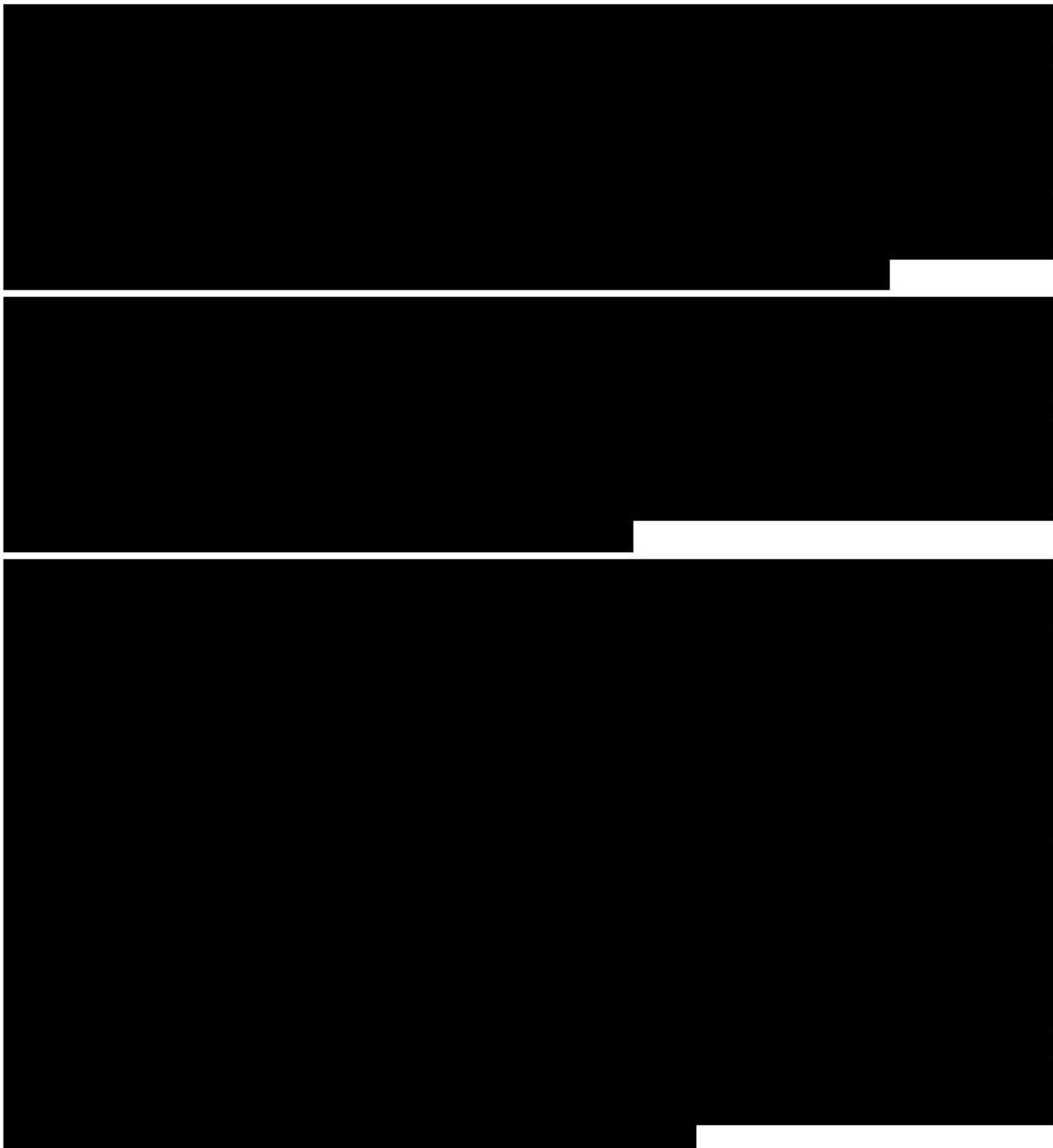
[REDACTED]

#### *8.3.2 Testing and monitoring devices within the borehole and annulus*

[REDACTED]



### *8.3.3 Drilling contingency plans and USDW Protection*



8.3.4 *Effect of average down-hole temperature*

8.3.5 *Structural strength of the proposed casing*

*8.3.6 Details of proposed cement job*

[REDACTED]

*8.3.7 Mechanical integrity of the cement and casing*

[REDACTED]

[REDACTED]

[REDACTED]

*8.3.8 Description of the well construction plan*

[REDACTED]

surveys for the wells.

[REDACTED]

[REDACTED]

[REDACTED]

[REDACTED]

[REDACTED]

[REDACTED]

[REDACTED]



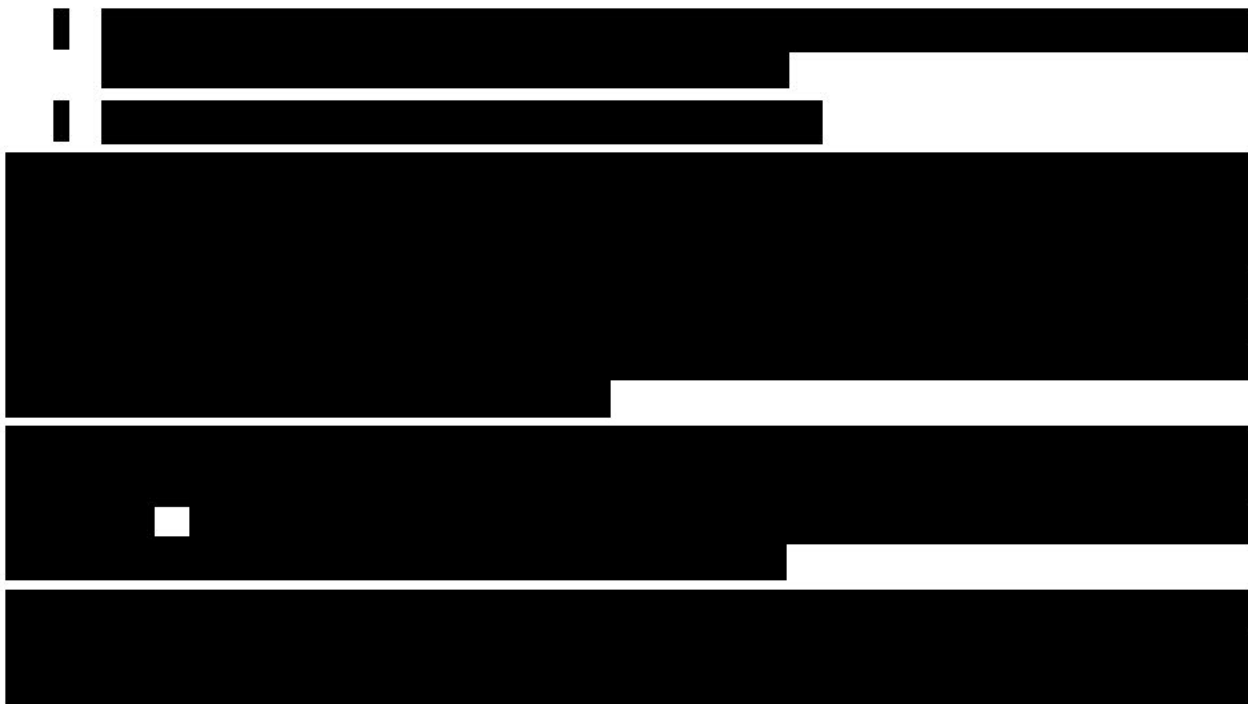
The image consists of a series of horizontal bars, primarily black, set against a white background. The bars are arranged in a staggered, non-uniform pattern. Some bars are very wide, while others are narrow. The vertical positions of the bars also vary, creating a stepped or layered effect. The overall appearance is abstract and could represent a digital signal, a specific data visualization, or a minimalist graphic design. The high contrast between the black bars and the white background makes the image stark and graphic.

The image consists of a series of horizontal bands of varying widths. The majority of the bands are black, while others are white. The white bands are irregular in width, with some being very narrow and others being relatively wide. The image is framed by a thick black border on the left and top, and a thin black border on the right and bottom. The overall effect is abstract and resembles a digital signal or a stylized landscape.

### 8.3.9 Description of the Tubing and Packers

40 CFR 146.86(c) requires that the tubing and packer must be compatible with the fluids which contact their surfaces and meet or exceed recognized standards for the industry. [REDACTED]

A high-contrast, black and white image showing a series of horizontal bars. The bars are mostly black, with white spaces between them. On the far left, there are small black dashes above the first bar. The bars vary in length, with some being very long and others very short. The image is set against a white background.



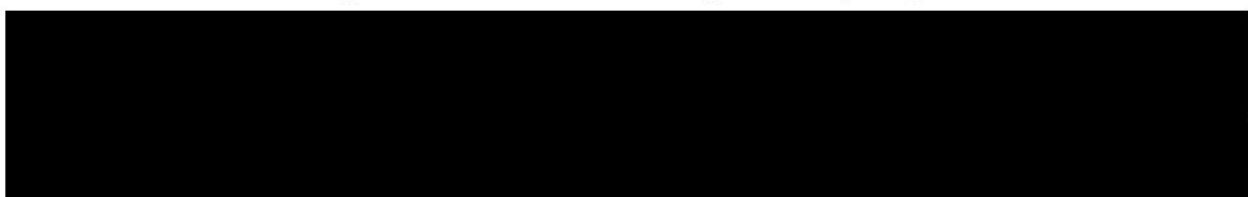
*8.3.10 Grade V5 liquid test*



*8.3.11 Grade V4 liquid test + axial loads*



*8.3.12 Grade V3 liquid test + axial loads + temperature cycling*





*8.3.13 Grade V1 gas test + axial loads + temperature cycling*



## **9.0 DESCRIPTION OF PRE-OPERATIONAL LOGGING AND TESTING PLAN**

### **9.1 Description of the documents that are submitted to the GSDT**

The fully completed Pre-Operational Logging and Testing Plan (“Data Acquisition Plan 40 CFR 146.87”) has been submitted via the GSDT in ‘Confidential Business Information’ form. All Tabs that require input data within the module have also been completed and submitted via the GSDT.

The Data Acquisition Plan 40 CFR 146.87 submission satisfies rule requirements. *40 CFR 146.82(a)(8) and 146.87*

<p><i>Pre-Operational Logging and Testing GSDT Submissions</i></p> <p><b>GSDT Module:</b> Pre-Operational Testing <b>Tab(s):</b> Welcome tab</p> <p><i>Please use the checkbox(es) to verify the following information was submitted to the GSDT:</i></p> <p><input type="checkbox"/> <i>Proposed pre-operational testing program [40 CFR 146.82(a)(8) and 146.87]</i></p>
--

## **10.0 DESCRIPTION OF WELL OPERATION PLAN**

The Well Operation Plan submission will be submitted when the CO<sub>2</sub> streams have been identified for the nameplate capacity of Project Goose Lake.

### **10.1 Operational Procedures**

The Operational Procedures [40 CFR 146.82(a)(10)] submission is currently being prepared and an update to this report will be filed via the GSDT when it is complete.

The outline of steps necessary to conduct injection at each injection well are provided in the following sections.

#### ***10.1.1 Injector Well No.1***

GCS has developed key objectives for operations which consist of a) maintaining and achieving a safe, reliable and available sequestration system; b) ensuring operations within prescribed safe limits; c) minimizing stop/start injection of CO<sub>2</sub> and cycling of the injection wells.

Please see [REDACTED] for the operational parameters for Injector Well No. 1. Values for the operational parameters were calculated using Prosper, a well modeling program, and Reveal, a reservoir simulation program, each developed by Petroleum Experts Limited of Edinburgh, UK (Petroleum Experts, 2020). Please see further discussion on the use of each program in Section 2.0 and 2.2 of the “Area of Review and Corrective Action Plan 40 CFR 146.84(b)” permit document.

Please note the bottom-hole pressures are significantly smaller than the estimated fracture pressure and induced seismicity pressure. [REDACTED]

Currently, it is assumed that the injection rates will be constant throughout the lifetime of the project, with the exception of maintenance periods.

In calculating the final total injected masses [REDACTED] was assumed. That is, the injection rate was discounted by [REDACTED] to calculate the total mass injected.

GCS will employ a rigorous testing and monitoring plan for Project Goose Lake which satisfies well operation planning required by 146.88, 146.89 and 146.90. Please see Class VI Permit Application Testing and Monitoring Plan 40 CFR 146.90 for a complete discussion of continuous recording of operational parameters and carbon dioxide stream analysis. Please also see Section 7.0 Description of Well Construction Plan which satisfies operational parameters specific to injection well and Injection Zone.

### ***10.1.2 Injector Well No.2***

GCS has developed key objectives for operations which consist of a) maintaining and achieving a safe, reliable and available sequestration system; b) ensuring operations within prescribed safe limits; c) minimizing stop/start injection of CO<sub>2</sub> and cycling of the injection wells.

Please see [REDACTED] for the operational parameters for Injector Well No. 2. Values for the operational parameters were calculated using Prosper, a well modeling program, and Reveal, a reservoir simulation program, each developed by Petroleum Experts Limited of Edinburgh, UK (Petroleum Experts, 2020). Please see further discussion on the use of each program in Section 2.0 and 2.2 in the Class VI Permit Application Area of Review and Corrective Action Plan 40 CFR 146.84(b).

Please note the bottom-hole pressures are significantly smaller than the estimated fracture pressure and induced seismicity pressure. [REDACTED]

Currently, it is assumed that the injection rates will be constant throughout the lifetime of the project, with the exception of maintenance periods.

In calculating the final total injected masses [REDACTED] was assumed. That is, the injection rate was discounted by [REDACTED] to calculate the total mass injected.

GCS will employ a rigorous testing and monitoring plan for Project Goose Lake which satisfies well operation planning required by 146.88, 146.89 and 146.90. Please see Class VI Permit Application Testing and Monitoring Plan 40 CFR 146.90 for a complete discussion of continuous recording of operational parameters and carbon dioxide stream analysis. Please also see Section 7.0 Description of Well Construction Plan which satisfies operational parameters specific to injection well and Injection Zone.

### **10.2 Description of the proposed Carbon Dioxide Stream**

The Description of the proposed Carbon Dioxide Stream [40 CFR 146.82(a)(7)(iii) and (iv)] submission is currently being prepared and will be filed via the GSDT when it is complete.

## **11.0 DESCRIPTION OF TESTING AND MONITORING PLAN**

### **11.1 Description of the documents that are submitted to the GSDT**

The Testing and Monitoring Plan Report has been submitted via the GSDT in ‘Confidential Business Information’ form. All tabs that require input data within the module have also been completed and submitted via the GSDT. A ‘Confidential Business Information’ version has been submitted to Region VI of EPA as well.

The report covers in detail the overall strategy and approach for testing and monitoring, carbon dioxide stream analysis, continuous recording of operational parameters, corrosion monitoring, above confining zone monitoring, external mechanical integrity testing, pressure fall off testing, carbon dioxide plume and pressure front tracking, environmental monitoring at the surface, sampling/analytical procedures. A Class IV well Quality Assurance and Surveillance Plan (QASP) was submitted as an appendix along with additional information relation to project management, data generation and acquisition, assessment and oversight and data validation and usability.

The Testing and Monitoring Plan Report satisfies rule requirements 40 CFR 146.82(a)(15) and 146.90.

#### ***Testing and Monitoring GSDT Submissions***

***GSDT Module:*** Project Plan Submissions

***Tab(s):*** Testing and Monitoring tab

*Please use the checkbox(es) to verify the following information was submitted to the GSDT:*

Testing and Monitoring Plan [40 CFR 146.82(a)(15) and 146.90]

## **12.0 DESCRIPTION OF INJECTION AND WELL PLUGGING PLAN**

### **12.1 Description of the documents that are submitted to the GSDT**

The Injection and Well Plugging Plan has been submitted via the GSDT in ‘Confidential Business Information’ form. All Tabs that require input data within the module have also been completed and submitted via the GSDT. A ‘Confidential Business Information’ version has been submitted to Region VI of EPA as well.

The report covers in detail the planned tests and measurements to determine the bottom hole reservoir pressure, Planned External Mechanical Integrity Test, Information on Plugs, methods used for volume calculations, notifications, permits and inspections required, plugging procedures and contingency procedures/measures.

The Injection and Well Plugging Plan satisfies rule requirements 40 CFR 146.82(a)(16) and 146.92(b).

<b><i>Injection Well Plugging GSDT Submissions</i></b>
<b><i>GSDT Module:</i></b> Project Plan Submissions
<b><i>Tab(s):</i></b> Injection Well Plugging tab
<i>Please use the checkbox(es) to verify the following information was submitted to the GSDT:</i>
<input checked="" type="checkbox"/> <i>Injection Well Plugging Plan [40 CFR 146.82(a)(16) and 146.92(b)]</i>

## **13.0 DESCRIPTION OF POST-INJECTION SITE CARE AND SITE CLOSURE PLAN**

### **13.1 Description of the documents that are submitted to the GSDT**

The Post Injection Site Care and Site Closure Plan (PISC) Plan has been submitted via the GSDT in ‘Confidential Business Information’ form. All Tabs that require input data within the module have also been completed and submitted via the GSDT. A ‘Confidential Business Information’ version has been submitted to Region VI of EPA as well.

The report covers in detail the pre and post injection pressure differential, post-injection monitoring plan, alternative post-injection site care timeframe, non-endangerment demonstration criteria, site closure plan and QASP.

An Alternative PISC timeframe has been proposed as part of the GSDT submission. GCS has indicated an alternative PISC timeframe of 10 years instead of the default 50 years.

The Post Injection Site Care and Site Closure Plan satisfies rule requirements 40 CFR 146.82(a)(17) and 146.93(a) and the Alternative PISC submission satisfies rule requirements 40 CFR 146.82(a)(18) and 146.93(c).

<p><b><i>PISC and Site Closure GSDT Submissions</i></b></p> <p><b>GSDT Module:</b> Project Plan Submissions <b>Tab(s):</b> PISC and Site Closure tab</p> <p><i>Please use the checkbox(es) to verify the following information was submitted to the GSDT:</i></p> <p><input checked="" type="checkbox"/> PISC and Site Closure Plan [40 CFR 146.82(a)(17) and 146.93(a)]</p>
<p><b>GSDT Module:</b> Alternative PISC Timeframe Demonstration <b>Tab(s):</b> All tabs (only if an alternative PISC timeframe is requested)</p> <p><i>Please use the checkbox(es) to verify the following information was submitted to the GSDT:</i></p> <p><input checked="" type="checkbox"/> Alternative PISC timeframe demonstration [40 CFR 146.82(a)(18) and 146.93(c)]</p>

## **14.0 DESCRIPTION OF EMERGENCY AND REMEDIAL RESPONSE PLAN**

### **14.1 Description of the documents that are submitted to the GSRT**

The Emergency and Remedial Response Plan has been submitted via the GSRT in 'Confidential Business Information' form. All Tabs that require input data within the module have also been completed and submitted via the GSRT. A 'Confidential Business Information' version has been submitted to Region VI of EPA as well.

The report covers in detail the local resources and infrastructure, potential risk scenarios, response personnel and equipment, emergency communications plan, a plan review and staff training and exercise procedures.

The Emergency and Remedial Response Plan Report satisfies rule requirements 40 CFR 146.82(a)(19) and 146.94(a).

<i><b>Emergency and Remedial Response GSRT Submissions</b></i>
<i><b>GSRT Module:</b></i> Project Plan Submissions
<i><b>Tab(s):</b></i> Emergency and Remedial Response tab
<i>Please use the checkbox(es) to verify the following information was submitted to the GSRT:</i>
<input checked="" type="checkbox"/> Emergency and Remedial Response Plan [40 CFR 146.82(a)(19) and 146.94(a)]

## **15.0 INJECTION DEPTH WAIVER AND ACQUIFER EXEPMTION EXPANSION**

Not applicable as GCS is not seeking a waiver or exemption.

## **16.0 DESCRIPTION OF ANY ADDITIONAL INFORMATION REQUESTED**

### **16.1 Description of the documents that has been requested by the UIC Program Director**

No documents have been requested by the UIC Program Director.

### **16.2 Optional Additional Project Information [40 CFR 144.4]**

#### ***16.2.1 Wild and Scenic Rivers Act, 16 U.S.C. 1273 et seq***

The National Wild and Scenic Rivers System was created by Congress in 1968 (Public Law 90-542; 16 U.S.C. 1271 et seq.) to preserve certain rivers with outstanding natural, cultural, and recreational values in a free-flowing condition for the enjoyment of present and future generations. The Act is notable for safeguarding the special character of these rivers, while also recognizing the potential for their appropriate use and development. It encourages river management that crosses political boundaries and promotes public participation in developing goals for river protection. Scenic River Areas are those rivers or sections of rivers that are free of impoundments, with shorelines or watersheds still largely primitive and shorelines largely undeveloped, but accessible in places by roads.

There are no scenic rivers within the project area.

#### ***16.2.2 National Historic Preservation Act of 1966, 16 U.S.C. 470 et seq***

The National Historic Preservation Act (NHPA) ensures that Federal agencies consider historic properties—defined as any prehistoric or historic site, district, building, structure, or object eligible for inclusion on the National Register of Historic Places (NRHP)—in their proposed programs, projects, and actions before initiation. There are no sites located within the project area that will be impacted.

#### ***16.2.3 Endangered Species Act, 16 U.S.C. 1531 et seq***

Federally listed species under the protection of the ESA in the vicinity of the Project were identified by a review of publicly available databases. A search using the USFWS Environmental Conservation Online System Information, Planning, and Conservation (IPaC) System consultation tool (Accessed in 2022) for the Project lease area was used to generate an official species list to fulfill the requirements of Section 7 of the ESA.

Based on the results of the IPaC consultation tool no species will be impacted for the proposed project. Species identified included: manatee (no suitable habitat), red-cockaded woodpecker (no suitable habitat), and the eastern black rail (critical habitat not defined). Additionally, according to IPaC, there are no critical habitats at this location.

#### ***16.2.4 Coastal Zone Management Act, 16 U.S.C. 1451 et seq***

The Coastal Zone Management Act (CZMA) defines the coastal zones wherein development must be managed to protect areas of natural resources unique to coastal regions. States are required to define the area that will comprise their coastal zone and develop management plans that will protect these unique resources through enforceable policies of state coastal zone management (CZM) programs. Federal as well as local actions must be determined to be consistent with the

CZM plans and policies before they can proceed. As defined in the Act, the coastal zone includes coastal waters extending to the outer limit of state submerged land title and ownership, adjacent shorelines, and land extending inward to the extent necessary to control shorelines. While this is a federal law, it is administered by the State of Louisiana.

The Permits/Mitigation Division of the Louisiana Department of Natural Resources is charged with implementing the Louisiana Coastal Resources Program (LCRP) under authority of the State and Local Coastal Resources Management Act, as amended (Act 361, La. R.S. 49:214.21 et seq). This law seeks to protect, develop, and, where feasible, restore or enhance the resources of the state's coastal zone. Its broad intent is to encourage multiple uses of resources and adequate economic growth while minimizing adverse effects of one resource use upon another without imposing undue restrictions on any user. Besides striving to balance conservation and resources, the guidelines, and policies of the LCRP also help to resolve user conflicts, encourage coastal zone recreational values, and determine the future course of coastal development and conservation. The guidelines are designed so that development in the Coastal Zone can be accomplished with the greatest benefit and the least amount of damage. The LCRP is an effort among Louisiana citizens, as well as state, federal and local advisory and regulatory agencies. The Permits/Mitigation Division regulates development activities and manages the resources of the Coastal Zone. A Coastal Use Permit (CUP) Program has been established by the Act as part of the LCRP to help ensure the management and reasonable use of the state's coastal wetlands. The project area is in the Louisiana coastal zone and will require a CUP.

#### *16.2.5 Subsurface cleanup sites*

Location searches within the project AoR for subsurface cleanup sites listed below:

- EPAs Superfund Sites (NPL)
- EPAs Brownfields
- EPAs Underground Storage Tanks (USTs)
- EPAs Resource Conservation and Recovery Act (RCRA) (Hazardous & Non-hazardous)

A geospatial search for all cleanup sites within the project AoR was completed using ArcGIS. The EPA data sources used are detailed in the following sections.

##### ***16.2.5.1 Data Sources (EPA)***

###### **EPA Geospatial Download Service <https://www.epa.gov/frs/geospatial-data-download-service>**

- Geospatial Data Download Service; To improve public health and the environment, the EPA collects information about facilities or sites subject to environmental regulation. The EPA Geospatial Data Access Project provides downloadable files of these facilities or sites.

###### **Superfund Sites (NPL) <https://www.epa.gov/superfund/search-superfund-sites-where-you-live>**

- EPA ArcGIS Web Map with source data for Superfund National Priorities (NPL). Where you live Map:  
<https://epa.maps.arcgis.com/apps/webappviewer/index.html?id=33cebcdfdd1b4c3a8b51d416956c41f1>

- Advanced Search: For National Priorities List and Non-NPL Sites. Search the Superfund data system for active and archived NPL and non-NPL sites: <https://cumulis.epa.gov/supercpad/cursites/srchsites.cfm>

## Brownfields

- EPA's Brownfields Program provides grants and technical assistance to communities, states, tribes and others to assess, safely clean up and sustainably reuse contaminated properties. To learn about EPA's broader efforts to put previously contaminated properties back into productive use, read about our Land Revitalization Program: <https://www.epa.gov/brownfields>
- Waste Origin: Wastes generated onsite and Wastes received from offsite facility: <https://enviro.epa.gov/envirofacts/br/search/results>

## Underground Storage Tanks (USTs)

- Underground Storage Tanks (USTs); Approximately 542,000 underground storage tanks (USTs) nationwide store petroleum or hazardous substances. The greatest potential threat from a leaking UST is contamination of groundwater, the source of drinking water for nearly half of all Americans. EPA, states, territories, and tribes work in partnership with industry to protect the environment and human health from potential releases: <https://www.epa.gov/ust>
- EPA developed UST Finder, a web map application containing a comprehensive, state-sourced national map of underground storage tank (UST) and leaking UST (LUST) data. It provides the attributes and locations of active and closed USTs, UST facilities, and LUST sites from states as of 2018-2019 and from Tribal lands and US territories as of 2020-2021. UST Finder contains information about proximity of UST facilities and LUST sites to: surface and groundwater public drinking water protection areas; estimated number of private domestic wells and number of people living nearby; and flooding and wildfires. UST Finder can import additional data layers and export UST facility and LUST site information for use by other software programs: <https://www.epa.gov/ust/ust-finder>
- EPA ArcGIS Web Map with source data for UST (UST Finder): <https://epa.maps.arcgis.com/apps/webappviewer/index.html?id=b03763d3f2754461adf86f121345d7bc>

## Resource Conservation and Recovery Act (RCRA) (Hazardous & Non-hazardous)

- Resource Conservation and Recovery Act (RCRA) Overview; RCRA gives EPA the authority to control hazardous waste from the "cradle-to-grave." This includes the generation, transportation, treatment, storage and disposal of hazardous waste. To achieve this, EPA develops regulations, guidance and policies that ensure the safe management and cleanup of solid and hazardous waste, and programs that encourage source reduction and beneficial reuse: <https://www.epa.gov/rcra/resource-conservation-and-recovery-act-rcra-overview>

#### ***16.2.5.2 Superfund Sites (NPL)***

Upon conducting the data search from the sources above, no Superfund sites were identified within the project AoR.

#### ***16.2.5.3 Brownfields***

Upon conducting the data search from the sources above, no Brownfields program sites were identified within the project AoR.

#### ***16.2.5.4 Underground Storage Tanks (USTs)***

Upon conducting the data search from the sources above, no UST Facilities were identified within the project AoR.

#### ***16.2.5.5 Resource Conservation and Recovery Act (RCRA) (Hazardous & Non-hazardous)***

Upon conducting the data search from the sources above, no Hazardous or Non-hazardous waste facilities were identified within the project AoR.

## **17.0 REFERENCES – See A.4.1 References**

(Alexander and Handschy, 1998): Alexander, L.L., and Handschy, J.W., 1998, Fluid flow in a faulted reservoir system: Fault trap analysis for the Block 330 Field in Eugene Island, South Addition, Offshore Louisiana: Am. Assoc. Petroleum Geologists Bull., v. 82 n. 3, p. 387-411.

(Allan, 1989): Allan, U.S., 1989, Model for hydrocarbon migration and entrapment within faulted structures: Am. Assoc. Petroleum Geologists Bull., v. 8, p. 803-811.

(Anadrill, 1987): Anadrill Schlumberger, "End of Well Report, E.I. DuPont De Nemours and Company, BMT Waster Well #3", Beaumont, Jefferson County, Texas", DuPont File 0111408, June 1987.

(Antonellini and Aydin, 1994): Antonellini, M., and Aydin, A., 1994, Effect of faulting on fluid flow in porous sandstones: petrophysical properties: Am. Assoc. Petroleum Geologists Bull., v. 78, n. 3, p. 355-377.

(Baker, 1979): Baker, E.T., 1979, Stratigraphic and hydrogeologic framework of part of the coastal plain of Texas, U.S. Department of the Interior Geology Survey, Open File report 77-712

(Baria et al., 1982): Baria, L.R., Stoudt, D.L., Victoria, P.M., and Crevello, P.D., 1982, Upper Jurassic reefs of Smackover Formation, United States Gulf Coast: Am. Assoc. Petroleum Geologists Bull., v. 66, n. 10, p. 1449-1482.

(Berg and Haveman, 1995): Berg, R.R., and Haveman, A.L., 1995, Sealing properties of Tertiary growth faults, Texas Gulf Coast: Am. Assoc. Petroleum Geologists Bull., v. 79, n. 3, p. 375-393.

(Berg, 1975): Berg, R.R., 1975, Capillary pressures in stratigraphic traps: Am. Assoc. Petroleum Geologists Bull., v. 59, p. 939-956.

(Bethke et al., 1988): Bethke, C.M., Harrison, W.J., Upson, C., and Altaner, S.P., 1988, Supercomputer analysis of sedimentary basins: Science, v. 239, Washington, D. C.

(Bouvier et al., 1989): Bouvier, J.D., Kaars-Sijpesteijn, C.H., Kluesner, D.F., and Onyejekwe, C.C., 1989, Three-Dimensional seismic interpretation and fault sealing investigations, Nigeria: Am. Assoc. Petroleum Geologists Bull., v. 72, p. 1397-1414.

(Clark, 1988): Clark, J.E., 1988, Groundwater flow in deep saline aquifers: Special Session on the Hydrologic and Geochemical Processes Involved in Deep Injection of Liquid Wastes, Groundwater Committee of the American Geophysical Union and the International Association of Hydrogeologists, Baltimore, Maryland.

(Clark et al., 1987): Clark, J.E., Howard, M.R., and Sparks, D.K., 1987, Factors that can Cause Abandoned Wells to Leak as Verified by Case Histories from Class II injection, Texas

Railroad Commission files: International Symposium on Subsurface Injection of Oilfield Brines, Underground Injection Practices Council, New Orleans, LA., p. 166-223.

(Clark et al., 1991): Clark, J.E., Papadeas, P.W., Sparks, D.K., and R.R. McGowen, 1991, Gulf Coast Borehole Closure Test Well, Orangefield, Texas; UIPC 1991 Summer Symposium, Reno, Nevada, talk presented July 30, 1991.

(Coker, 2006): Coker, M.O., 2006, Aquitanian (Lower Miocene) Depositional Systems: Vinton Dome, Onshore, Gulf of Mexico, Southwest Louisiana. The Faculty of The Department of Geosciences University of Houston.

(Core Laboratories, 1987a): Core Laboratories, DuPont de Nemours and Company, DuPont File 00008564, 1987

(Core Laboratories, 1987b): Core Laboratories, Petrographic study of selected sidewall core samples from a Beaumont Disposal Well for DuPont Chemicals, DuPont File 00008603, 1987

(Coleman and Galloway, 1990): Coleman, J. and Galloway, W.E., 1990, Petroleum Geology of the Vicksburg Formation, Goliad County, Texas: South Texas Geological Society Bulletin, v. 30, no. 19, p. 9-25

(Davis, 1986): Davis, K.E., 1986, Factors Effecting the Area of Review for Hazardous Waste Disposal Wells: Proceedings of the International Symposium on Subsurface Injection of Liquid Wastes, New Orleans, National Water Well Association, Dublin, OH, p. 148-194.

(Davis et al., 1989): Davis, S.D., Pennington, W.D., and Carlson, S.M., 1989, A compendium of earthquake activity in Texas: The University of Texas at Austin, Bureau of Economic Geology, Geological Circular 89-3, 27 p. doi.org/10.23867/gc8903D

(DEQ of Louisiana, 2009): DEQ of Louisiana, 2009, Appendix 4 to the 2009 Triennial Summary Report in the Evangeline Summary Report, 2007

(Diamond and Akinfiev, 2003): Diamond, L.W., and Akinfiev, N.N., 2003, "Solubility of CO<sub>2</sub> in water from -1.5 to 100 oC and from 0.1 to 1000 MPa: evaluation of literature data and thermodynamic modelling", Fluid Phase Equilibria, 208 (2003) 265-290.

(Doughty, 2007): Doughty, C., Freifeld, B., and Trautz, R., 2007, "Site characterisation for CO<sub>2</sub> geologic storage and vice versa: the Frio brine pilot, Texas, USA as a case study", Environ Geol 54, 1635–1656.

(Downey, 1984): Downey, M.W., 1984, Evaluating seals for hydrocarbon accumulations: Am. Assoc. Petroleum Geologists Bull., v. 68, n. 11, p. 1752-1763.

(Eaton, 1969): Eaton, B.A., 1969, Fracture gradient prediction and its application in oil field operations: Journal of Petroleum Technology, pp. 1353-1360.

(Ellsworth, 2013): Ellsworth, W.L., 2013, Injection-induced earthquakes: *Science*, v.341, p. 6142-6148.

(Engelder, 1974): Engelder, J.T., 1974, Cataclasis and the generation of fault gouge: *Geological Society of America*.

(Engelder et al., 1997): Engelder, J.T., and Leftwich Jr., J.T., 1997, "A pore-pressure limit in overpressured South Texas oil and gas fields", AAPG Memoir 67: Seals, Traps, and the Petroleum System, Edited by R. C. Surdam, p 255-267.

(Foote et al., 1984): Foote, R.Q., Martin, R.G., Khan, A.S., Garrison, L.E., Massingill, L.M., Wells, R.H., Berryhill Jr., H.L., 1984, Summary report on the regional geology, petroleum potential, environmental consideration for development, and estimates of undiscovered recoverable oil and gas resources of the United States Gulf of Mexico Continental Margin in the area of proposed Oil and Gas Lease Sales Nos. 81 and 84.

(Frohlich et al., 2010): Frohlich, C., Potter, E., Hayward, C., and Stump, B., 2010, Dallas-Fort Worth earthquakes coincident with activity associated with natural gas production: *The Leading Edge*, v. 29, p. 270-275.

(Galloway, 1985): Galloway, W.E., 1985, Depositional framework of the lower Miocene (Fleming) episode Northwest Gulf Coast Basin: *Gulf Coast Association of Geologists Society Transactions*, v. 35, pp. 67-73.

(Galloway et al., 1982a): Galloway, W.E., Hobday, D.K., and Magara, K., 1982a, Frio Formation of the Texas Gulf of Mexico Basin-depositional systems, structural framework, and hydrocarbon origin, migration, distribution, and exploration potential: *Bureau of Economic Geology, Report of Investigations No. 122*, The University of Texas at Austin, Austin, Texas, p. 78.

(Galloway et al., 1982b): Galloway, W.E., Henry, C.G., and Smith, G.E., 1982b, Depositional framework, hydrostratigraphy, and uranium mineralization of the Oakville sandstone (Miocene) Texas Coastal Plain: *Bureau of Economic Geology, Report of Investigations No. 113*, The University of Texas at Austin, Austin, Texas, 59 p.

(Ghanbari et al., 2006): Ghanbari, S., Al-Zaabi, Y., Pickup, G.E., Mackay, E., Gozalpour, F., and Ford, A.C., 2006, "Simulation of CO<sub>2</sub> storage in saline aquifers", *Trans. IChemE, Part A* September 2006, *Chemical Engineering Research and Design*, 84 (A9), 764-775.

(Gray et al., 1980): Gray, G.R., Darley, H.C.H., and Rodgers, W.F., 1980, *Composition and Properties of Oil Well Drilling Fluids*: Gulf Publishing Company, Houston Texas.

(Gregory, 1966): Gregory, J.L., 1966, A lower Oligocene delta in the subsurface of southeastern Texas: *Gulf Coast Assoc. Geol. Soc. Trans.*, v. 16, p. 227-241

(Gundogan, 2011): Gundogan, O., 2011, *Geochemical Modelling of CO<sub>2</sub> storage*, submitted for the degree of Doctor of Philosophy, *Hariot-Watt University, Institute of Petroleum Engineering*

(Handin, 1963): Handin, H., 1963, Experimental deformation of sedimentary rocks under confining pressure: Pore pressure tests: Am. Assoc. Petroleum Geologists Bull., v. 47, pp. 717-755.

(Harder, 1960): Harder, A.H., 1960, The geology and groundwater resources of Calcasieu Parish, Louisiana, Geological Survey Water-Supply Paper 1488

(Harding and Tuminas, 1989): Harding, T.P., and Tuminas, A.C., 1989, Structure of hydrocarbon traps sealed by basement normal block faults at stable flank of foredeep basins and at rift basins: Am. Assoc. Petroleum Geologists Bull., v. 73, p. 812-840.

(Hiland, 2010): Hiland, P., 2010, Generic Issue 199 (GI-199), Implications of updated probabilistic seismic hazard estimates in central and eastern United States on existing plants, Safety Risk Assessment: Nuclear Regulatory Commission (<https://web.archive.org/web/20170525170632/http://msnbcmedia.msn.com/i/msnbc/Sect ions/NEWS/quake%20nrc%20risk%20estimates.pdf>)

(Horton, 2012): Horton, S., 2012, Disposal of hydrofracking waste fluid by injection into subsurface aquifers triggers earthquake swarm in central Arkansas with potential for damaging earthquake: Seismological Research Letters, v. 83, no. 2, p. 250-260.

(Hosseini, 2019): Hosseini, Seyyed of the Bureau of Economic Geology at the University of Texas in Austin, Texas, USA (private communication).

(Hovorka et al., 2008): Hovorka, S.D. et al., 2008, “Frio final technical report – OSTI.gov” [www.osti.gov](http://www.osti.gov).

(Hovorka et al., 2018): Hovorka, S.D., Tutton. P., Ramón H. Treviño, 2018, “Feasibility study of CO<sub>2</sub> storage in saline formations in the region of the planned Lake Charles Methanol Plant”, Final Report, Gulf Coast Carbon Center, Bureau of Economic Geology, Jackson School of Geosciences, The University of Texas at Austin, July 30, 2018.

(Jackson and Galloway, 1984): Jackson, M.P.A., and Galloway, W.E., 1984, Structural and depositional styles of Gulf Coast Tertiary continental margins: Application to hydrocarbon exploration: Am. Assoc. Petroleum Geologists, Continuing Education Course Note Series No. 25, p. 226.

(Jev et al., 1993): Jev, B.I., Kaars-Sijpesteijn, C.H., Peters, M.P.A.M., Watts, N.L., and Wilkie, J. T., 1993, Akoso Field, Nigeria: Use of integrated 3-D seismic, fault slicing, clay smearing, and RFT pressure data on fault trapping and dynamic leakage: Am. Assoc. Petroleum Geologists Bull., Volume 77, p. 1389-1404.

(Johnston and Greene, 1979): Johnston, O.C., and Greene, C.J., 1979, Investigation of Artificial Penetrations in the Vicinity of Subsurface Disposal Wells: Texas Department of Water Resources.

(Jolley et al., 2007): Jolley, S.J., Dijk, H., Lamens, J.H., Fisher, Q., Manzocchi, T., Eikmans, H., Huang, Y., 2007, Faulting and fault sealing in production simulation models: Brent Province, northern North Sea: *Petroleum Geoscience*, v. 13, p. 321-340

(Jones and Haimson, 1986): Jones, T.A., and Haimson, J.S., 1986, Demonstration of Confinement: An Assessment of Class 1 Wells in the Great Lakes and Gulf Coast Regions: *Journal of the Underground Injection Practices Council*, Number 1, pp. 279-317.

(Juanes et al., 2006): Juanes, R., Spiteri, E.J., Orr Jr., F.M., and Blunt, M.J., 2006, "Impact of relative permeabilities on geological CO<sub>2</sub> storage", *Water Resources Research*, Vol.42 W12418.

(Jung et al., 2017): Jung, H., Singh, G., Espinoza, N., and Wheeler, M.F., 2017, "An integrated case study of the Frio CO<sub>2</sub> sequestration pilot test for safe and effective carbon storage including compositional flow and geomechanics", *SPE Reservoir Simulation Conference*, Montgomery, Texas, USA, 20-22 February 2017, SPE 182710-MS.

(Keranen et al., 2013): Keranen, K.M., Savage, H.M., Abers, G.A., and Cochran, E.S., 2013, Potentially induced earthquakes in Oklahoma, USA: Links between wastewater injection and the 2011 M 5.7 earthquake sequence: *Geology*, v. 41, p. 699-702.

(Kharaka et al., 2006): Kharaka, Y.K., Cole, D.R., Hovorka, S.D., Gunter, W.D., Knauss, K.G., and Freifield, B.M., 2006, "Gas-water-rock interactions in Frio formation following CO<sub>2</sub> injection: Implications for the storage of greenhouse gases in sedimentary basins", *Geology*, July 2006, v.34, no.7, 577-580.

(Knipe, 1992): Knipe, R.J., 1992, Faulting processes and fault seal: in R.M. Larsen, H. Brekke, B.T. Larsen, and E. Talleras, eds., *Structural and tectonic modeling and its application to petroleum geology*: Elsevier, Amsterdam, p. 325-342.

(Knipe, 1997): Knipe, R.J., 1997, Juxtaposition and seal diagrams to help analyze fault seals in hydrocarbon reservoirs: *Am. Assoc. Petroleum Geologists Bull.*, v. 81, n. 2, pp. 187-195.

(Knott, 1993): Knott, Steven D., 1993, Fault seal analysis in the North Sea: *The American Association of Petroleum Geologists Bulletin*, v. 77, p. 778-792.

(Kreitler, 1986): Kreitler, C.W., 1986, Hydrogeology of sedimentary basins as it relates to deep-well injection of chemical wastes: *Proceedings of the International Symposium Subsurface Injection of Liquid Wastes*, New Orleans, National Water Well Assoc., Dublin, Ohio, p. 398-416.

(Krevor et al., 2012): Krevor, S.C.M., Pini, R., Zuo, L., and Benson, S.M., 2012, "Relative permeability and trapping of CO<sub>2</sub> and water in sandstone rocks at reservoir conditions", *Water Resources Research*, Vol.48, W02532.

(Kumar et al., 2005): Kumar, A., Ozah, R., Noh, M., Pope, G.A., Bryant, S., Sepehrnoori, K., and Lake, L. W., 2005, "Reservoir simulation of CO<sub>2</sub> storage in deep saline aquifers", SPE Journal, September 2005, pp 336 – 348.

(Leeds and Associates, 1989): Leeds, D.J. and Associates, 1989, Seismic Effects: Dupont Sabine Works, DuPont Sabine River Works HWDIR Exemption Petition

(Lehner and Pilaar, 1991): Lehner, F.K., and Pilaar, W.F., 1991, On a mechanism of clay smear emplacement in synsedimentary normal faults: Am. Assoc. Petroleum Geologists Bull., v. 75, p. 619.

(Lindsey et al., 1993): Lindsey, N.G., Murphy, F.C., Walsh, J.J., and Watterson, J., 1993, Outcrop studies of shale smear on fault surfaces; International Association of Sedimentologists Special Publication 15, p. 113-123.

(Loucks et al., 1986): Loucks, R.G., Dodge, M.M., and Galloway, W.E., 1986, Controls on porosity and permeability of hydrocarbon reservoirs in lower Tertiary sandstones along the Texas Gulf Coast: Bureau of Economic Geology, Report of Investigations No. 149, The University of Texas at Austin, Austin, Texas, 78 p.

(Lovelace et al., 2004): Lovelace, J.K., Fontenot, J.W., and Frederick, C.P., 2004, Withdrawals and water levels, and specific Conductance in the Chicot Aquifer System in Southwestern Louisiana, 2000-03, Scientific Investigations Report 2004-5212

(Mancini et al., 1985): Mancini, E.A., Mink, R.M., Bearden, B.L., and Wilkerson, R.P., 1985, Norphlet Formation (Upper Jurassic) of southwestern and offshore Alabama: environments of deposition and petroleum geology: Am. Assoc. Petroleum Geologists Bull., v. 69, n. 6, p. 881-889.

(Manzocchi et al., 1999): Manzocchi, T., Walsh, J.J., Nell, P., Yielding, G., 1999, Fault transmissibility multipliers for flow simulation models: Petroleum Geoscience, v. 5, p. 53-63.

(Matthews and Kelly, 1967): Matthews, W. R., and Kelly, J., 1967, How to Predict Formation Pressure and Fracture Gradient from Electric and Sonic Logs: Oil and Gas Journal.

(McCubbin, 1981): Donald G. McCubbin, 1981. "Barrier-Island and Strand-Plain Facies", Sandstone Depositional Environments, Peter A. Scholle, Darwin Spearing

(Meckel et al., 2017): Meckel, T.A., Nicholson, A.J., and Trevino, R.H., 2017, "Capillary Aspects of Fault-Seal Capacity for CO<sub>2</sub> Storage, Lower Miocene, Texas Gulf of Mexico", Chapter 4 in Geological CO<sub>2</sub> Sequestration Atlas of Miocene Strata, Offshore Texas State Waters, Bureau of Economic Geology.

(National Earthquake Information Center): [https://www.usgs.gov/natural-hazards/earthquake-hazards/national-earthquake-information-center-neic?qt-science\\_support\\_page\\_related\\_con=3#qt-science\\_support\\_page\\_related\\_con](https://www.usgs.gov/natural-hazards/earthquake-hazards/national-earthquake-information-center-neic?qt-science_support_page_related_con=3#qt-science_support_page_related_con)

(Nicholson, 2012): Nicholson, A.J., 2012, "Empirical analysis of fault seal capacity for CO2 sequestration. Lower Miocene, Texas Gulf Coast," University of Texas, Austin, MSc Thesis.

(Nyman et al., 1990): Nyman, D.J., Halford, K.J., and Martin, A.M., 1990, Geohydrology and Simulation Flow in the Chicot Aquifer System of Southwestern Louisiana, Water Resources Technical Report No. 50, Louisiana Department of Transportation and Development, Baton Rouge, Louisiana

(Nyman, 1984): Nyman, D.J., 1984, The occurrence of high concentrations of chloride in the Chico aquifer system in southwestern Louisiana, 200 03: US Geological Survey Scientific Investigations Report 2004-5212, 56 p.

(Ohio DNR, 2012): Ohio Department of Natural Resources, 2012, Executive Summary: Preliminary report on the Northstar I Class II injection well and the seismic events in the Youngstown, Ohio area: State Report, p 1- 23, Columbus, Ohio.

(Peng and Robinson, 1976): Peng, Y., and Robinson, D.B., 1976, "A new two-constant equation of state", Industrial and Engineering Chemistry: Fundamentals, 15 59-64.

(Petroleum Experts Limited): Petex House, 10 Logie Mill, Edinburgh, EH7 4HG, United Kingdom; [www.petex.com](http://www.petex.com); email: [edinburgh@petex.com](mailto:edinburgh@petex.com).

(Pittman, 1981): Pittman, E.D., 1981, Effect of fault-related granulation on porosity and permeability of quartz sandstones, Simpson Group (Ordovician), Oklahoma: Am. Assoc. Petroleum Geologists Bull., v. 65, n. 11, p. 2381-2387.

(Porter and Newsom, 1987): Porter, W.M., and Newsom, S.W., 1987, "Shale Porosity and Permeability".

(Rainwater, 1968): Rainwater, E.H., 1968, Geological History and Oil Potential of the Central Gulf Coast: Gulf Coast Association of Geological Societies, Transactions, Vol. XVIII, pp.124165.

(Ramos et al. 1994): Ramos, G., Katahara, K., Keck, R., and Batzle, M., 1994, "In-situ stress predictions and measurements in an unconsolidated sandstone formation, the Lower Frio, East Texas", Rock Mechanics, Nelson and Laubach (eds), Balkema, Rotterdam, Netherlands.

(Schlumberger, 1987): Log Interpretation Principles/Applications, Schlumberger Educational Services, Houston, Texas, p. 198.

(Schlumberger, 1988): Archie's Law: Electrical Conduction in Clean, Water-bearing Rock, The Technical Review, v. 36, n. 3, Schlumberger Educational Services, Houston, Texas, pp. 4-13.

(Sargent, 2004): Sargent, B.P, 2004, Thickness of the Chicot aquifer system surficial confining unit and location of shallow sands, southwestern Louisiana; Louisiana Department of Transportation and Development Water Resources Technical Report no. 73, 34 p.

(Secor, 1965): Secor, D.T., 1965, Role of fluid pressure in jointing: American Journal of Science, v. 263, p. 633-646.

(Seni et al., 1997): Seni, S.J., Hentz, T.F., Kaiser, W.R., and Wermund, E.G., editors, 1997, Atlas of northern Gulf of Mexico gas and oil reservoirs, Volume 1, Miocene and older reservoirs, Texas, University of Texas, Austin, Bureau of Economic Geology.

(Shake Out website): <https://www.shakeout.org/centralus/louisiana/>

(Skoumal et al., 2018): Skoumal, R.J., Brudzinski, M.R., Currie, B.S., 2018, Proximity of Precambrian basement affects the likelihood of induced seismicity in the Appalachian, Illinois, and Williston Basins, central and eastern United States: *Geosphere* v. 14, p. 1365–1379.

(Smith, 1966): Smith, D.A., 1966, Theoretical Considerations of Sealing and Non-Sealing Faults: *Am. Assoc. Petroleum Geologists Bull.*, v. 50, n. 12, p. 363-374.

(Smith, 1980): Smith, D.A., 1980, Sealing and Non-Sealing Faults in Louisiana Gulf Coast Salt Basin: *Am. Assoc. Petroleum Geologists Bull.*, v. 64, n. 2, p. 145-172.

(Smoot, 1988): Smoot, C.W., 1988, Louisiana hydraulic atlas map No. 3: Altitude of the base of the Freshwater in Louisiana: U.S. Geological Survey Water-Resources Investigation Report 86-4314, 1 sheet, <http://pubs.er.usgs.gov/publication/wri864314>

(Snee and Zoback, 2016): Snee, J.E. and Zoback, M.D., 2016, State of Stress in Texas: Implications for induced seismicity: *AGU Publications Geophysical Research Letters*, 43, 10,208-10,214.

(Stevenson and Agnew, 1988): Stevenson, D.A., and Agnew, J.D., 1988, Lake Charles Louisiana, earthquake of 16 October 1983: *Bulletin of the seismological Society of America* 78 (4), p. 1,463-1,474.

(Stevenson and McCulloh, 2001): Stevenson, D.A., and McCulloh, R.P., 2001, Earthquakes in Louisiana: *Louisiana Geological Survey, Public Information Series* No. 7, 8 p.

(Stolper, 1994): Stolper, K., 1994, Calculate a More Accurate Water Salinity by Visually Estimating “m”: *Houston Geological Society Bulletin*, September 1994, p. 34.

(Swanson and Karlsen, 2009): Swanson, S.M., and Karlsen, A.W., 2009, PSUSGS Assessment of Undiscovered Oil and Gas Resources for the Oligocene Frio and Anahuac Formations, Onshore Gulf of Mexico Basin, USA, *Search and Discovery Article #10178*.

(Swanson et al., 2013): Swanson, S.M., Karlsen, A.W., and Valentine, B.J., 2013, *Geologic Assessment of Undiscovered Oil and Gas Resources—Oligocene Frio and Anahuac*

Formations, United States Gulf of Mexico Coastal Plain and State Waters, Open-File Report 2013-1257.

(Teas and Miller, 1933): Teas, L.P., and Miller, C.R., 1933, Racoob Bend oil field, Austin County, Texas: Am. Assoc. Petroleum Geologists Bull., v. 17, p. 1459-1491.

(Todd and Mitchum, 1977): Todd, E.G., and Mitchum, R.M., 1977, Seismic sequences and global changes in sea level, part 8: Identification of Upper Triassic, Jurassic, and Lower Cretaceous seismic sequences in Gulf of Mexico and offshore West Africa: in Payton, C. E., ed., Seismic Stratigraphy- Applications to Hydrocarbon Exploration: Am Assoc. Petroleum Geologists, Memoir 26, p. 145-163.

(Vail et al., 1977): Vail, P.R., Mitchum, R.M, and Thompson, S., 1977, Seismic Stratigraphy and Global Changes in Sea Level, Part 4: Global Cycles of Relative Changes in Sea Level, in Payton, C. D., ed., Seismic Stratigraphy - Applications to Hydrocarbon Exploration: AAPG, Memoir 26, pp. 52-97.

(Warner and Syed, 1986): Warner, D. L., and Syed, T., 1986, Confining layer study-supplemental report: prepared for U.S. EPA Region V, Chicago, Illinois.

(Warner, 1988): Warner, D.L., 1988, Abandoned oil and gas industry wells and their environmental implications: prepared for the American Petroleum Institute.

(Weber, 1978): Weber, K.J., 1978, The role of faults in hydrocarbon migration and tapping in Nigerian growth fault structures: Annual Offshore Technology Conference Proceedings, Volume 4, p. 2643-2653.

(Weber and Daukoru, 1975): Weber, K. J., and Daukoru, E., 1975, Petroleum geology of the Niger Delta: in Proceedings of the 9th World Petroleum Conference, Volume 2, p. 209-221.

(Weingarten et al., 2015): Weingarten, M., Ge, S., Godt, J. W., Bekins, B. A., Rubinstein, J. L., 2015, High-rate injection is associated with the increase in U.S. mid-continent seismicity: Science, v. 348, p. 1336-1340.

(Wesselman and Aronow, 1971): Wesselman, J.B. and Aronow, S., 1971, Groundwater Resources of Chambers and Jefferson Counties, Texas: Texas Water Development Board Report No. 133.

(Wesson and Nicholson, 1987): Wesson, R.L., and Nicholson, C., 1987, Earthquake Hazard Associated With Deep Well Injection, a Report to the U.S. Environmental Protection Agency: Open-File Report 98-331, U.S. Geological Survey, Reston, Virginia, p. 72.

(Yale et al., 1993): D.P. Yale, G.W. Nabor and J.A. Russell, "Application of variable formation compressibility for improved reservoir analysis", presented at the 58th Annual Technical Conference and Exhibition of the Society of Petroleum Engineers, Houston, Texas, USA, 3 – 6 October 1993, SPE 26647.

(Yielding et al., 1997): Yielding, G., Freeman, B., and Needham, D.T., 1997, Quantitative fault seal prediction: Am. Assoc. Petroleum Geologists Bull., v. 81, n. 6, p. 897-917.

(Zeidouni et al., 2009): Zeidouni, M., Pooladi-Darvish, M., and Keith, D., 2009, “Sensitivity analysis of salt precipitation and CO<sub>2</sub>-brine displacement in saline aquifers”, 2009 SPE International Conference on CO<sub>2</sub> Capture, Storage and Utilisation, San Diego, California, USA, 2-4 November 2009, SPE 126690.

(Zheng et al., 2019): Zheng, X., Sun, Z., and Espinoza, D.N., 2019, “Uniaxial strain unloading compressibility of Frio sand: Measures and implications of reservoir pressure management for CO<sub>2</sub> storage”, 53rd US Rock Mechanics/Geomechanics Symposium, New York, NY, USA, 23-26.

(Zimmerman, 1990): R.W. Zimmerman, “Compressibility of sandstones”, Developments in Petroleum Science 29”, Elsevier, 1990

(Zoback, 1980): Zoback, M.L., and Zoback, M., 1980, “State of stress in conterminous United States”, Journal of Geophysical Research, v.85, p 6113-6156.